

ANALYSIS OF SOLAR PHOTOVOLTAIC MODULE PERFORMANCE UNDER
TROPICAL SAVANNAH CLIMATIC CONDITIONS OF KENYA (UASIN GISHU
COUNTY)

MUSAAVY BELINDAH

A Thesis Submitted to the School of Engineering, Department of Mechanical,
Production and Energy Studies in Partial Fulfillment of the Requirements for the
Award of the degree of Master of Science in Renewable Energy


Moi University

2023

DECLARATION

Declaration by Candidate

This thesis is my original work and has not been presented for a degree in any other University. No part of this thesis may be reproduced without the prior written permission of the author and/or Moi University.

Sign:  _____

Date: 25-07-2023

BELINDAH MUSAAVY

ENG/MES/10/19

Declaration by Supervisors

This thesis has been submitted for examination with our approval as University Supervisors.

Sign:  _____

Date: 25-07-2023

PROF. (ENG.) AUGUSTINE.B MAKOKHA

Department of Mechanical, Production and Energy studies

Moi University, Eldoret, Kenya

Sign:  _____

Date: 25-07-2023

DR. LAWRENCE LETTING

Department of Electrical and Communication Engineering

Moi University, Eldoret, Kenya

DEDICATION

I dedicate this thesis to my mum, husband and our daughters Blessing and Brandy.

ABSTRACT

Solar Photovoltaic (PV) is essential for the transition to clean and renewable energy in Kenya. However, it remains underutilized accounting for only 2.2 % of the country's electricity generation mix as of December 2020. The obstacle in harnessing solar PV in Kenya has been linked to a lack of site specific design parameters and limited data on solar PV performance under different climatic conditions. This has been exacerbated by the overdependence on imported solar PV modules that are tested under standard conditions by manufactures. Therefore, the main objective of this study was to analyse solar PV module performance under Uasin Gishu County climatic conditions. The specific objectives were: To measure the power output of the PV modules under combined effect of temperature and irradiance, measure the I-V, P-V characteristics of the PV modules and simulate the PV modules performance using MATLAB/Simulink. The methodology involved rooftop installation of two 100W solar PV modules, one of mono-crystalline and the other of poly-crystalline technology, at Moi University (0.2861° N, and 35.2943° E). Data was collected daily from 7.00am to 6.00pm for five months (November 2020 - March 2021). The data on solar irradiance and module temperature was captured using light intensity and temperature sensors respectively while the data on voltage and current from the solar PV modules was captured by the electric power sensors. Analysis of the data collected indicated that both mono-crystalline and poly-crystalline modules were affected by module temperature and solar irradiance variation. As the temperature increased beyond 25°C the current increased slightly while the power output and voltage dropped. However, the increase in solar irradiance increased the power output, current and voltage. At irradiance of 1023 W/m², the results revealed a higher current and power output by mono-crystalline module at 6.27% and 5.62% respectively above the poly-crystalline while at irradiance of 702 W/m², the current was 3.6% and power at 2.86% above that of polycrystalline. In the case of module temperature the mono-crystalline module still performed better. The current and power output increased by 3.87% and 6.7% respectively above the polycrystalline performance at 13°C while at 28.5°C the current of 4.11% and power of 2.97% above the poly-crystalline performance was recorded. In conclusion, the cell temperature and solar irradiance have a strong influence on the performance of solar PV modules and this varies with the type of solar cells technology. Based on the findings of this study the mono-crystalline solar PV technology is recommended for the Kenyan tropical savannah climate of Uasin Gishu.

TABLE OF CONTENT

DECLARATION.....	I
DEDICATION.....	II
ABSTRACT.....	III
TABLE OF CONTENTS.....	IV
LIST OF TABLES.....	VIII
LIST OF FIGURES.....	IX
ACKNOWLEDGMENT.....	XIII
CHAPTER ONE: INTRODUCTION.....	1
1.2 Background and Motivation.....	1
1.2.1 Energy Consumption in Kenya.....	5
1.2.2 Solar Photovoltaic (PV) Energy.....	6
1.2.3 The Characteristics of PV Solar Cell.....	6
1.2.4 Short circuit current (I_{sc}) of solar cell.....	7
1.2.5 Open circuit voltage (V_{oc}) of solar cell.....	7
1.2.6 The Meteorological Conditions in Kenya.....	9
1.3 Statement of the Problem.....	10
1.4 Objectives.....	11
1.4.1 General objective.....	11
1.4.2 Specific objectives.....	11
1.5 Justification of the Study.....	12
1.6 Significance of the Study.....	12
CHAPTER TWO: LITERATURE REVIEW.....	13
2.1 Introduction.....	13
2.2 Renewable Energy.....	13

2.3	Solar Photovoltaic Systems.....	14
2.4	Empirical Review.....	15
2.5	I-V Curves of Different Solar PV Modules.....	16
2.6	Outdoor effects on I–V characteristics.....	17
2.7	Impact of temperature on IV characteristics.....	20
2.8	Impact of Irradiance on IV characteristics.....	21
2.9	Tropical Savannas.....	21
2.10	Types of PV Modules.....	22
2.11	Factors affecting Power Output of Solar Photovoltaic Modules.....	26
2.11.1	Temperature.....	26
2.11.2	Solar irradiance.....	27
2.12	Performance Parameters of PV module.....	28
2.13	PV Outdoor and Standard Test Conditions (STC).....	30
2.14	Degradation of PV Modules.....	31
2.15	Data Logger operations theory.....	32
2.16	Microprocessor Based Data Logger.....	33
2.17	Microcontroller Units ATMEGA328.....	33
2.18	Network Operator Requirements.....	36
	CHAPTER THREE: METHODOLOGY.....	40
3.1	Introduction.....	40
3.1	Research Design.....	41
3.2	Data Source.....	41
3.3	Data Collection Technique.....	41
3.4	Reliability and Validity.....	42
3.5	Sampling Technique.....	42

3.6	Data Analysis and Interpretation.....	42
3.7	Conceptual Framework.....	44
3.8	Data logger system set-up.....	45
3.9	Experiment setup.....	45
3.10	Limitation of the study.....	48
3.11	Assumption of the study.....	48
CHAPTER FOUR: RESULTS AND DISCUSSIONS.....		50
4.1	Introduction.....	50
4.2	MEASURED (EXPERIMENTAL) VALUES GRAPHS.....	50
4.2.1	Testing parameters for Module 1 for the Period of November 2020 (set one).....	50
4.2.2	Testing parameters for Module 1&2 for the Period of 1 st Jan – 10 th Feb 2021.....	58
4.2.3	The I-V and P-V curves for module 1 (monocrystalline).....	59
4.2.4	Testing parameters for Module 1&2 for the Period of 17 th Feb – 31 st March 2021. .	65
4.2.5	The I-V and P-V curves for module 1 under the meteorological conditions.....	65
4.3	The I-V and P-V curves for module 2 (Polycrystalline).....	68
4.4	SIMULATED GRAPHS.....	70
4.4.1	The I-V and P-V curves for monocrystalline (November 2020).....	70
4.4.2	The I-V and P-V curves for module 2 (polycrystalline).....	73
4.4.3	I-V and P-V curves at constant temperature but varying irradiance.....	75
4.4.4	I-V and P-V curves at constant temperature but varying irradiance.....	78
4.4.5	I-V and P-V curves at constant temperature but varying irradiance.....	80
4.5	SIMULATED AND MEASURED VALUES COMPARED.....	86
4.6	Schematic Simulink setup.....	90

CHAPTER FIVE: CONCLUSIONS AND RECOMMENDATIONS.....91

5.1 Conclusions.....91

5.2 Recommendations.....92

REFERENCES.....93

APPENDICES.....100

 Appendix A: Installation on the roof.....101

 Appendix B: More measured results.....101

LIST OF TABLES

Table 2.1: PV Module Characteristics.....	25
Table 2.2: MCU Key Parameters.....	34
Table 2.3: Program Parallel Mode.....	35
Table 2.4: Serial Programming.....	36
Table 3.1: Specification and orientation parameters.....	43
Table 3.2: Conceptual Framework Key.....	44
Table 4.1: Specification of the modules used, angle of inclination 33°.....	50
Table 4.2: Measured parameters for monocrystalline.....	52
Table 4.3: Measured parameters for polycrystalline.....	54
Table 4.4: Measured parameters for monocrystalline solar PV.....	57
Table 4.5: Measured parameters for module 1.....	67
Table 4.6: Measured parameters for Polycrystalline solar PV.....	69

LIST OF FIGURES

Figure 1.1 : Kenya renewable capacity in 2021.....	8
Figure 2.1: Photovoltaic systems (Source: Blueplanet-energy, 2014).....	14
Figure 2.2 MCU ATMEGA 328.....	34
Figure 2.3: Arduino communication shield.....	37
Figure 2.4: Digital pins.....	37
Figure 3.1: Map of the study Area (Source: Author, 2022).....	40
Figure 3.2: Conceptual Framework.....	44
Figure 3.3: Data logger schematics.....	45
Figure 3.4: PV panels on the clear roof.....	46
Figure 3.5: Data logger and batteries (storage).....	46
Figure 3.6: Data logger and charge controllers.....	47
Figure 3.7: Inverter and load (bulbs).....	48
Figure 4.1: I-V and P-V characteristics Module 1 (monocrystalline) Temperature =25°C	52
Figure 4.2: I-V and P-V characteristics Module 2 Temperature =25°C.....	54
Figure 4.3: I-V and P-V characteristics Module 1 Irradiance =1000W/m ²	55
Figure 4.4: I-V and P-V characteristics Module 2 Irradiance =1000W/m ²	56
Figure 4.5: I-V and P-V characteristics of monocrystalline Module Temperature =25°C	57
Figure 4.6: I-V and P-V characteristics Module 2 Temperature =25°C.....	58
Figure 4.7: I-V and P-V characteristics Module 1 Irradiance =1000W/m ²	60
Figure 4.8: I-V and P-V characteristics Module 2 Irradiance =1000W/m ²	62
Figure 4.9: I-V and P-V characteristics of Monocrystalline Module Temperature =25°C	63
Figure 4.10: I-V and P-V characteristics Polycrystalline module Temperature =25°C	64
Figure 4.11: I-V and P-V characteristics of monocrystalline Module Irradiance =1000W/m ²	67

Figure 4.12: I-V and P-V characteristics of polycrystalline Module Irradiance =1000W/m ²	69
Figure 4.13: Simulink setup for mono-crystalline at constant Temperature.....	70
Figure 4.14: I-V and P-V characteristics of monocrystalline Module Temperature =25°c	71
Figure 4.15: Simulink setup for mono-crystalline at constant irradiance.....	72
Figure 4.16: I-V and P-V Curves at constant irradiance 1000W/m ² (mono-crystalline)	72
Figure 4.17: Simulink set-up for poly-crystalline.....	73
Figure 4.18: I-V and P-V Curves at constant temperature at 25°c (Poly-crystalline)..	73
Figure 4.19: Simulink set-up for poly-crystalline at constant irradiance.....	74
Figure 4.20: I-V and P-V Curves at constant irradiance 1000 W/m ² (Poly-crystalline)	75
Figure 4.21: Simulink set-up for mono-crystalline for constant temperature.....	75
Figure 4.22: I-V and P-V Curves at constant temperature (mono-crystalline).....	76
Figure 4.23: Simulink set-up for mono-crystalline at constant irradiance.....	77
Figure 4.24: I-V and P-V Curves at constant irradiance (mono-crystalline).....	77
Figure 4.25: Simulink set-up for poly-crystalline at constant temperature.....	78
Figure 4.26: I-V and P-V Curves at constant temperature (poly-crystalline).....	78
Figure 4.27: Simulink set-up for poly-crystalline at constant irradiance.....	79
Figure 4.28: I-V and P-V Curves at constant irradiance (poly-crystalline).....	80
Figure 4.29: Simulink set-up for mono-crystalline at constant temperature.....	81
Figure 4.30: I-V and P-V Curves at constant temperature (mono-crystalline).....	81
Figure 4.31: Simulink set-up for mono-crystalline at constant irradiance.....	82
Figure 4.32: I-V and P-V Curves at constant irradiance (mono-crystalline).....	83
Figure 4.33: Third Simulink set-up for poly-crystalline.....	84
Figure 4.34: I-V and P-V Curves at constant temperature (poly-crystalline).....	84
Figure 4.35: Third Simulink set-up for poly-crystalline.....	85

Figure 4.36: I-V and P-V Curves at constant irradiance (poly-crystalline).....	85
Figure 4.37: I-V characteristics for simulated and measured values for monocrystalline	86
Figure 4.38: I-V characteristics for monocrystalline and polycrystalline measured values at varied irradiance.....	87
Figure 4.39: P-V characteristics for monocrystalline and polycrystalline at varied temperatures.....	88
Figure 4.40: I-V characteristics comparison between Mono and Poly at different temperature level but constant irradiance.....	89
Figure 4.41: Simulink Setup for the simulation.....	90

ACRONYMS

AC	Alternative Current
DC	Direct Current
EPRA	Energy and Petroleum Regulatory Authority
ERC	Energy Regulatory Commission
GMPP	Global Maximum Power Point
GW	Gigawatt
Inc	Incremental Conductance
IRENA	International Renewable Energy Agency
MPPT	Maximum Power Point Techniques
P&O	Perturb and Observe
PECVD	Plasma Enhancement Chemical Vapour Deposition
PV	Solar Photovoltaic
PVT	Photovoltaic-Thermal
RAPS	Remote Area Power Supply
SWE	Staebler-Wronski Effect
PCE	power conversion efficiency
PO	Power Output

ACKNOWLEDGMENT

I am indebted to the almighty God, who has been so gracious to me. He gave me the excellent health, intellect, wisdom, perseverance, and strength necessary to complete this work. I am also grateful to ACEII Centre of Excellence in Phytochemicals, Textiles and Renewable Energy (PTRE) for sponsoring me financially through the program. I am also deeply indebted to my supervisors, Prof. Augustine Makokha and Dr. Lawrence Letting, for their guidance and support. I would a like to appreciate my mum Mary Mutola for her unconditional support through the entire period as student, my husband Felix Yaola for the support and patience in taking care of our young family time I was unavailable, as I take care of my studies. I extend my gratitude to my sister Isabella for coming in to assist my family while I was away studying. Lastly am grateful to Amisi Amuyunzu and all the lab technicians in the school of Engineering and Elton in chemistry Laboratory for helping me set up the apparatus for the experiment. God bless all.

CHAPTER ONE: INTRODUCTION

1.1 Introduction

This chapter provides information on the background of the study, Solar Photovoltaic (PV) Energy, meteorological conditions in Kenya, Statement of the Problem, Objectives, and Justification of the research and Significance of the study

1.2 Background and Motivation

Renewable energy now provides 5% of the world's power (EASE-CA, 2020). Renewable capacity is expected to further increase over 8% in 2022, reaching almost 320 GW (IEA, 2022). There were 160 GW of clean energy installations worldwide in 2016 (EASE-CA, 2020). Global renewable generation capacity was 2 799 GW by the end of 2020, according to International Renewable Energy Agency (IRENA, 2020). 2020 will see an increase in renewable energy capacity of 260 GW (+10.3 percent) (Santos *et al.*, 2021). Wind energy came in second with an increase of 111 GW (+18%), closely behind solar energy, which continues to increase its capacity by 127 GW (+22%) (Santos *et al.*, 2021). Annual additions to global renewable electricity capacity are expected to average around 305 GW per year between 2021 and 2026 in the IEA main case forecast (IEA, 2021).

At the end of 2017, there were around 415 GW of photovoltaic (PV) electricity installed worldwide (ISE, 2018). From 2010 to 2017, the compound annual growth rate of PV installations was 24 percent (ISE, 2018). The capacity of the installed PV systems globally increased by 100 GW in 2018, bringing the total installed PV system capacity to 515 GW. Approximately two billion PV modules were functioning in various regions and under various weather conditions by the end of 2020, representing over 760 GW of photovoltaic (PV) systems installed globally and 3.7% of the world's electricity demand (IRENA, 2022).

With 132.8 GW of solar PV installations, up from 125.6 GW in 2020, the world set a new milestone in 2021. There was 53 GW (40%) of the additions in 2021 which came from China (IRENA, 2022). Brazil, India, and the United States came next, all of which set new annual marks (IRENA, 2022). The next-largest locations for PV solar installations were in Spain, the Netherlands, Germany, Japan, the Republic of Korea, and the Republic of Korea, although none of them were able to outperform their earlier peak volumes (IRENA, 2022). The total amount of photovoltaic (PV) electricity installed globally is 892 GW.

Photovoltaic modules are used to convert solar energy to electrical energy. A group of photovoltaic cells make up a solar photovoltaic module (Amuda, Adeleke & Orotayo, 2017). When sunlight shines on a photovoltaic cell, a semiconductor device, direct current (DC) power is produced (Gardas & Tendolkar, 2012). The first PV cells were created by Bell Laboratories in 1954, and since then, technical advancements have increased efficiency while lowering prices (Tyagi, Kaushik & Tyagi, 2012). The most efficient PV modules usually employ single crystal silicon cells, with efficiencies up to 15% (Işık, 2015). Polycrystalline cells are less expensive to manufacture but yield module efficiencies of about 11% (Işık, 2015).

The main component in generating electricity from solar energy is the PV module, which has a nonlinear relationship between current and voltage (Bonthagorla & Mikkili, 2020). The number of cells in a solar panel can vary from 36 cells to 144 cells and these elements are connected in series. The two most common solar panel options on the market today are 60-cell and 72- cell (www.lithiumvalley.com). It is an energy source that directly transforms solar energy into electrical energy (Pradhan & Panda, 2017)

Solar insolation, temperature, potential induced deterioration, and age are the elements that have an impact on the functionality and effectiveness of PV systems. Changes in temperature and sun insolation are thought to be the two factors that have the greatest influence (Bonthagorla & Mikkili, 2020; Ogbomo *et al.*, 2017). There is only one global maximum power point (GMPP) for the output power-voltage characteristic of the PV module/array under uniform insolation conditions, and it can be easily identified using conventional maximum power point techniques (MPPT), such as hill-climbing techniques, perturb and observing (P&O), and incremental conductance (Inc) (Ahmad, Murtaza & Sher, 2019).

PV modules are frequently regarded as the component of PV systems with the highest level of dependability. Photovoltaic technology, according to Ghoneim *et al.* (2011), has a significant positive impact on the environment because it doesn't need fuel and generates no additional pollutants or trash outside of that produced naturally during manufacture. Researchers and manufacturers have made significant advancements in their understanding of the performance and conceptual modelling of photovoltaic (PV) modules under a variety of meteorological conditions, including temperature and solar irradiance, which are frequently harsh and may cause PV modules to degrade (Abdullahi *et al.*, 2017). Because there are significant hazards both inside and outside of PV power systems that produce uncertainty and unpredictability in PV capacity, it is essential to assess the dependability of PV modules (Sawin & Martinot, 2010). The systems that make up PV module components and environmental elements present considerable design issues for effective and massive PV power systems, according to Roy, Kedare & Bandyopadhyay (2010).

PV modules made of silicon crystalline are widely utilized worldwide (Ramadan *et al.*, 2020). These days, novel PV technologies including amorphous silicon, copper

indium selenide (CIS), and cadmium telluride are accessible with lower production costs than conventional silicon crystalline-based modules (Ramadan *et al.*, 2020). The fact that silicon is so readily available on earth is the main benefit of silicon cells (Shukla & Khare, 2015). Several layers of semiconductor materials with various electronic characteristics make up the photovoltaic cell (Ishaque, Salam & Taheri, 2011). There are several types of solar PV cells on the market, including amorphous silicon, thin-film, multi-crystalline, and monocrystalline silicon cells (Ahmed, Habib & Javaid, 2015).

The key external and internal elements that affect a photovoltaic cell's performance include radiation, wind, electrical losses, structural characteristics, pollution, visual losses, age, temperature, and shading (Hasan & Parida, 2016). To understand the output characteristics, efficiency, and performance of PV systems and to analyze the system using solar insolation, temperature, and output voltage, theoretical modelling and computer simulation are thus crucial (Abdullahi, Saha & Jinks, 2017). Many simulation tools, including MATLAB-Simulink, Spice, SABER, and electromagnetic transient, have been used in extensive research on PV modelling and parameterizations over the last few decades to comprehend the non-linear I-V/P-V characteristic of the PV module (Apostolou, Reinders & Verwaal, 2016). According to studies of the IV curve, the current falls as the voltage rises, but maximum power is created at a point known as the knee point, thus the name maximum power point (Pradhan & Panda, 2017).

The world's sunniest continent is Africa (Sow, 2017). The continent could be able to meet its energy demands with average radiation of 2650 kWh/m²/year and expected sunlight duration of 3500 hours/year (Sow, 2017). For the first time in sub-Saharan Africa in 2014, electrification initiatives exceeded population growth (IEA, 2017).

Despite this progress, 675 million people, 90% of whom live in sub-Saharan Africa, may still lack access to electricity in 2030 (down from 1.1 billion today), and 2.3 billion people may still use kerosene, coal, or biomass for cooking (down from 2.8 billion today) (Muok, 2021).

Africa's potential for solar energy (10 TW), hydropower (350 GW), wind energy (110 GW), and geothermal energy (15 GW) is practically limitless (African Development Bank, 2018). Installed Renewable Energy Capacity in Africa is 56 GW (IRENA, 2022). By 2030, it is predicted that Africa's renewable energy capacity would increase to 310 GW (IRENA, 2018). The overall installed solar PV capacity in Africa has increased fourfold during the past two years (IRENA, 2016). Even if the market increased to around 1.2 GW in 2018, Africa's contribution of the global PV industry is still rather tiny (German Solar Association, 2019). At the end of 2018, Africa's installed solar PV capacity was 5.1 GW (Becquerel Institute, 2019).

1.2.1 Energy Consumption in Kenya

Hydroelectric resources provide for a sizable portion of Kenya's home and industrial energy usage. Due to the fact that the majority of homes are not grid-connected, this is prohibitive in nature. Solar energy is an alternate source that the general public may easily access. The number of individuals purchasing and using solar PV for their energy requirements has dramatically grown, according to reports from the Energy Regulatory Commission in Kenya (ERC, 2017). In Kenya, more than 30,000 tiny solar panels with a capacity of 12 to 30 Watts were marketed as of 2010 (Ngeno *et al.*, 2018). As more individuals continue to use solar energy as an option to meet their energy needs, the numbers have considerably increased. In Kenya, almost 1.2 percent

of residences use solar energy, primarily for lighting and television set charging (Takase, Kipkoech & Essandoh, 2021).

1.2.2 Solar Photovoltaic (PV) Energy

Through the photovoltaic effect, photovoltaic modules produce electricity by converting radiant energy to electricity (Pandiarajan & Muthu, 2011). This happens when solar cells are combined to boost their power. Photovoltaic cells are a very dependable, long-lasting, and quiet way to generate electricity (Cui *et al.*, 2019). Semi-conducting components, such as silicon-based materials, make up the majority of photovoltaic modules (Ahmad *et al.*, 2020). Semiconducting components create electrical charges when the photovoltaic module is exposed to radiation, and these charges are carried away by metal carriers (Guo & Facchetti, 2020). A single cell may create a tiny quantity of direct current (DC), while a string of connected multiple cells can produce a bigger amount of DC (Wolfs & Tang, 2005; Jovicic, 2019).

1.2.3 The Characteristics of PV Solar Cell

The majority of photovoltaic cells are made on silicon-based semiconductor materials and have two distinct layers of semiconductors (Cho *et al.*, 2008). N-type silicon is the kind with surplus electrons, and P-type silicon is the type with extra holes (Cho *et al.*, 2008). When these two layers are placed together, they produce a P-N junction. Some of the photons from the sun's energy are absorbed by the cell when it is exposed to it. The energy of the absorbed photons will be greater than the energy difference between the valence and conduction bands of the semiconductor (Trupke, Green & Würfel, 2002). The electrons become excited and fly out to form one electron-hole pair when they receive energy from the photons. Due to the electrostatic field, these electron-hole pairs close to the p-n junction move to the n-type side of the intersection

(Walter *et al.*, 2010). This is how a solar cell works, and various solar cell parameters determine how efficient the cell is (Walter *et al.*, 2010).

1.2.4 Short circuit current (I_{sc}) of solar cell

A solar cell can only deliver the short circuit current without endangering its own constriction (Christians, Manser & Kamat, 2015). It is determined by short-circuiting the cell's terminals when it is operating at its peak efficiency to provide the greatest output (Christians, Manser & Kamat, 2015).

1.2.5 Open circuit voltage (V_{oc}) of solar cell

When there is no load attached to the cell, it is measured by observing the voltage between the terminals (Mirzaev & Abdullaev, 2020). This voltage is slightly dependent on the manufacturing processes and temperature, but not much on the amount of light and exposed surface area (Mirzaev & Abdullaev, 2020). Kenya is seen to be an appropriate location for the spread of solar energy technology (including PV systems, micro grids, nano grids, and similar technologies) (EPRA, 2020). Through the Draft Energy Solar Photovoltaic Systems Regulation of 2020, the nation is now creating laws to ensure the sustainable exploitation of solar power resources (EPRA, 2020).

Sadly, despite having strong solar radiation, the nation is neither as ambitious nor as effective in developing PV (Samoita *et al.*, 2020). According to data, as of 2019, Kenya had a total installed PV capacity of just approximately 50.25 MW (ERC, 2019). In Kenya, solar PV is expected to expand at a rate of 15% yearly ERC (2019), mostly because to falling PV prices, which will make it more competitive. However, this is still a small increase relative to the potential. Developments frequently include off-grid solutions. In Kenya, more than 30,000 tiny solar panels with a capacity of 12

to 30 Watts were marketed as of 2010 (Ngeno *et al.*, 2018). According to estimates, Kenya's whole solar market has grown by more than 100% during the past ten years (Muok & Makokha, 2017).

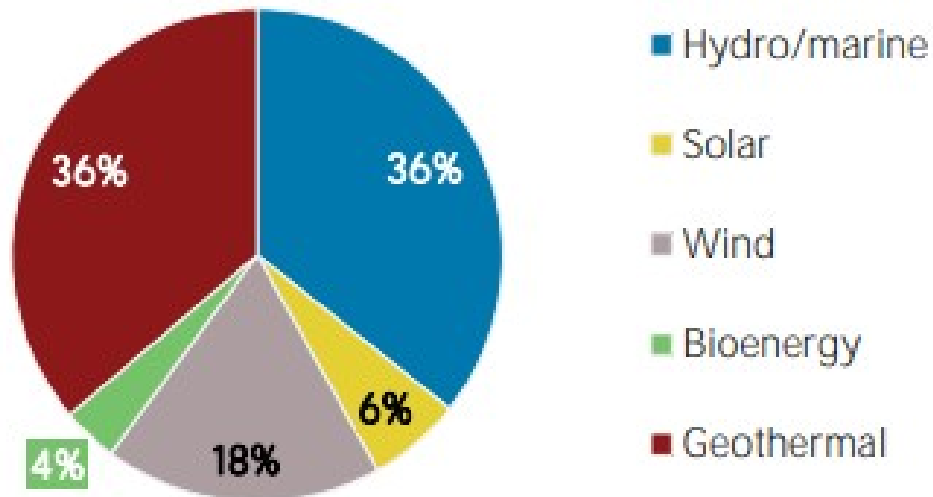


Figure 1.1 : Kenya renewable capacity in 2021

Source: IRENA, 2022

In this work, solar PV module performance for Uasin Gishu County climatic conditions was analyzed and modelled using several widely available photovoltaic modules. In addition, the impact of other climatic factors irradiance and temperature change on the functionality and dependability of modules was investigated.

1.2.6 The Meteorological Conditions in Kenya

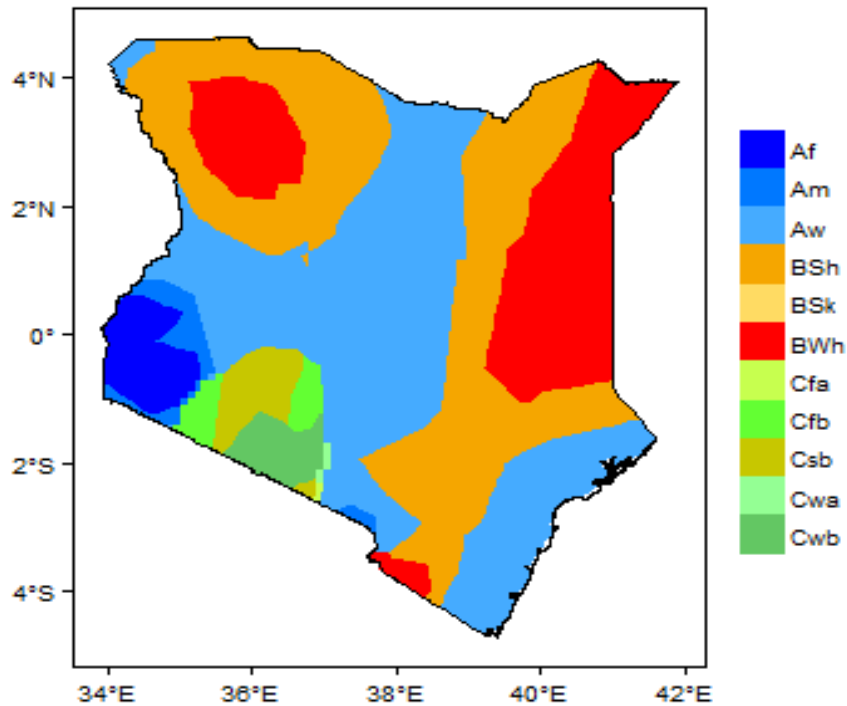


Figure 1.2 Meteorological Conditions in Kenya

Key:

Climate for Af region (Tropical Rainforest)

Climate for Am region (Tropical Monsoon)

Climate for Aw region (Tropical Savannah)

Climate for BSh region (Arid Steppe (hot))

Climate for BWh region (Arid Desert (hot))

Climate for Cfb region (Temperate without dry season (warm summer))

Climate for Csb region (Temperate with dry summer (warm summer))

Climate for Cwb region (Temperate with dry winter (warm summer))

Climate for Aw region (Tropical Savannah)

The savanna environments are characterised by a rainy period with warm to hot conditions followed by a virtually rainless dry period with warm to cool conditions. Uasin Gishu can be found in the tropical savannah region on the map of Kenya's weather conditions. Areas with savanna vegetation experience a predominantly tropical wet and dry environment. Averaging 762 and 1270 millimeters (mm) of precipitation annually, mean monthly temperatures are at or above 17.7°C (php.radford.edu). Though, most of the savannah temperature range is between 20-30°C (Worldatlas.com). The dry season, however, has less rainfall than 101 mm every month (php.radford.edu). Africa has an average yearly irradiance of 260W/m², yet Germany produces 13.7% of the world's solar energy with an annual irradiance of 125W/m² (Korir, 2020). One of the least-used energy sources in the world is solar, and this is even truer in Africa (Korir, 2020). According to the Energy and Petroleum Regulatory Authority of Kenya (2015), Kenya receives an average daily solar insolation of 4-6 KWh/m² and mostly uses solar energy for PV systems, drying, and water heating. Uasin Gishu has an average yearly temperature of 18.94°C, which is -3.56% lower than Kenya's norms. It is situated at an altitude of 2164.67 meters above sea level. Annual precipitation in Uasin Gishu averages out to 220.3 millimeters, with 253.01 rainy days (or 69.32%) (tcktcktck.org).

1.3 Statement of the Problem

The quantity of incident global radiation on the surface is influenced by environmental factors such as air transmissivity, shading, diffuse ratios, the effect of altitude, and terrain, which also affects the system's overall performance and power production (Opiyo, 2015; Bimenyimana *et al.*, 2017). To ensure a dependable system for the duration of its anticipated lifetime, the operator is informed of the necessary maintenance

Tropical savannah environments are characterised by a rainy period with warm to hot conditions followed by a virtually rainless dry period with warm to cool conditions is perfect area to study the module performance. The study area falls under such conditions. Moreover, the study area experiences annual rainfall of about 1200mm, mean temperature range of 20-30°C and solar radiation of 5.3kWh/m² (Worldatlas.com). Though, on the performance of various solar PV modules in Kenyan environments, there is, however, a paucity of information. Also, consumers buy solar module from their vendors or solar shops with no information on the performance in various climatic conditions and types of solar modules. Such information is essential as it has an impact on the economics of the consumer. Therefore, the goal of this work was to provide an experimental analysis of solar PV module performance that was appropriate for the weather in Uasin-Gishu County.

1.4 Objectives

1.4.1 General objective

The main objective of this study was to conduct an experimental analysis of solar photovoltaic module performance under tropical savannah climatic conditions of Uasin Gishu County

1.4.2 Specific objectives

- i. To measure the power output) of the PV modules under the combined effect of the temperature and irradiance.
- ii. To measure the I-V, P-V characteristics of the PV modules
- iii. To model and simulate the PV modules performance using MATLAB/Simulink.

1.5 Justification of the Study

The Kenyan market is currently home to a variety of PV modules that have been developed throughout time by various producers. The performance and dependability of these PV modules are, however, calibrated using Standard Test Conditions, which don't reflect the reality across all of the country's climatic conditions. According to research, when exposed to external circumstances, PV modules' performance and dependability vary greatly (Ryan *et al.*, 2012; Oloo *et al.*, 2015; Gatakaa *et al.*, 2010 and Fouad *et al.*, 2017). As a result, it is uncertain how well or reliably PV modules will work under various weather situations. The performance of the PV modules was examined in this study using measurements of temperature and irradiance; and how these variables impact PV modules under tropical savannah climate of Uasin-Gishu.

1.6 Significance of the Study

The results of this study are believed to be useful to manufacturers, energy industry investors, consumers, and various governments. To achieve the anticipated return on investment for the solar PV investor, the PV modules' dependable performance and durability under warranty circumstances are critical. As a result, the findings assist investors comprehend how PV modules function in Uasin-Gishu weather conditions. Module makers try to reassure customers by offering warranties, much like other product manufacturers do. In order to make wise judgments on warranties, this study's findings is crucial in giving crucial information on the performance of PV modules in Uasin-Gishu climatic circumstances. The result is important for customers, the Uasin-Gishu County energy department, and the different regulatory agencies about the

performance of PV modules under tropical savannah climatic conditions of Uasin Gishu County.

CHAPTER TWO: LITERATURE REVIEW

2.1 Introduction

The performance of several solar PV module types under various climatic and meteorological circumstances is covered in this chapter through a review of some of the research that has been completed to date. A discussion of earlier attempts by other researchers to experiment with and model the performance of solar PV is also provided. Thus, the knowledge and understanding provided in this chapter serve as the foundation for the study.

2.2 Renewable Energy

Today, everyday energy consumption includes a significant amount of renewable energy (Faye *et al.*, 2019). Solar photovoltaic (PV) technology energy is the renewable energy source that is producing electricity at the quickest rate (Oliva *et al.*, 2017). Over the years, solar photovoltaic (PV) have been one of the leading renewable energy technologies (Letcher, 2018). By the end of 2018, the installed capacity of solar PV has grown to 480 GW globally (excluding CSP), making it the second-largest renewable energy source after wind (IRENA, 2020). Solar PV additions reached almost 94 GW last year, dominating total renewable and electric capacity additions once more, adding twice as much capacity as wind as and more than all fossil fuels and nuclear combined (IRENA, 2019).

In order to construct a photovoltaic (PV) system, it is important to forecast the output of a certain solar cell array under various circumstances (Jakica, 2018; Roy, 2018).

There are two main categories of PV power prediction modeling methods: data-driven approaches that require PV power output measurements and deterministic methods that use physics-based models and demand detailed design and rated performance information about the PV system (Hesse *et al.*, 2017; Moslehi *et al.*, 2018; Scioletti *et al.*, 2017). The latter group consists of artificial intelligence methods, linear or time series models, and statistical models (Raza *et al.*, 2016).

2.3 Solar Photovoltaic Systems

By harnessing the photovoltaic effect, solar PV systems use sunlight to generate electricity (Akorede, 2022). Semiconductors undergo this process, which causes them to produce voltage and current when they are exposed to light. Solar cells—individual devices whose electrical properties change when exposed to light—are typically used in practical applications to achieve this effect. These silicon cells, which are either polycrystalline or monocrystalline, can be coupled in series or parallel to provide the desired voltage and current (Akorede, 2022). The form in which solar PVs are commercially made accessible for usage is known as a solar module or solar panel and consists of a number of solar cells packed onto a metal frame (Akorede, 2022).

The major materials used to make solar cells are gallium arsenide, copper and copper indium diselenide. Due to its unique optical characteristics, silicon is the best of these materials (Contreras *et al.*, 2006). Applications for PV cells include spacecraft, maritime navigational aids, telephony, cathodic protection, water pumping, remote area power supply (RAPS) systems, and a wide range of other things (Kalogirou *et al.*, 2007).

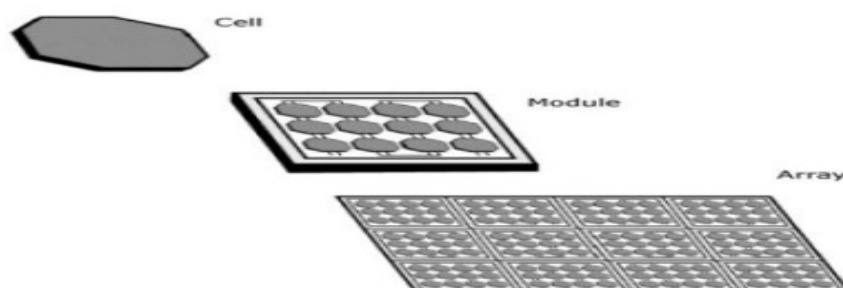


Figure 2.2: Photovoltaic systems (Source: Blueplanet-energy, 2014)

2.4 Empirical Review

Ike (2015) conducted research on the impact of ambient temperature on solar panel efficiency in tropical Nigeria. His research shows a negative correlation between power output and outside temperature. He added that the PV modules in the test area displayed high PO at low ambient temperatures, whereas the inverse was true at high ambient temperatures.

PV module durability in Senegal's tropical environment was examined by Ndiaye *et al.* (2015). They were particularly concerned with the decline of PO and PCE, which is indicated by short circuit current (I_{sc}) and open-circuit voltage (V_{oc}). They reported declines in I_{sc} and V_{oc} of 13% and 11%, respectively, over a ten-month period.

Kurnik *et al.* (2011) conducted outdoor testing of PV module performance under various mounting and operating conditions. The results revealed that regardless of irradiance, wind speed, or mounting restrictions, the relative temperature difference between the module and the ambient temperature was about similar to the conversion efficiency.

In their review of the literature on the relationship between cell temperature and solar cell performance, Dubey *et al.* (2013) came to the conclusion that because the expressions used in the literature to estimate solar cell temperature only work for specific mounting geometries, caution must be exercised when using them.

Ndiaye (2013) studied the performance deterioration of PV panels under various presentation styles. The key reasons of the PV performance deterioration that the research concentrated on were corrosion, discolouration, delamination, and breaking. Corrosion and discolouration were shown to be the main causes of PV cell

deterioration, despite the fact that modeling of various degradation types is still not well-examined in the literature. In their 2008 study, Hamrouni *et al.* (2008) examined the impact of solar irradiation and ambient temperature on the effectiveness of solar pumping systems and came to the conclusion that high ambient temperatures reduced pump flow rate and total system efficiency.

Under the tropical climatic conditions of Singapore, Dubey and Tay (2013) tested the performance of two types of photovoltaic-thermal (PVT) modules. According to the study, the regular PV module's average PV efficiency was roughly 0.4% lower than that of the PV-Thermal modules. Tiba & Beltro (2012) investigated the performance of thin-film and amorphous silicon, polycrystalline silicon, monocrystalline silicon, subjected to Recife and Araripina's environmental conditions. The findings revealed an energy yield decrease of around 4%. In general, it was found that the energy yield decreased with increasing temperature and vice versa. Finally, Kumar *et al.* (2014) conducted a thorough experimental analysis by taking into account the installation, operating performance, and economic aspects of a 20 kWp solar photovoltaic power plant.

The technologies are mainly the different types of solar PV panels like; thin films, monocrystalline, and polycrystalline. So, these are the main technological concerns.

2.5 I-V Curves of Different Solar PV Modules

The photovoltaic properties of a PV module, often known as the I-V curve, are crucial for determining its quality and performance in response to changing environmental factors (Marwan, 2006; Chen *et al.*, 2020). The curve displays the characteristics of the PV module that would allow for maximum efficiency (Dajuma *et al.*, 2016). These factors are essential for constructing any PV system, no matter how big or little

(Dajuma *et al.*, 2016). Therefore, it is crucial to accurately quantify the I-V properties in a real setting (Dajuma *et al.*, 2016).

The efficiency of the module and the capability of solar energy conversion are both described in depth by this curve. The output performance and solar efficiency of the module may thus be determined by understanding the electrical I-V characteristics of the module. The output performance of several PV modules is compared in this study. The trials are carried out under enough sunshine. When a load is applied to a module, the current values that grow with the voltage at each load level are monitored. This method allows for the experimental acquisition of each module's I-V curve. The curves of the modules are then compared to one another.

The modules' performance is displayed and discussed. The findings show that each panel has unique characteristics. Therefore, it is possible to classify the modules using information obtained from the I-V curves of the modules. The current and voltage (I-V) characteristics of a certain photovoltaic (PV) module are represented by curves. The efficiency of the module and the capability of solar energy conversion are both described in depth by this curve. The output performance and solar efficiency of the module may thus be determined by understanding the electrical I-V characteristics of the module. The module's I-V characteristics affect its output performance and solar efficiency.

2.6 Outdoor effects on I–V characteristics

Before being installed in the field, modules are normally assessed indoors under Standard Test Conditions (STC, per IEC TS 61836) (Augusto *et al.*, 2022). Indoor STC measurements are governed by a predetermined irradiance (1000 W m^2), temperature (25°C), and a predetermined AM 1.5G standard spectrum (Dash *et al.*,

2017). STC are designed to give a fair baseline for useful comparison in the industry, not to replicate the precise range of conditions that modules encounter in the field (Augusto *et al.*, 2022). Although it is difficult to replicate the sun's spectrum, these inside measurements are easier since they are not affected by the fleeting impacts of the outside (Augusto *et al.*, 2022).

Field conditions will have a significant impact on the modules' electrical characteristics (Augusto *et al.*, 2022). As a result, it is essential to measure these factors and comprehend how they affect the performance of the modules because otherwise, it will be impossible to determine whether potential deviations in the performance of the modules are caused by changes in the environmental factors or by the modules themselves (Meral & Dinçer, 2011).

Despite the fact that the solar spectrum outdoors is constantly changing due to factors such as angle of incidence, particulates, and water vapor, among others, AM 1.5G is the only reference spectrum used for interior STC measurements of modules (Fernández-Solas *et al.*, 2021). Module irradiance outside is rarely comparable to the AM 1.5G spectrum utilized for inside STC testing (Augusto *et al.*, 2022). Amorphous silicon modules are more severely impacted by the spectrum variations from the AM 1.5G standard, which directly affects current production (Nofuentes *et al.*, 2014). Because of the variations dependent on the season, hour of the day, and location, the spectral impact on module performance must be understood (Augusto *et al.*, 2022).

The amount of incident light and a module's output current are inversely correlated (Augusto *et al.*, 2022). Therefore, partial shadowing may cause significant interference with performance and outdoor measurements. Some of the causes of partial shadowing include cloud cover, telephone poles, bird droppings, soiling

(Augusto *et al.*, 2022). A solar module's front surface may be covered in soiling, which is a collection of dust, snow, or other particles (Shaju & Chacko, 2018). Due to the limited precipitation and high levels of dust deposition, soiling is essential in desert locations, particularly in northern Africa and the Middle East (Li, Mauzerall & Bergin, 2020).

I-V measurements can be used to assess how much of an impact soiling has, but cleaning can lessen it (Schill, Brachmann & Koehl, 2015). Due to the conventional series architecture of solar modules, shading results in a significant drop in current at the module output (Augusto *et al.*, 2022; Kawamura *et al.*, 2003). When a cell is shaded, the bypass diode for the corresponding string is activated, greatly lowering the current component (or "step" of the I-V curve) (Alonso-Garca, Ruiz, & Chenlo, 2006). A study of the relationship between the electrical properties of crystalline silicon cell diodes and cell temperature was conducted by (Choi *et al.*, 2012). They discovered that the ideality factor rises in the quasi-neutral zone and decreases with cell temperature in the space charge region.

Tsuno *et al.* (2005) used the linear interpolation method to investigate the relationship between the cell temperature and various solar cell characteristics. They found that the physical validity of the linear interpolation for the cell temperature was based on the current-voltage characteristics of the junction p-n. The series resistance of silicon solar cells is shown to vary with cell temperature, according to a study by Sabry & Ghitas (2008). As a result, the temperature of the cell is an important parameter to assess the performance of crystalline silicon solar cells (Dubey *et al.*, 2013).

The expression of current-voltage of a crystalline silicon solar cell as illustrated by Khan *et al.* (2010)

$$I = I_0 \left[\exp \left(\frac{q(V - IR_s)}{nkT} \right) - 1 \right] + \left(V - \frac{IR_s}{R_{sh}} \right) - I_L$$

Here, I_0 stands for reverse saturation current, q for electron charge, n for the diode's ideality factor, T for temperature, k for the Boltzmann constant, R_{sh} for shunt resistance, R_s for series resistance, and I_L for the silicon solar cell's light generation current. Accurate knowledge of the environmental conditions is required to regulate the quality and determine the performances of a solar module. The performance properties of silicon solar modules are constantly influenced by environmental factors.

2.7 Impact of temperature on IV characteristics

Temperature plays an important factor in determining solar cell efficiency because if a site that records high temperatures is being considered, mitigation measures should be included in the selection of PV technology (Zaini *et al.*, 2015)

Temperature plays an important factor in determining solar cell efficiency because if a site that records high temperatures is being considered, mitigation measures should be included in the selection of PV technology (Zaini *et al.*, 2015)

em, it is essential to have data relating to orientation of the plane and inclination to the horizontal of the
The effect of varying the light intensity and temperature on solar modules changes all of their properties, including short-circuit current, open-circuit voltage, fill factor, efficiency, and the effect of series and parallel resistances (Luque & Hegedus, 2003). Studying how temperature and light intensity affect the solar module's output performance is crucial. As a result of changing the electrons' travel speed, temperature alters how electricity moves across an electrical circuit (Karki, 2015). Increasing temperature decreases the open-circuit voltage. This effect simultaneously increases the short-circuit current (Barukcic *et al.*, 2014; Baig *et al.*, 2015). The efficiency of

the photovoltaic energy conversion thus decreases with the increasing temperature (Kara-tepe *et al.*, 2007).

Temperature rises causes a semiconductor's band gap to narrow, which affects the majority of the semiconductor material properties (Dash & Gupta, 2015). The energy of the electrons in the material can be thought of as increasing as the band gap of a semiconductor decreases with temperature (Bisquert, 2020). The open circuit voltage is the element most impacted by temperature changes (Bisquert, 2020). The temperature coefficient calculates the reduction in power output that will occur if the PV module temperature deviates from the STC (Dash & Gupta, 2015). Additionally, different solar cell technologies have different temperature coefficients (Dash & Gupta, 2015).

2.8 Impact of Irradiance on IV characteristics

The same is true for irradiance, with a decrease in sunshine predominantly causing a decrease in current and, as a result, a decrease in power production (Mustafa *et al.*, 2020). Evidently, irradiance significantly affects short-circuit current, which corresponds to the relatively horizontal arm of the I-V curve, whereas the effect on open circuit voltage, which corresponds to the somewhat vertical arm of the curve, is comparatively minor (Chenni *et al.*, 2007). It is evident that a solar cell may produce its greatest amount of power when the irradiance is higher (Chenni *et al.*, 2007).

2.9 Tropical Savannas

Approximately 10% of India and South-East Asia, over half of Africa, Australia, 45% of South America, and close to a third of the world's total area are claimed to be covered by tropical savannas (Phalan *et al.*, 2013). The intensity of the sun in tropical savannas creates an extremely hot environment throughout most of the

year. The average monthly temperature in tropical savannas is 17.7 degrees Celsius (Grace *et al.*, 2006). Tropical savannas experience two seasons per year: the dry season and rain season (Preece, 2002). The savanna climate has a temperature range of (20° - 30° C). In the winter, it is usually about (20° - 25° C) (Laakso *et al.*, 2008). In the summer the temperature ranges from 78° to 86° F (25° - 30° C). In a Savanna the temperature does not change a lot (Laakso *et al.*, 2008). When it does, it's very gradual and not drastic. There is an annual precipitation of 10 to 30 inches (100 to 150 cm) of rain (Kricher, 2011).

2.10 Types of PV Modules

The solar module is the heart of a photovoltaic system. A solar module is created by the manufacturer by wiring several photovoltaic cells together (Godfrey, 2017). Silicon, copper indium selenium, cadmium telluride, gallium arsenide, and copper indium selenide are among the materials frequently utilized to create solar cells (Chu & Chu, 2010). Thin-film solar cells and crystalline solar cells are the two types of solar cells constructed from these materials, respectively (Luceo-Sánchez, Dez-Pascual & Pea, 2019). To produce thin-film solar cells with broad absorption spectrum properties and improved diffuse radiation performance, layers of photovoltaic materials are deposited on a substrate (Lin *et al.*, 2020).

The wavelengths absorbed by the various glass types are what cause the performance variance (Lin *et al.*, 2020). On days with a lot of clouds or little sun energy, thin-film solar cells absorb short-wave blue light whereas crystal solar cells absorb long-wave radiation. Instead of being constructed and joined in lengthy series, thin-film solar cells are made. Hegedus (2006), for instance, said that the main distinction between crystalline and thin-film module technologies is the latter's superior shadow resistance

because of the length of the string. Thin-film photovoltaic modules can function more effectively in environments with lower light levels, such as those with shadow, clouds, or gloomy weather (Wu *et al.*, 2010). Zhou *et al.* (2018) claimed that by modifying the absorption spectra to correspond to the broad frequency range of sunlight, thin-film solar cells perform better at low light intensities (Lin *et al.*, 2020). Additionally, compared to crystal modules, thin-film modules are adjusted to absorb a wider spectrum of infrared wavelengths, resulting in a higher output at low light intensities (Lin *et al.*, 2020). Single crystal, polycrystalline, and ribbon solar cells are all types of crystal solar cells. Amorphous silicon, cadmium telluride, copper indium, selenium, and organic solar cells are examples of thin-film solar cells (Lin *et al.*, 2020).

Crystalline silicon is the most well-established and commonly utilized of the aforementioned PV technologies. With an 80% market share, c-Si leads the PV technology sector, according to Ribeyron (2017). Mono-c-Si stands out for having an organized crystalline structure with all of its atoms arranged in a continuous crystalline lattice. Despite its great efficiency, mono-c-Si is expensive owing to the manufacturing procedures, making it unaffordable for impoverished rural communities who are in desperate need of dependable, clean energy (Reese *et al.*, 2018).

Small grains of mono-c-Si are used to make multi-c-Si PV cells, which are less expensive than mono-c-Si. Sarkeret *et al.* (2018) assert that multi-c-affordability, Si's although having a little lower efficiency, is a result of the less complex manufacturing process. Recombination at the grain boundaries in the multi-c-Si structure is to blame for the decreased efficiency in multi-c-Si PV cells (Sarker *et al.*, 2018). Another

multi-c-Si technology made from multi-c-Si that is appropriate for the solar sector is ribbon silicon. High-temperature resistant wires are pushed through molten silicon during this technology's production process to create a ribbon, which is then cut and processed as usual to create PV cells. This technique has the benefit of having lower manufacturing costs than other c-Si technologies while maintaining the same efficiency and cell quality as other multi-c-Si technologies but at a lower cost than mono-c-Si (Reese *et al.*, 2018).

When compared to their c-Si equivalents, thin-film technologies' key benefit has been their low production costs. Thin-film technologies have developed in a highly encouraging way over the past several years, with the worldwide manufacturing capacity reaching about 3.5GW in 2010 and being predicted to reach between 6-8.5GW in 2012 (Makrides *et al.*, 2010). Some of the most promising thin-film technologies include CdTe, a-Si, micro morph tandem cells (a-Si, c-Si), and CIGS.

Since amorphous silicon has been used in PV technology longer than other thin-film technologies, researchers and producers have had more time to study the material's behavior. Since its first commercialization in the early 1980s, this technology has continuously become more efficient (Ngeno *et al.*, 2018). Plasma-enhanced chemical vapor deposition is one of the most common deposition methods used in the production of a-Si technology (PECVD). As a result, flexible and affordable substrates like thin foil polymer and stainless steel may be employed in huge spaces.

Amorphous silicon PV cells lack the crystalline order of mono-c-Si, which results in dangling bonds that significantly affect the material's characteristics and behavior. Due to the Staebler-Wronski phenomenon, which causes this technology to degrade when exposed to light, there is still another crucial material constraint (SWE). The

first performance drop that occurs when a-Si modules are initially exposed to light is described by SWE (Agroui *et al.*, 2011). Using double- or triple-junction devices and creating micro morph tandem cells, a hybrid c-Si and a-Si technology, has generally reduced the impact. The high absorption coefficient of a-Si, which is around ten times greater than that of c-Si and leads to significantly thinner cells, is a key benefit. To increase the stability of a-Si tandem cells, the idea of micro morph (micro crystalline/amorphous silicon) tandem cells was presented. The placement of a micro-crystalline silicon (c-Si) layer of the order of 2 μm onto the substrate has optimized the structure of the micro morph device's a-Si cell.

By helping the device boost its absorption in the red and near infrared portions of the light spectrum, the application of the c-Si layer can increase efficiency by up to 10%. CdTe, a group II-VI semiconductor with a direct band gap of 1.45 eV, is another sort of thin-film technology. Due to the high optical absorption co-efficient of this technology, which absorbs over 90% of the available photons in a layer with a thickness of 1 μm , thin-film solar cells only require sheets between 1-3 μm thick. Thin-film PV technologies that can be made reasonably cheaply and with high module efficiencies, like CdTe, are leading the pack. The efficiency of this technique has so far been higher than triple-junction a-Si but lower than c-Si. Additionally, the CdTe PV technology does not initially degrade like a-Si does. In contrast to c-Si-based technology, temperature fluctuations do not have the same impact on the power.

Table 2.1: PV Module Characteristics

Technology	Material Thickness (mm)	Area (m^2)	Efficiency (%)	Surface area for 1KWp system (m^2)
Mono-c-Si	200	1.4-1.7 (typical)	14-20	>>7
Multi-c-Si	160	1.4-1.7	11-15	>>8

		(typical)		
A-Si	1	1.5	4-8	>>15
A-Si/m c-Si	2	1.4	7-9	>>12
CdTe	>>1-3	>>0.6-1	10-11	>>10
CIGS	>>2	>>0.6-1	7-12	>>10

Source: Makrides *et al.*, 2010

2.11 Factors affecting Power Output of Solar Photovoltaic Modules

Several things influence power output. Opiyo (2015) claims that elements including sun irradiation, shadowing, and solar cell temperature affect the general effectiveness/power output of solar PV modules.

2.11.1 Temperature

Due to higher internal carrier recombination rates brought on by higher carrier concentrations, the performance of solar cells diminishes with temperature (WCE, 2018). An important factor in the photovoltaic conversion process is the operating temperature (WCE, 2018). Only up to 20% of the incident solar energy from the radiation hitting a PV panel is transformed into electricity (Zhang *et al.*, 2014). The majority of what is left is transformed into heat. As a result, the operational temperature of the PV panel rises due to the stored heat energy, which lowers its electrical efficiency (Amelia *et al.*, 2016). Solar cells are susceptible to temperature changes, much like any other semiconductor technology (Sani & sule, 2020). Most of the characteristics of semiconductor materials are impacted by a semiconductor's band gap, which is decreased as temperature rises (Sani & sule, 2020).

It is possible to interpret the narrowing of a semiconductor's band gap with rising temperature as an increase in the energy of the material's electrons (Sani & sule, 2020). Thus, a solar cell's band gap is reduced when temperature rises; the open-circuit voltage is the characteristic that is most impacted (Sani & sule, 2020). As a

result, the solar module's output power and efficiency were decreased. According to El- Amin & Al-Maghrabi (2018), the operating temperature is crucial to the PV conversion process. A crystalline PV module's performance and power production are both influenced by the operating temperature. They also noted that solar cells change as a result of temperature variations, and that these changes have an impact on the power production of the cells.

According to Dubey *et al.* (2013), PV modules that are less sensitive to temperature are best for high-temperature locations, whereas those that are more sensitive to temperature will perform better in low-temperature regions. Operators must thus take into account the geographic distribution of photovoltaic energy potential, taking into account the impact of irradiance and ambient temperature on the performance of PV systems. Additionally, Chikate & Sadawarte (2015) discovered a clear correlation between the solar parameter and the efficiency of solar modules. Consequently, changes in solar parameters have an impact on the solar module's efficiency. They discovered that the irradiance and temperature are the two most important solar cell working state factors.

However, Charfi *et al.* (2018) have noted that one of the primary drawbacks of this technology continues to be the impact of solar cell temperature on the performance and longevity of photovoltaic panels. A linear relationship between output power and ambient temperature was discovered by Sanusi *et al.* (2011) after three years of studying the impact of ambient temperature on PV modules.

2.11.2 Solar irradiance

The power density of sunlight or the total amount of power from all radiant sources falling on a given area is measured by irradiance (Ibrahim, Gyukand Aliyu, 2019).

The irradiance that Earth receives from the sun via the atmosphere is the solar constant for Earth (Karim *et al.*, 2011). On a clear day, the average solar spectrum's total irradiance on the earth's surface is 1 kW/m² (Zaharim *et al.*, 2009). However, because of the rotation of the globe and the weather, the available irradiance is often much lower than 1 kW/m² (Ibrahim, Gyuk & Aliyu, 2019). For instance, irradiance is higher on sunny days than it is on cloudy days. When clouds are absent, direct sun radiation is not hindered; resulting in higher irradiance and combining dazzling light and radiant heat (Ibrahim *et al.*, 2019). The output of PV modules has been discovered to be impacted by solar irradiation. According to Buni *et al.* (2018), solar irradiance and the output current of PV modules are directly related. On the other hand, Rani *et al.* (2018) found that the power of PV modules fluctuates with solar irradiance because solar panels don't always convert light into electricity at a rate of 40 percent, while most PV panels do so at a rate of 15 to 18 percent. The PV energy conversion systems must thus run close to the maximum power point in order to maximize the output efficiency of PV (MPP).

2.12 Performance Parameters of PV module

The open-circuit voltage (V_{oc}), short-circuit current (I_{sc}), maximum voltage (v_{max}), maximum current (I_{max}), full power (p_{max}), conversion efficiency (η), and fill factor are the electrical characteristics of a PV device (FF). Some of these metrics are measured by manufacturers under regular test circumstances (STC). Only a small portion of solar radiation is converted into electrical energy by solar cells. Instead, the extra incident energy is converted to heat and released into the silicon solar cell's main body, raising its temperature above ambient levels. For a given irradiance, a solar cell's short circuit current (I_{sc}) increases as its working temperature rises because a smaller band gap allows for more energy absorption.

The band gap energy $E_g(T)$ of the material as a function of temperature can be written as equation (a);

$$E_g(T) = E_g(0) - \frac{\alpha T^2}{T + b} \quad (2.1)$$

Where $E_g(0)$ is the band gap energy of the material at room temperature, a and b are constants.

This effect alone raises the theoretical maximum output power of the solar cell. At the same time an increase in the temperature increases the population of electrons exponentially. This enhances the dark saturation current (I_0) that is a minority carrier current, and its variation with temperature can be written in equation (b);

$$I_0 = A T_0^3 e^{\left(\frac{-E_g}{K_B T}\right)} \quad (2.2)$$

Where A_0 and K_B are the areas of the device and Boltzmann's constant. The increase in the dark saturated current decreases the open-circuit voltage (V_{oc}) of the device that is expressed in equation (c);

$$V_{oc} = \frac{K_B T}{e} \ln\left(\frac{I_{sc}}{I_0} + 1\right) \quad (2.3)$$

Theoretically, a decrease in the open-circuit voltage would reduce the device's output power. The short circuit current and the open circuit Voltage are related to an essential property of a PV device known as the fill factor (FF) which is defined as the ratio of the maximum power of the PV device to the product of I_{sc} and V_{oc} as indicated in equation (d)

$$FF = \frac{V_{max} I_{max}}{V_{oc} I_{sc}} \quad (2.4)$$

The fill factor diminishes as the temperature of the device is increased. The decrease in Voc and fill factor (FF) with the working temperature of the device outweighs the slight increase in the short circuit current.

Jefari *et al.* (2011) reported that Solar cell's performance parameters vary due to temperature changes. The temperature change will affect the power output from the cells. The voltage is highly dependent on the temperature, and an increase in temperature will decrease the voltage. When the module's temperature rises from 10°C to 70°C, its short-circuit current slightly declines but its open-circuit voltage considerably drops from 25V to 18V (Jefari *et al.*, 2011). In accordance with Jefari *et al.* (2011), the photovoltaic cell (PV) does not produce power from more than 80% of the solar radiation that reaches it. It is either refracted or converted into heat energy. The heat produced raises the temperature of the cell, which lowers the cell's conversion efficiency. As a result, the cell's output power drastically declines as the cell's temperature rises.

The performance of two PV modules—one polycrystalline and the other amorphous—was assessed by Cornaro and Musella (2010) over a medium-term exposure at an ideal tilt angle, along with a thorough assessment of the weather. The polycrystalline module's average performance ratio (P.R.) of 0.88 revealed that it was very stable. Due to the influence of temperature on module performance, a seasonal trend in the monthly performance was seen. The Staebler-Wronski degradation effect caused the amorphous silicon module to degrade in the first few months of operation.

2.13 PV Outdoor and Standard Test Conditions (STC)

PV cells are prone to electrical deterioration, much like all other semi-conducting materials. PV cells are subjected to temperature fluctuations between 10 and 50

degrees Celsius. Temperature affects the solar cells' performance, efficiency, and output characteristics (Singh *et al.*, 2011). It is difficult to produce measurement circumstances that are equal to standard test standards (STC), which include irradiation intensity of 1000 W/m², module temperature of 25°C, and air mass of 1.5 for assessing PV performances in outdoor working conditions for practical usage (Singh *et al.*, 2011). Carr (2005) studied PV modules made of various technologies and the effects they had on Australian PV system design techniques. The trials showed that the STC values claimed by the PV module manufacturers did not always correspond to those found in STC measurements.

Malik *et al.* (2010) investigated how the environment of Brunei affected how well photovoltaic polycrystalline silicon modules performed. Data for I-V was gathered twice every week. Additionally, studies on the effects of temporal variation on the electrical performance of the devices were conducted. This included looking at variations in solar radiation intensity and its distribution across different components, including direct, diffused, and global radiation, as well as ambient and working temperatures. In accordance with the findings, polycrystalline modules performed well under low irradiance. Last but not least, Siddiqui *et al.* (2014) examined polycrystalline silicon PV modules in both indoor and outdoor circumstances. The findings demonstrated that STC values claimed by manufacturers for their multi-crystalline silicon photovoltaic modules may not always correspond to actual STC measurements.

2.14 Degradation of PV Modules

PV modules depend on packaging materials including protective superstrate, substrate, sealants, and encapsulants to offer the necessary dependability for them to survive in challenging working environments. For a PV module to be successful

commercially, a number of important reliability-related features are essential. Low moisture permeability via all packaging materials, Adequate adhesion of encapsulants to substrate, superstrate, and PV cells, Adequate adhesion of encapsulants to all working conditions, and Good mechanical qualities such as tensile elongation and creep resistance. Therefore, it is crucial to look at how polymeric materials used in PV modules change over time or degrade, as well as the relationship between material degradation and field failures of PV module systems. Ethan & Edwin (2012) claim that the breakdown of packing materials under a variety of conditions, including as heat, moisture, and UV, can result in PV modules failing. Additionally, according to Rong *et al.* (2011), the external weather conditions where solar photovoltaic modules are used are related to their deterioration.

The effectiveness of indoor and outdoor photovoltaic modules based on thin-film solar cells was assessed by Agroui *et al.* in 2011. The experiments revealed that the STC values manufacturers claimed for their amorphous modules did not correspond to those found in STC measurements. The Staebler-Wronski effect on the amorphous silicon material caused the modules to disintegrate during the first 8–10 weeks of exposure. Snail trails were used by Yang *et al.* (2018) to evaluate the power degradation and dependability of crystalline silicon solar modules. According to the findings, snail trails have no impact on the long-term dependability and longevity of solar modules. According to a Duke *et al.* (2010) survey, just 9% of Kenyan customers of PV modules believe they are familiar with the brand. The dependability of their PV modules is unknown to more than 40% of the responders.

2.15 Data Logger operations theory

A data logger is an electronic device that captures data over time or about location using either an internal instrument or sensor or external instruments and sensors (also

known as a data recorder or data logger). They are based on a digital processor, but not totally (or computer). They often come with a microprocessor, internal memory for data storage, sensors, and are compact, battery-powered, portable devices. Some data recorders connect to a computer through a software program, which is used to turn on the data logger and display and analyze the data it has gathered. Others, on the other hand, have a local interface device and can function as a standalone device (keypad, LCD).

Data loggers range from general-purpose models for a wide range of measurement applications to specialized models for only one environment or application type. Although it is usual for general-purpose types to be programmable, many still function as static machines with few or no adjustable settings. In many applications, electronic data loggers have taken the position of chart recorders.

The automated 24-hour collection of data is one of the main advantages of employing data loggers. Data loggers are normally activated, deployed, and unattended while they gather data for the monitoring time. This enabled the monitoring of environmental variables like solar irradiance and temperature to provide a complete and accurate picture.

2.16 Microprocessor Based Data Logger

This employs an embedded system for system monitoring; it consists of an Arduino board with a microcontroller unit (the system's brain), sensors for temperature, and light as well as an LCD for local monitoring and GSM for distant monitoring.

2.17 Microcontroller Units ATMEGA328

The ATmega328 is a single-chip microcontroller created by Atmel in the mega AVR family (later Microchip Technology acquired Atmel in 2016). It has a modified Harvard architecture 8-bit RISC processor core.

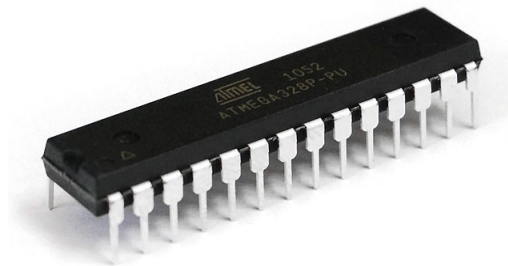


Figure 2.3 MCU ATMEGA 328

Specifications

The Atmel 8-bit AVR RISC-based microcontroller includes a byte-oriented 2-wire serial interface, SPI serial port, 6-channel 10-bit A/D converter (8-channels in TQFP and QFN/MLF packages) Ojha *et al.* (2016), programmable watchdog timer, 1 KB EEPROM, 2 KB SRAM, 23 general-purpose I/O lines, 32 general-purpose working registers Jain, Rawat & Morbale (2017), three flexible timer/counters with compare modes, internal and external interrupts, and the gadget runs on 1.8 to 5.5 volts. The system's throughput is close to 1 MIPS per MHz (Jain *et al.*, 2017).

Table 2.2: MCU Key Parameters

Parameter	Value
CPU Type	8-bit AVR
Performance	20 MIPS at 20 MHz
Flash Memory	32KB
SRAM	2KB
EEPROM	1KB
Pin count	28 or 32 pin: PDIP-28, MLF-28, TQFP-32, MLF-32
Maximum operating frequency	20MHz
Number of touch channels	15

Hardware QTouch Acquisition	No
Number of I/O Pins	23
External interrupts	2
USB interface	No
USB Speed	-

Series alternatives

A common alternative to the ATmega328 is the "picoPower" ATmega328P. A

- ATmega328
- ATmega328P and ATmega328P-AUTOMOTIVE
- ATmega328PB and ATmega328PB-AUTOMOTIVE (superset of ATmega328P)

It has more UART, I2C and SPI Interfaces than ATmega328P

Applications

As of 2013, the ATmega328 is frequently employed in several projects and autonomous systems that need for a straightforward, inexpensive micro-controller. The Arduino Uno and Arduino Nano versions, which are part of the well-known Arduino programming platform, may be where this chip is used the most frequently.

Programming

Reliability qualification shows that the projected data retention failure rate is much less than 1 PPM over 20 years at 85 °C or 100 years at 25 °C.

Table 2.3: Program Parallel Mode

Programming signal	Pin Name	I/O	Function
RDY/BSY	PD1	O	High means the MCU is ready for a new command, otherwise busy.
OE	PD2	I	Output Enable (Active low)
WR	PD3	I	Write Pulse (Active low)
BS1	PD4	I	Byte Select 1 ("0" = Low byte, "1" = High byte)

XA0	PD5	I	XTAL Action bit 0
XA1	PD6	I	XTAL Action bit 1
PAGEL	PD7	I	Program memory and EEPROM Data Page Load
BS2	PC2	I	Byte Select 2 (“0” = Low byte, “1” = 2nd High byte)
DATA	PC[1:0]:PB[5:0]	I/O	Bi-directional data bus (Output when OE is low)

The programming model is entered when PAGEL (PD7), XA1 (PD6), XA0 (PD5), BS1 (PD4) is set to zero (Khodzhaev, 2016). RESET pin to 0V and VCC to 0V. VCC is set to 4.5 - 5.5V. Wait 60 μ s, and RESET is set to 11.5 - 12.5 V. Wait for more than 310 μ s (Khodzhaev, 2016). Set XA1:XA0:BS1:DATA = 100 1000 0000, pulse XTAL1 for at least 150 ns, pulse WR to zero (Khodzhaev, 2016). This starts the Chip Erase. Wait until RDY/BSY (PD1) goes high. XA1:XA0:BS1:DATA = 100 0001 0000, XTAL1 pulse, pulse WR to zero. This is the Flash write command.

Table 2.4: Serial Programming

Symbol	Pins	I/O	Description
MOSI	PB3	I	Serial data in
MISO	PB4	O	Serial Data out
SCK	PB5	I	Serial Clock

Serial data to the MCU is clocked on the rising edge, and data from the MCU is clocked on the falling edge. Power is applied to VCC while RESET and SCK are set to zero. After at least 20 minutes, the Programming Enabled serial instruction 0xAC, 0x53, 0x00, 0x00 to be sent to the MOSI pin. The second byte (0x53) will be echoed back by the MCU.

2.18 Network Operator Requirements

A Subscriber Identity Module (SIM) card, a GSM-compliant equipment like the GSM shield, and a subscription with a mobile phone operator (prepaid or contract) in order to access a network is needed. The SIM card was provided by the network provider and contains data like the mobile number. A Connection Point Name (APN) and a

username/password from the network operator is needed in order to utilize GPRS for internet access and for the Arduino to request or deliver websites (Nagarjun, 2019).



Figure 2.4: Arduino communication shield

Sketches to the board are uploaded by connecting to the computer with a USB cable and upload sketch with the Arduino IDE (Monk, 2016). Once the sketch has been uploaded, the board can be disconnected and the computer powered with an external power supply (Pan & Zhu, 2018).

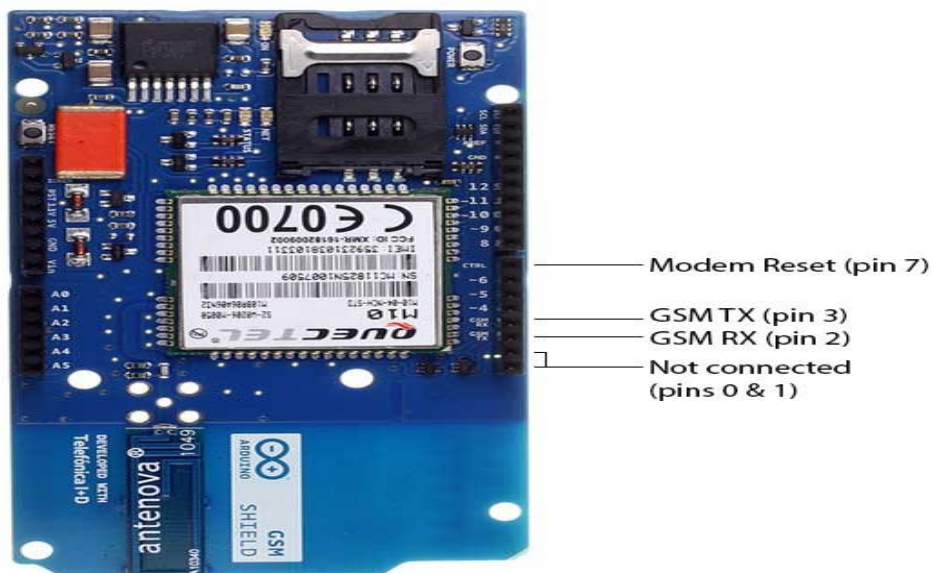


Figure 2.5: Digital pins

On pins 2 and 3, the Software Serial library handles communication between the modem and Arduino. For modem reset, pin number seven was used. The modem is

switched on when the yellow status LED illuminates, this is the point connection to the network is done. For the modem to be switched on in developer versions of the GSM shield, the Power button is held down for a while. A jumper might be connected to the CTRL/D7 pad on the back of the board if the protection is an early model and it doesn't switch on automatically.

Knowledge Gap

In Kenya several studies have been done on solar photovoltaic; Duke *et al.* (2002) looked at Photovoltaic module quality in the Kenyan solar home systems market, Gatakaa (2010) researched on performance evaluation of silicon-based photovoltaic modules found in the Kenyan market, Otakwa (2012) sought to understand the performance and characterization of a dye-sensitized photovoltaic module under tropical weather conditions in Nairobi. Choge (2015) did analysis of wind and solar energy potential in Eldoret, Kenya while Muok *et al.* (2015) solar pv for enhancing electricity access in Kenya

Further, Oloo *et al.* (2015) did a study on spatial modelling of solar energy potential in Kenya on the same Opiyo (2015) also work on modelling of PV-based communal grids potential for rural western Kenya. More recently, Hansen (2018) worked on a case study about off-grid solar PV in rural Kenya, Biwott (2018) assessing the solar energy resource potential in Trans-Nzoia County for decentralized domestic power generation, Ngeno *et al.* (2018) looked at opportunities for transition to clean household energy in Kenya: application of the household energy assessment rapid tool and Musanga *et al.* (2018) studied the effect of irradiance and temperature on the performance of monocrystalline silicon solar module in Kakamega.

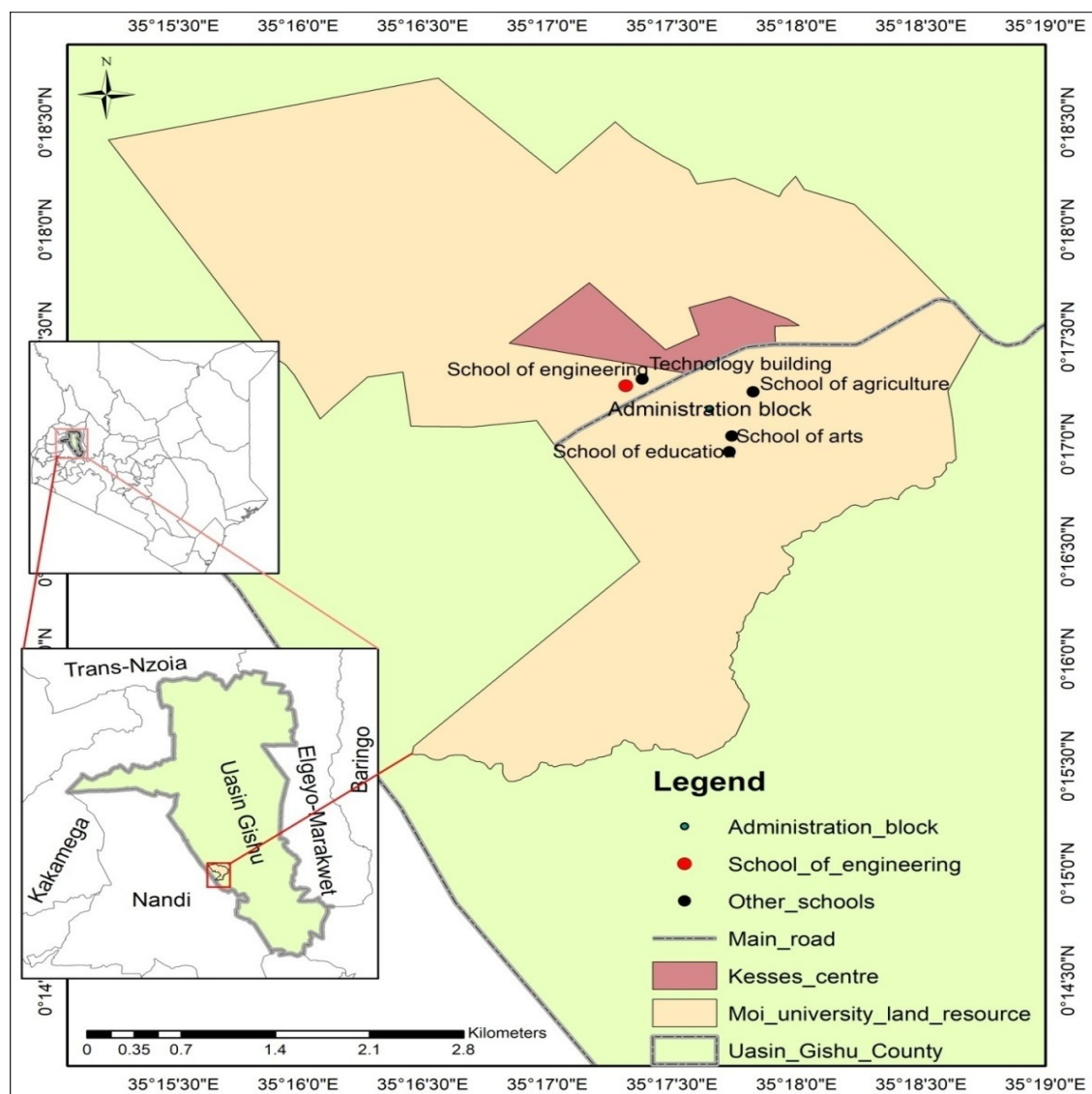
Finally, Korir (2020) assessed factors Affecting Consumer Adoption of Solar Energy Technology in Uasin Gishu County in Kenya , Njoku *et al.* (2020) investigated the typical performance reductions in PV modules subject to soiling in a tropical climate, Muchiri *et al.* (2021) looked at solar pv potential and energy demand assessment in machakos county, .Mwende (2021) assessed the photovoltaic (pv) system performance forecasting and modelling using real-time observation and weather data and Kidegho (2022) did a study on hybrid solar photovoltaic and thermoelectric energy generation in the Lake Victoria environment.

From the literature cited only Musanga *et al.* (2018) who studied the effect of irradiance and temperature on the performance of monocrystalline silicon solar module in Kakamega and Njoku *et al.* (2020) who investigated the typical performance reductions in PV modules subject to soiling in a tropical climate who have done their research on solar photovoltaic but tackled different variables. Musanga *et al.* (2018) dealt with only monocrystalline though they researched on effect of irradiance and temperature while Njoku *et al.* (2020) studied performance reductions in PV modules subject to soiling in a tropical climate. The gap of knowledge which the current research has filled is by successfully studying photovoltaic module performance under tropical savannah climatic conditions of Uasin Gishu for both monocrystalline and polycrystalline modules.

CHAPTER THREE: METHODOLOGY

3.1 Introduction

The study used a mixed approach (qualitative and quantitative) to conduct the research on solar PV module performance analysis. The quantitative approach was used to choose the parameters to be studied and the appropriate tools for the analysis, while the qualitative approach established the prevailing parameters and how each parameter varies the performance of different solar PV modules.



Moi University coordinates 0.2861° N, 35.2943° E

Figure 3.6 : Map of the study Area (Source: Author, 2022)

According to the Uasin Gishu County profile report 2013 from the Office of the Governor, the county's total area is 3327.8 Km² with arable land covering 2603.2 Km² and non-arable ground covering 682.6 Km² (Murgor, 2015). The County extends between longitude 34° 50' and 35 ° 37' east and 0° 03' and 0° 55' north (Murgor, 2015). It shares common borders with Trans Nzoia County to the North, the Marakwet and Keiyo County to the East, Baringo County to the southeast, Kericho County to the South, and Nandi County to the West 96 and Lugari Sub-County to the North West (Murgor, 2015). The County, divided into six sub-counties, has the following sizes in terms of land distribution:-Kapsaret 400 Km², Ainabkoi 383 Km², Kesses 611 Km², Soy 762 Km², Turbo 324 Km² and Moiben 738 Km² (GoK, 2008).

3.1 Research Design,

The project's design made use of sensors to monitor on the weather and electricity sensors to monitor the voltage and current from the solar PV modules.

3.2 Data Source

The data sources were from; solar PV module manufacturer and from an experimental set-up at Moi University

3.3 Data Collection Technique

Most of the data were recorded on the memory card in the data logger and then transferred to Ms-Excel. Others from the open-source were downloaded and stored in the computer, and photographing the required areas were collected from archives. The data collected from the experimental set was collected through datalogging andGMS communication.

3.4 Reliability and Validity

To ensure the reliability on the data, the researcher compared data from different sources and considered the system simulation results with experimental results. The GSM data was stored in a secure gadget for future use.

3.5 Sampling Technique

The sample period for the weather conditions was from November 2020 to March 2021, and the researcher needed 118 days to gather and evaluate the data. The researcher took into account the outcomes of two modules' manufacturer tests for the solar PV model.

Data logging is the collection of data over a period of time and is something often used in scientific experiments. Data logging systems typically monitor a process using sensors linked to a computer.

The transceiver is a device that can both transmit and receive communications, in particular, a combined radio transmitter and receiver

3.6 Data Analysis and Interpretation

Ms-Programs (excel) was utilized for the analysis, and MATLAB was then used to model and simulate the data. One of the first programs for resolving mathematical equations and models in mathematical techniques was Mat lab. As a result, it is excellent software that provides a vast array of options for dealing with a variety of problems in a real-time system.

Table 3.5: Specification and orientation parameters

	Module 1: Mono-Crystalline	Module 2: Poly-Crystalline
Out Peak Power (W)	100	100
Open Circuit Voltage (V)	21	22.5
Short Circuit Current (A)	6.4	6.18
Max.Power Voltage (V)	18	18
Max.Power Current (A)	5.71	5.56

The angle of inclination was 33°C

The conceptual knowledge was used in the built-up data logger for the experiment set-up, with the meteorological sensors, electrical, and remote communication. The set-up had a solar PV module powering the given load. The current and voltage was monitored simultaneously with the meteorological conditions and communicated through the GSM module to the remote monitor every 30 minutes from 7:00am to 6:00pm for five months; November 2020 to march 2021. This was the period that the researcher was ready to begin the experimental study.

3.7 Conceptual Framework

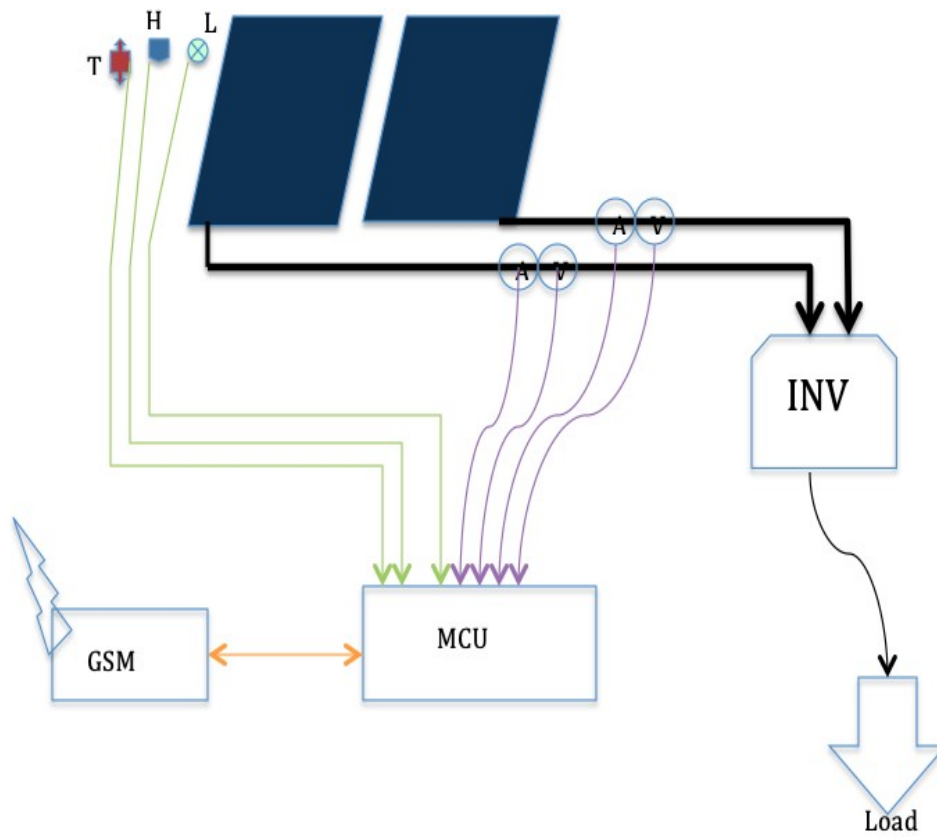


Figure 3.7: Conceptual Framework

Table 3.6: Conceptual Framework Key

T	Temperature Sensor
L	Light Sensor
A	Ammeter
V	Voltage
INV	Inverter
MCU	Microcontroller

3.8 Data logger system set-up

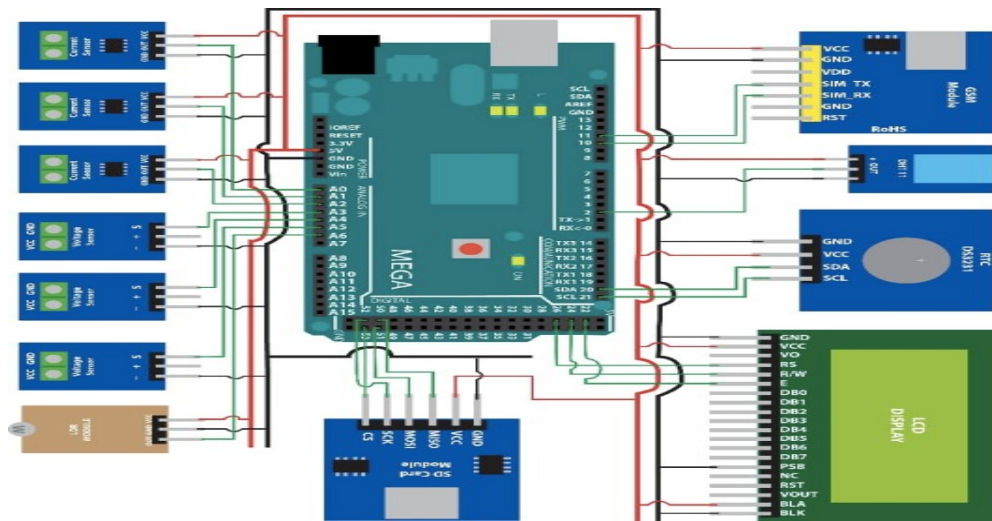


Figure 3.8: Data logger schematics

The logger was delicate and very sensitive to power and meteorological parameters variations. The logger could store the data in the card then the researcher could later read. The logger also was able to send an alert message that enabled the researcher to confirm its operations

3.9 Experiment setup

The study of the performance of solar PV modules used this solar modules, 100W monocrystalline and 100W polycrystalline setup as shown below on the roof top at Moi University (0.2861° N, and 35.2943° E) that were inclined at 33° to the roof.



Figure 3.9: PV panels on the clear roof

Fig 3.5 shows the setup of data logger connected to the modules using cables used to collect, store data on its memory card and send part of it to the cell phone of the researcher; batteries for power storage in the laboratory at Moi University designed for the study.



Figure 3.10: Data logger and batteries (storage)

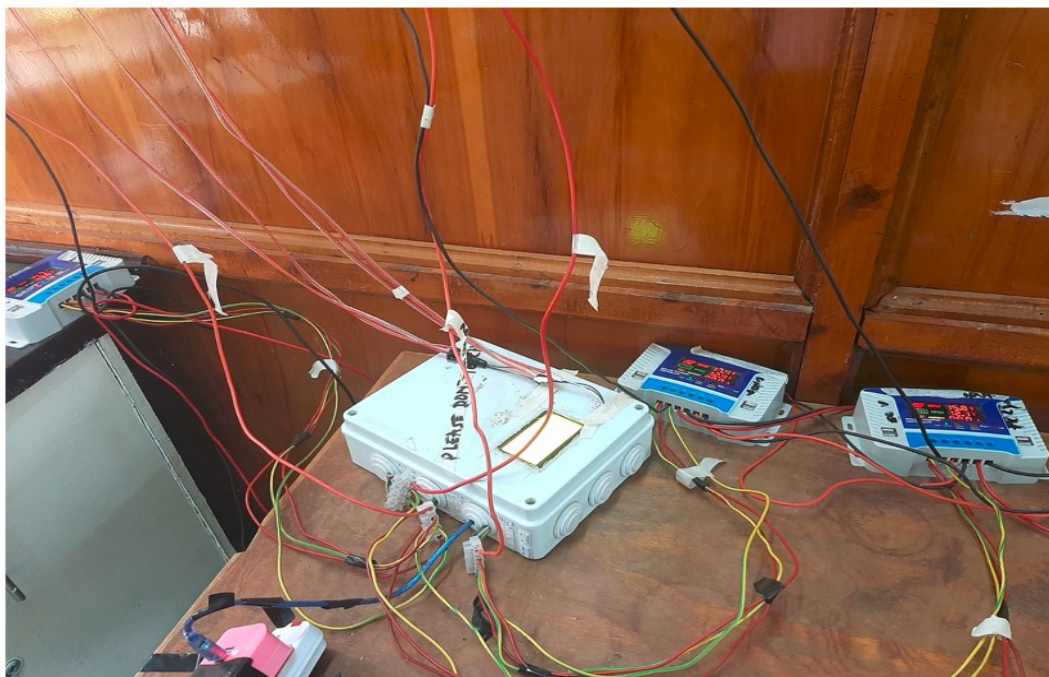


Figure 3.11: Data logger and charge controllers.

The figure (3.6) above shows the data logger and charge controllers used to regulate the voltage and current from the modules to prevent overcharging and over discharging of the batteries, both are connected to the modules.

The figure (3.7) below shows inverters, used in the experimental setup that converted current from DC to AC and even monitor and hunt for MPPT to help in maximizing power generated from the solar module; loads used 75 W bulbs.



Figure 3.12: Inverter and load (bulbs)

3.10 Limitation of the study

The study was limited to the study solar photovoltaic module performance under tropical savannah climatic conditions of Uasin-Gishu. The study also assessed the performance of only 100W monocrystalline and 100W polycrystalline modules. Data on temperature and irradiance was recorded for 12hours daily and after every 5 minutes during the study period.

3.11 Assumption of the study

The study assumed that the temperature and irradiance had constant reading throughout the study period. It was assumed that clouds or rain did not affect temperature and irradiance. The effect of humidity and wind, shading from clouds was not considered. All the equipments used during the study period performance to

the optimal level as described by the manufacturer. The apparatus used did not malfunction.

CHAPTER FOUR: RESULTS AND DISCUSSIONS

4.1 Introduction

The chapter presents the findings of the experiments and then brief explanations of the outcomes of the research. The model is that every result follows the discussion and the overall conclusions at the end. The meteorological conditions then considered were the temperature and irradiance.

Table 4.7: Specification of the modules used, angle of inclination 33°

Parameters	Module 1: Mono-Crystalline	Module 2: Poly-Crystalline
Out Peak Power (W)	100	100
Open Circuit Voltage (V)	21	22.5
Short Circuit Current (A)	6.4	6.18
Max.Power Voltage (V)	18	18
Max.Power Current (A)	5.71	5.56

4.2 MEASURED (EXPERIMENTAL) VALUES GRAPHS

4.2.1 Testing parameters for Module 1 for the Period of November 2020 (set one)

A. Temperature readings

From the data collected, the researcher picked the lowest, average, and maximum temperature; this data was collected for 20days for 12hours daily and after every 5 minutes

The minimum, average, and maximum temperatures are:

Temperature range: [13.0, 28.5, 44.0]°C

B. Irradiance readings

From the data collected, the researcher picked the lowest, average, and maximum irradiance; this data was collected for 20days for 12hours daily and after every 5 minutes

The minimum, average, and maximum irradiance are:

Irradiance Range: [675.0, 848.5, 1023.0] W/m²

Parameters for plotting I-V and P-V curves from the data collection for the given period

At constant irradiance

The Mono_voltage: Average, Minimum and Maximum

Mono_Voltage (V) [9.94 0.02 19.23] at 44°C

Mono_Voltage (V) [10.91 0.01 20.43] at 28.5°C

Mono_Voltage (V) [11.71 0.01 21.6] at 13°C

The Mono_Current: Average, Minimum and Maximum

Mono_Current (A) [5.48 0.05 6.22] at 44°C

Mono_Curren (A) [5.40 0.03 6.12] at 28.5°C

Mono_Curren (A) [5.36 0.01 6.02] at 13°C

At constant Temperature

Mono_Voltage (V) [11.11 0.02 20.72] at 1023W/m²

Mono_Voltage (V) [11.00 0.01 20.55] at 848.5W/m²

Mono_Voltage (V) [10.86 0.01 20.38] at 675W/m²

The Mono_Current: Average, Minimum and Maximum

Mono_Current (A) [5.51 0.01 6.25] at 1023W/m²

Mono_Curren (A) [4.53 0.03 5.13] at 848.5 W/m²

Mono_Curren (A) [3.69 0.02 4.19] at 675 W/m²

Table 4.8: Measured parameters for monocrystalline

Parameters for monocrystalline solar PV	Parameters	Units
A_V	10.92	V
V_{min}	0.02	V
V_{max}	20.49	V
I_{min}	0.00	A
I_{max}	5.66	A
I_{sc}	6.40	A
I_{mp}	5.18	A
V_{oc}	21.00	V
V_{mp}	18.48	V

Temp=25 degrees; Monocrystalline (Module 1)

Irradiance= [1023, 848.5, 675]

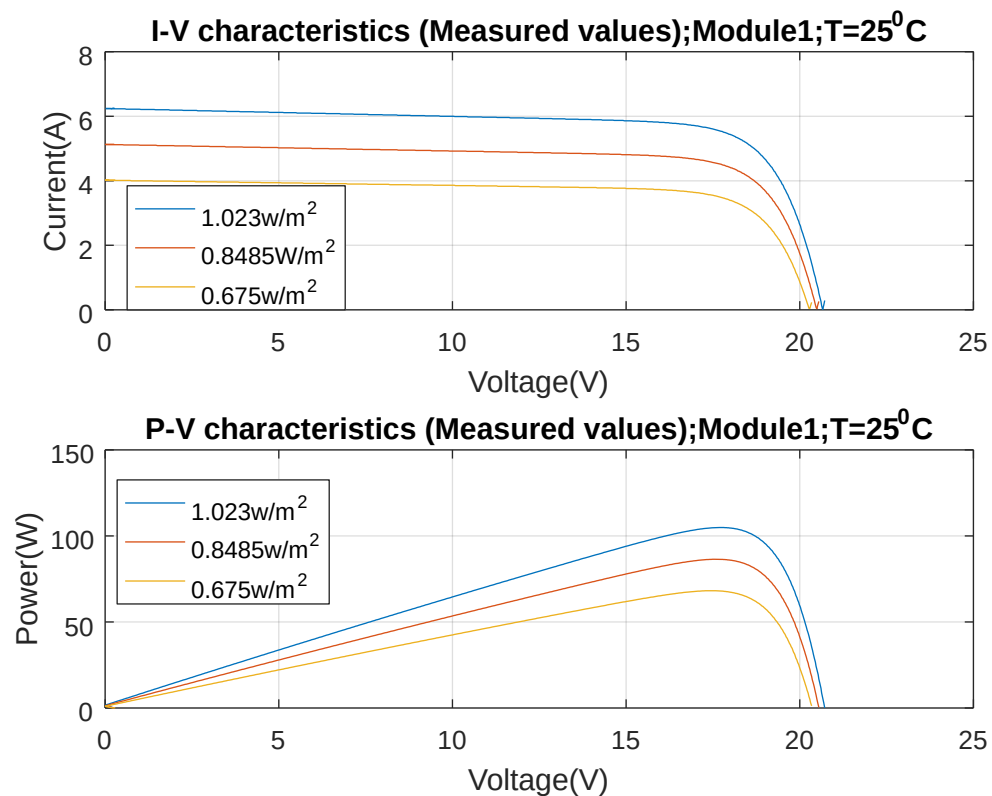


Figure 4.13: I-V and P-V characteristics Module 1 (monocrystalline) Temperature =25°C

From the graph above period of November at constant temperature of 25°C monocrystalline module gave a short circuit current of 6.4A, 5.5A, 4.15A at 1023W/m², 848.5W/m², 675 W/w² respectively. With higher irradiance it was seen that the module still gave a higher power output as compared to lower irradiance levels. P_{max} at irradiance level of 1023W/m², 848.5W/m², 675 W/w² were 109W, 84W, and 72W respectively. The open circuit voltage was least affected by the irradiance level variance which varied within 20V-21V while the short circuit current and power output varied distinctly for the three irradiance levels.

Set1 (Nov2020)

Parameters for plotting I-V and P-V curves from the data collection for the given period

At constant irradiance

The Poly 100W_voltage: Average, Minimum and Maximum

Poly_Voltage (V) [9.87 0.02 20.53] at 44°C

Poly Voltage (V) [10.98 0.02 21.86] at 28.5°C

Poly Voltage (V) [11.78 0.00 23.05] at 13°C

The Ploy100W_Current: Average, Minimum and Maximum

Poly Current (A) [5.20 0.01 5.9] at 44°C

Poly Current (A) [5.24 0.05 5.9] at 28.5°C

Poly Current (A) [5.10 0.06 5.7] at 13°C

At constant Temperature

Poly_Voltage (V) [11.12 0.02 22.12] at 1023W/m²

Poly Voltage (V) [11.12 0.01 21.93] at 848.5W/m²

Poly Voltage (V) [11.07 0.01 21.75] at 675W/m²

The Mono_Current: Average, Minimum and Maximum

Poly Current (A) [5.24 0.01 5.92] at 1023W/m²

Poly Current (A) [4.29 0.03 4.85] at 848.5 W/m²

Poly Current (A) [3.48 0.00 3.94] at 675 W/m²

Table 4.9: Measured parameters for polycrystalline

Parameters for Polycrystalline solar PV	Values	Units
A_V	10.99	V
V_{min}	0.00	V
V_{max}	21.87	V
I_{min}	0.00	A
I_{sc}	6.00	A
I_{max}	5.36	A
V_{oc}	22.00	V
V_{mp}	18.48	V

Temp=25 degrees; Module 2 (polycrystalline)

Irradiance= [1023 848.5 675]

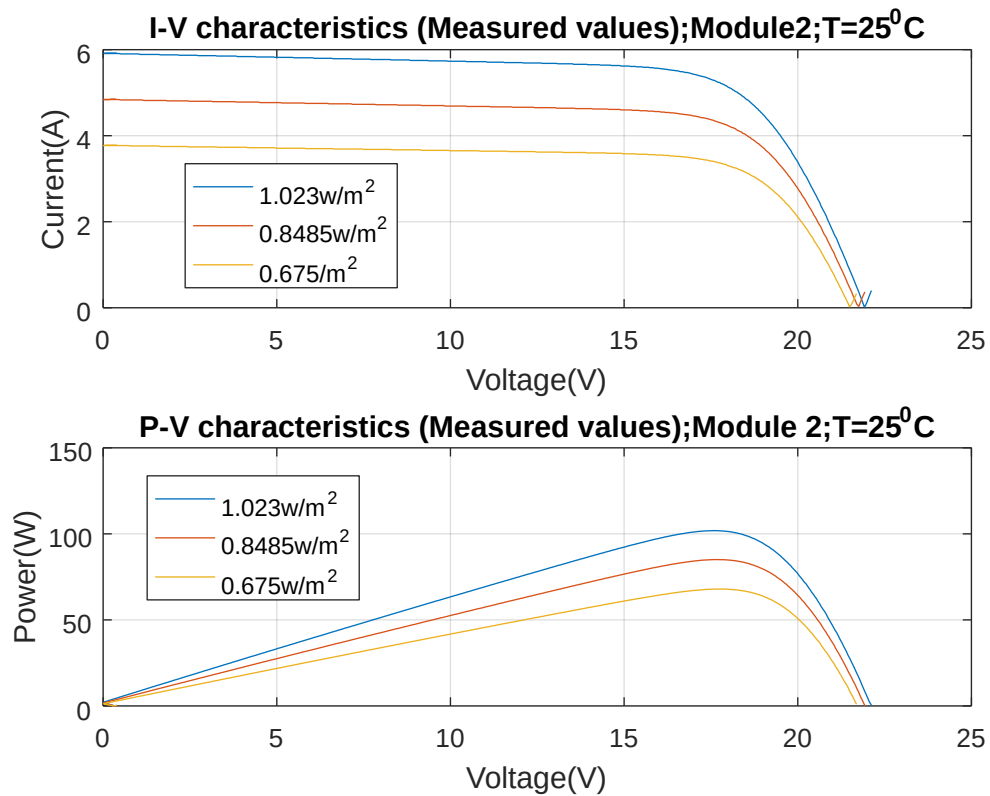


Figure 4.14: I-V and P-V characteristics Module 2 Temperature =25⁰c

As seen in the figure above, at constant temperature of 25°C the polycrystalline module gave an output short circuit current of 5.9 A, 4.8 A, 4.0 A at irradiance level of 1023W/m², 848.5W/m²,675W/m² respectively, the maximum power at this irradiance levels were 100W, 80W, 68W respectively, voltage of this module was still least affected with irradiance level variation. At this irradiance levels the open circuit voltage ranged closely within 22V for the three irradiance levels.

Set1 (Nov2020)

Irradiance=1000W/m²; Module 1

Temp=[44 28.5 13]°C

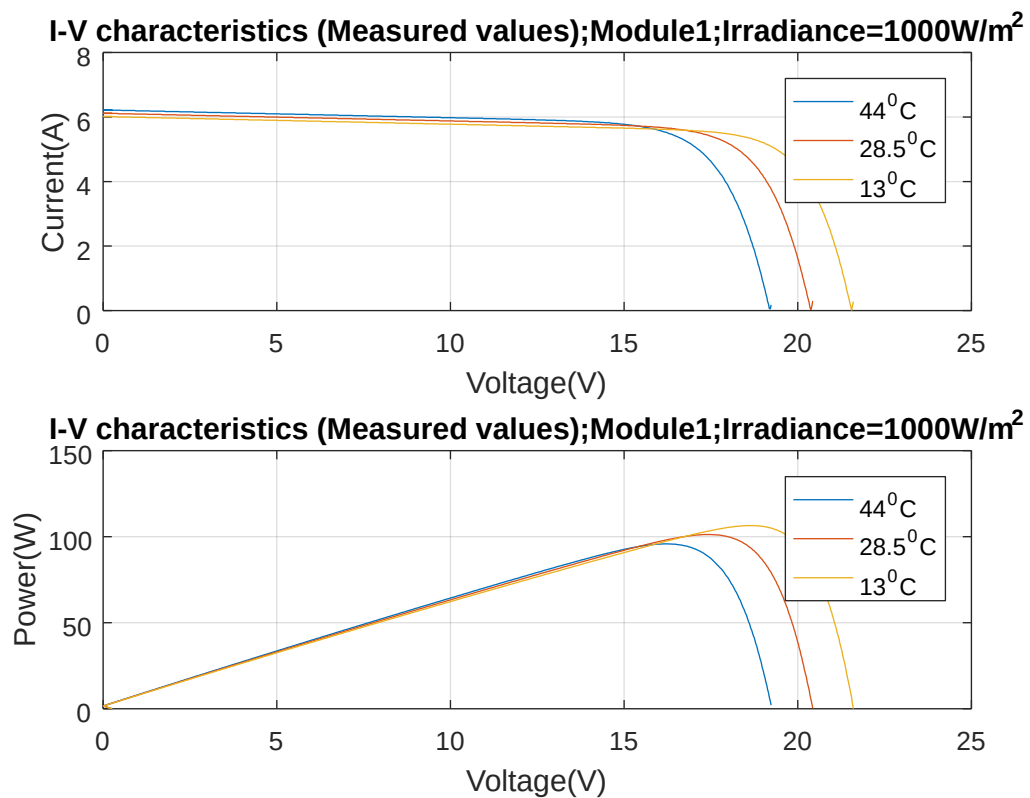


Figure 4.15: I-V and P-V characteristics Module 1 Irradiance =1000W/m²

At constant irradiance of 1000W/m², variation in module temperature on monocrystalline module gave different values of open circuit voltage 19V, 20.5V and 21.8V at 44°C, 28.5°C, and 13°C respectively; there was still power output variation

in these temperatures, 90W, 100W and 109W respectively. At higher temperature there was a slight increase in short circuit current at 44°C it was 6.2A as compared to 6.0 A at 13°C. The outcomes are in line with those of Chitrlekha and Arjadhara (2013)

Irradiance=1000W/m²; polycrystalline (Module 2)

Temp=[44 28.5 13]°C

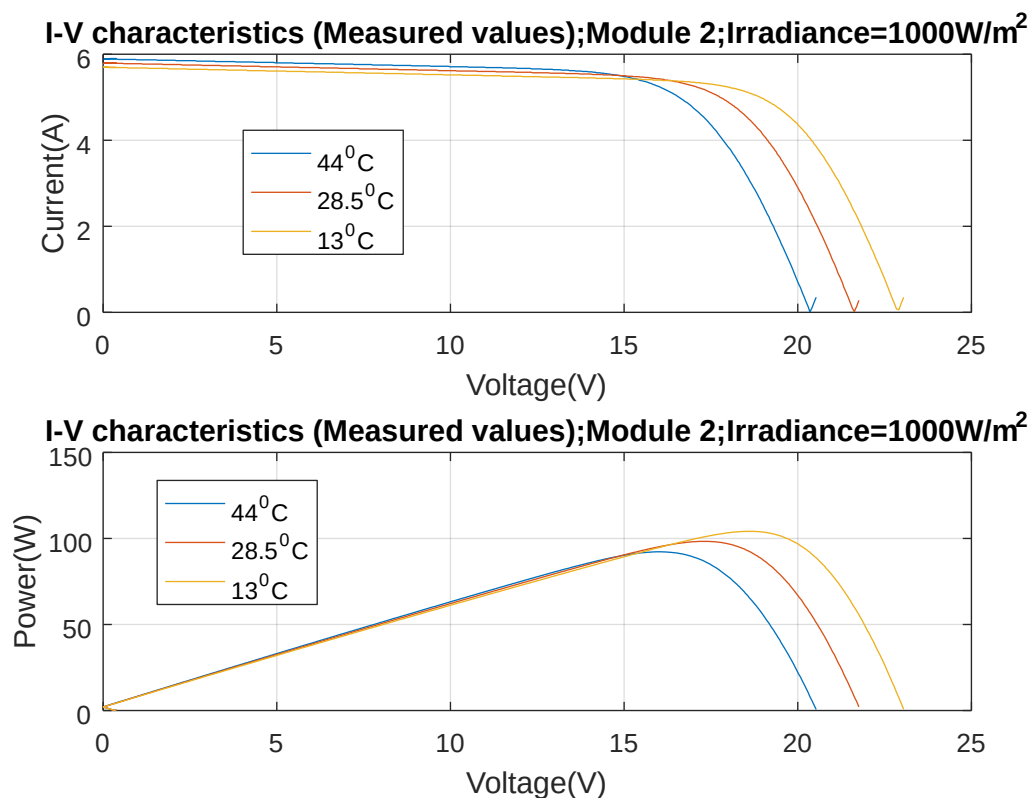


Figure 4.16: I-V and P-V characteristics Module 2 Irradiance =1000W/m²

At constant irradiance of 1000W/m², polycrystalline module's open circuit voltage and maximum power output varied at different temperature levels 20.5V, 21V, 22.6V and 86W, 97W, and 102W, at 44°C, 28.5°C, and 13°C respectively. The findings conformed with those founded by Irwanto *et al.* (2010) where they observed that if the solar irradiance is constant and the temperature increase will cause the open circuit voltage, the maximum power and the efficiency decrease. It also agreed with the

findings of Abdelkader *et al.* (2010), who found out that as ambient temperature raises, the open-circuit voltage decreases in their study of a comparative analysis of the performance of monocrystalline and multicrystalline PV cells in semi-arid climate conditions. The short circuit current for the three temperatures didn't show great variation from each other at 44°C it gave 5.9A while at 13°C it gave 5.7A.

Set2 (JanFeb2021)

Table 4.10: Measured parameters for monocrystalline solar PV

Parameters for monocrystalline solar PV	Values	Units
A_v	10.94	V
V_{min}	0.01	V
V_{max}	20.50	V
I_{min}	0.03	A
I_{max}	5.66	A
I_{sc}	6.30	A
I_{mp}	5.92	A
V_{oc}	23.00	V
V_{mp}	18.48	V

Temp=25 degrees; Monocrystalline (module 1)
Irradiance= [1023 862.5 702]

Figure 4.17:I-V and P-V characteristics of monocrystalline Module Temperature =25°C

From the graph above period of January/February at constant temperature of 25°C monocrystalline module gave a short circuit current of 6.3A, 5.3A, 4.2A at 1023W/m², 862.5 W/m² and 702W/m² respectively. With higher irradiance it was seen that the module still gave a higher power output as compared to lower irradiance levels, similar results by Takyi *et al.* (2021). P_{max} at irradiance level of 1023W/m², 862.5W/m², 702 W/m² were 106W, 85W, and 71W respectively. The open circuit voltage was least affected by the irradiance level variance while the short circuit current and power output varied distinctly. The finding is similar to earlier result by chedid *et al.* (2014) where they found that as irradiance increases, the current

increases greatly while little effect on the voltage, dependence of PV current and voltage on solar irradiance lead to dependence of output power on irradiance too.

Temp=25 degrees; polycrystalline (module 2)

Irradiance=[1023 848.5 701]

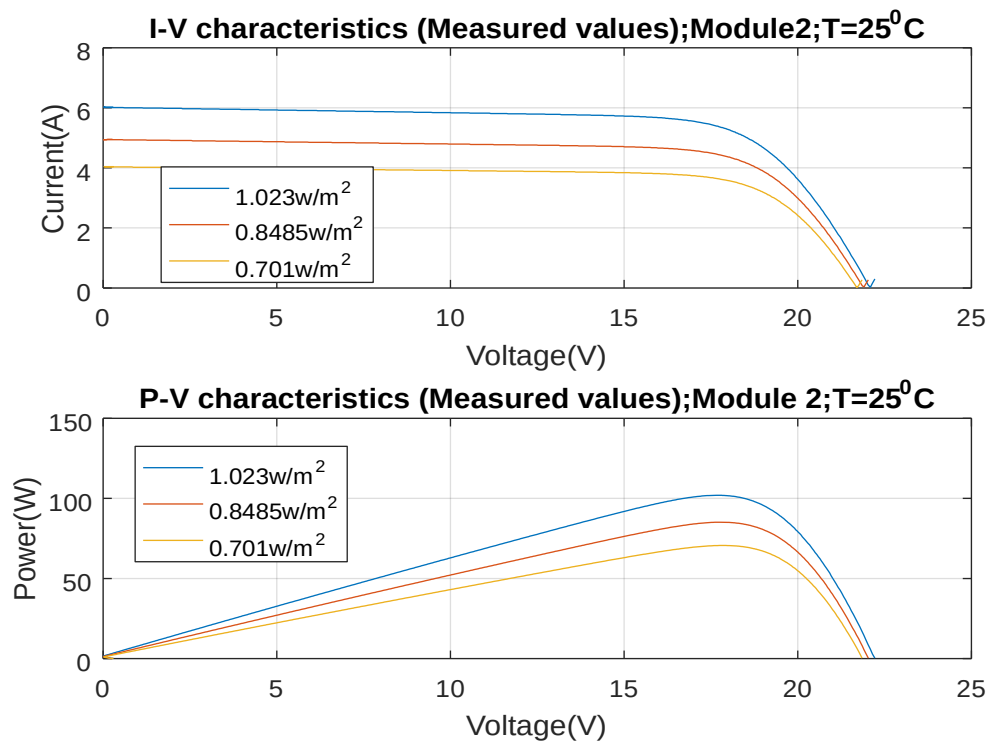


Figure 4.18 : I -V and P-V characteristics Module 2 Temperature =25°C

As seen in the figure above, at constant temperature of 25°C the polycrystalline module gave an output short circuit current of 6.0 A, 5.0 A, 4.0A at irradiance level of 1023W/m², 848.5W/m²,701W/m² respectively, the maximum power at this irradiance levels were 100W, 82W, 68W respectively, voltage of this module was still least affected with irradiance level variation. At this irradiance levels the open circuit voltage ranged closely between 21V to 22V.

4.2.2 Testing parameters for Module 1&2 for the Period of 1st Jan – 10th Feb 2021

A. Temperature readings

The minimum, average, and maximum temperatures are:

Temperature range: [14.0, 28.0, 42.0]°C

B. Irradiance readings

The minimum, average, and maximum irradiance are:

Irradiance Range: [701.0, 862.0, 1023.0] W/m²

4.2.3 The I-V and P-V curves for module 1 (monocrystalline)

Parameters for plotting I-V and P-V curves from the data collection for the given period

At constant irradiance:

Mono_Voltage (V) [10.09 0.02 19.40] at 42 °C

Mono_Voltage (V) [10.92 0.01 20.46] at 28 °C

Mono_Voltage (V) [11.66 0.01 21.52] at 13°C

The Mono_Current: Average, Minimum and Maximum

Mono_Current (A) [5.45 0.02 6.21] at 42°C

Mono_Curren (A) [5.40 0.05 6.12] at 28 °C

Mono_Current (A) [5.35 0.03 6.03] at 13°C

At constant Temperature

Mono_Voltage (V) [11.11 0.02 20.72] at 1023W/m²

Mono_Voltage (V) [11.00 0.01 20.55] at 848.5W/m²

Mono_Voltage (V) [10.86 0.01 20.35] at 701W/m²

The Mono_Current: Average, Minimum and Maximum

Mono_Current (A) [5.51 0.01 6.25] at 1023W/m²

Mono_Curren (A) [4.52 0.03 5.13] at 848.5 W/m²

Mono_Curren (A) [3.69 0.02 4.19] at 701 W/m²

Irradiance=1000W/m²; Module 1

Temp=[42 29 13]

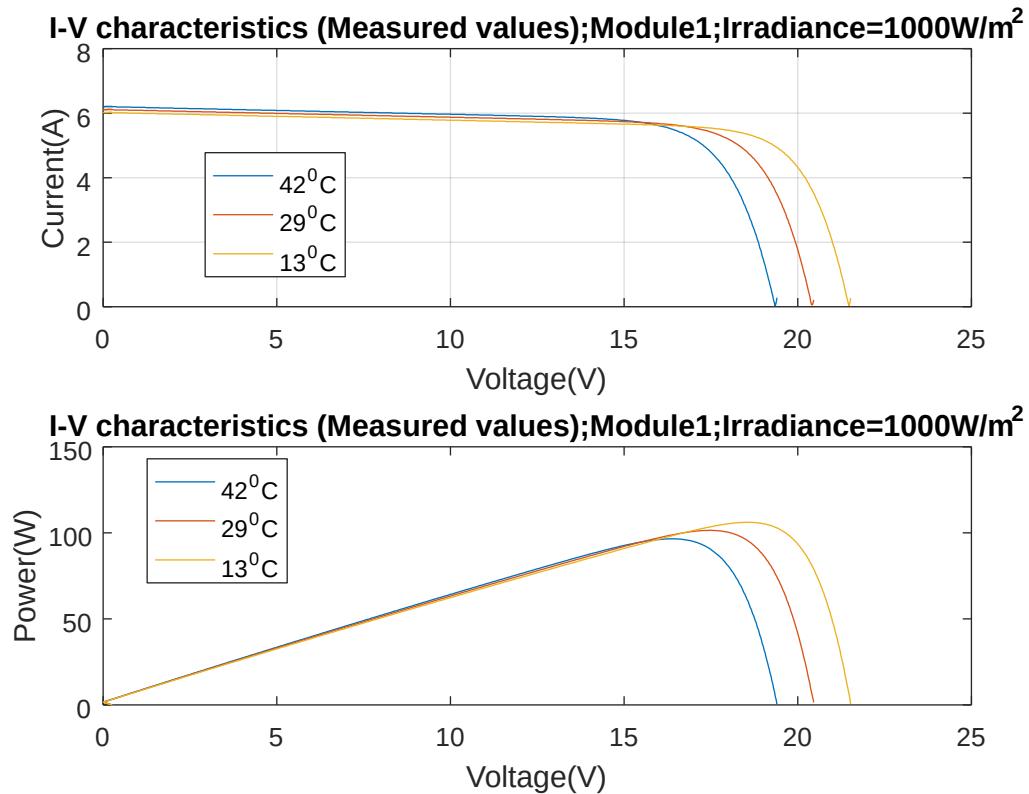


Figure 4.19: I-V and P-V characteristics Module 1 Irradiance =1000W/m²

At constant irradiance of 1000W/m², variation in temperature on monocrystalline module gave different values of open circuit voltage 19V, 20.5V and 21.8V at 42°C, 29°C, and 13°C respectively; there was still power output variation in these temperatures, 90W, 102W and 111W respectively. At higher temperature there was a slight increase in short circuit current at 42°C it was 6.2A as compared to 6.0 A at 13°C. The finding agrees with Zaini *et al.* (2015) where it showed that increasing the temperature, the maximum power (P_{max}) and the open circuit voltage (V_{oc}) showed a decreasing trend while the short circuit current (I_{sc}) indicated an increasing trend. Though, differed with Bioudun and Adeleke's (2017) research, neither photovoltaic

module's open-circuit voltage (Voc) increased much with temperature (monocrystalline and polycrystalline). The results agreed with those of Abdelkader *et al.* (2010), who found out that as ambient temperature raises, the open-circuit voltage decreases in their study of a comparative analysis of the performance of monocrystalline and multicrystalline PV cells in semi-arid climate conditions. It also agreed with study conducted by Irwanto *et al.* (2010) which indicated that if solar irradiance is constant and the temperature increases will cause the open circuit voltage, the maximum power and the efficiency decrease.

Set2 (JanFeb2021)

At constant irradiance

Irradiance=1000W/m²; Polycrystalline (Module 2)

The Poly voltage: Average, Minimum and Maximum

Poly_Voltage (V) [10.02 0.01 20.68] at 42°C

Poly Voltage (V) [10.93 0.01 21.82] at 29°C

Poly Voltage (V) [11.72 0.00 22.96] at 13°C

The Ploy Current: Average, Minimum and Maximum

Poly Current (A) [5.18 0.05 5.89] at 42°C

Poly Current (A) [5.12 0.06 5.80] at 28 °C

Poly Current (A) [5.09 0.05 5.71] at 13°C

At constant Temperature

Poly_Voltage (V) [11.11 0.02 22.12] at 1023W/m²

Poly Voltage (V) [11.11 0.01 21.93] at 848.5W/m²

Poly Voltage (V) [11.07 0.01 21.75] at 701W/m²

The Mono_Current: Average, Minimum and Maximum

Poly Current (A) [5.92 0.01 5.92] at 1023W/m²

Poly Curren (A) [4.29 0.03 4.85] at 848.5 W/m²

Poly Curren (A) [3.45 0.00 3.94] at 701 W/m²

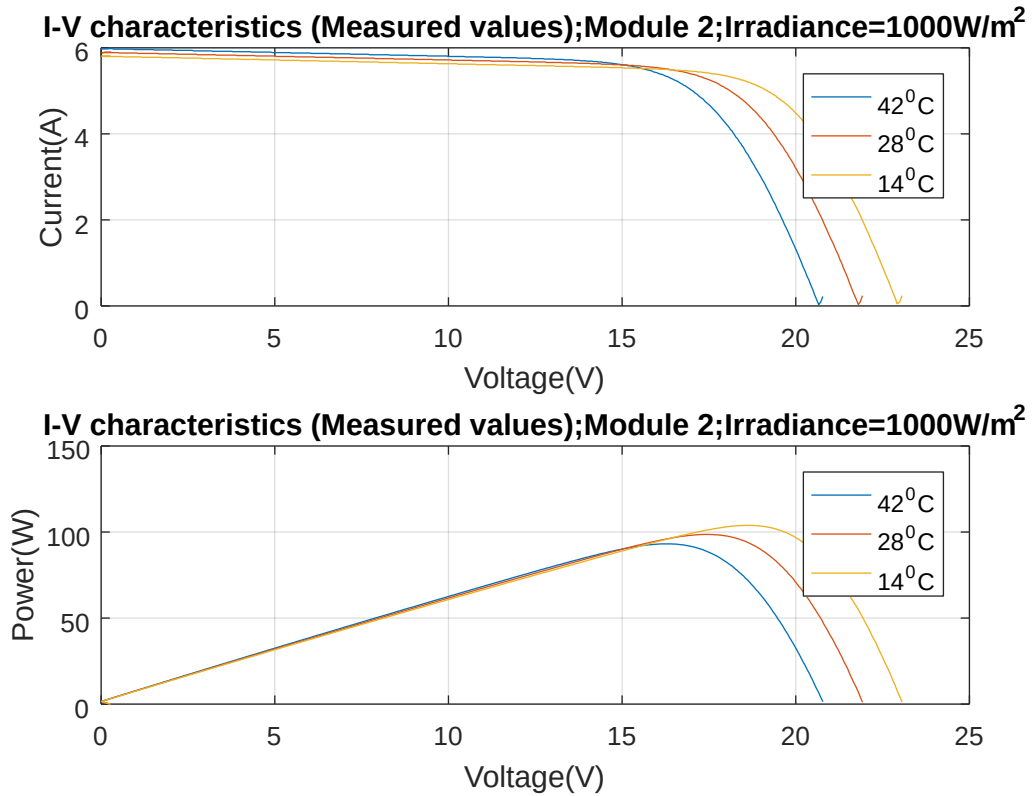


Figure 4.20: I-V and P-V characteristics Module 2 Irradiance =1000W/m²

At constant irradiance of 1000W/m², polycrystalline module's open circuit voltage and maximum power output varied at different temperature levels, 20.8V, 22V, 23V and 90W, 98W, and 102W, at 42°C, 28°C, and 14°C respectively. The short circuit current for the three temperatures was least affected by temperature variance at 42°C it gave 6.0A while at 14°C it gave 5.8A. The findings agreed with those done by WanQuan *et al.* (2020) where the open circuit voltage is observed to decrease gradually with increase in temperature. On the other hand, the short circuit increases with increase in temperature.

Set3 (FebMarch2021)

Temp =25 degrees; Monocrystalline

Irradiance = [1023 862.5 702]

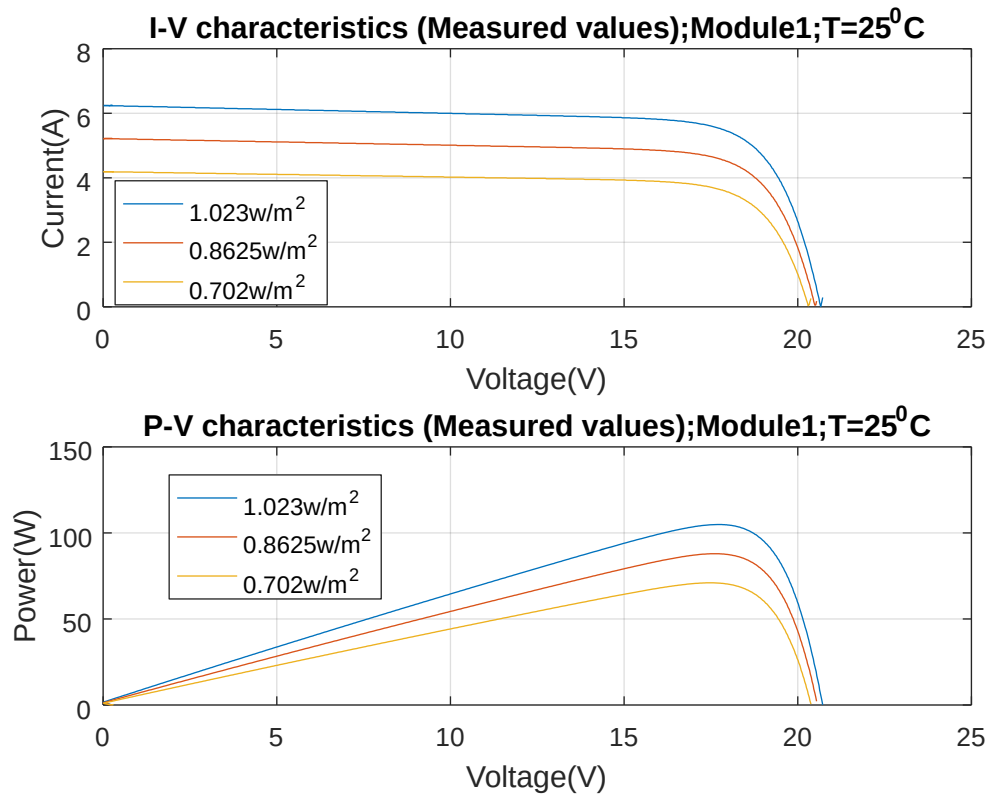


Figure 4.21: I-V and P-V characteristics of Monocrystalline Module Temperature = 25°C

From the graph above period of Feb/March at constant temperature of 25°C monocrystalline module gave a short circuit current of 6.2A, 5.2A, 4.2A at 1023W/m², 862.5 W/m² and 702W/m² respectively. With higher irradiance it was seen that the module still gave a higher power output as compared to lower irradiance levels, the finding agrees with Rani *et al.* (2018) where they found that output power of a solar panel increases with increasing solar irradiance. P_{max} at irradiance level of 1023W/m², 862.5W/m², 702 W/w² were 104W, 82W, and 69W respectively .The

open circuit voltage was least affected by the irradiance level variance while the short circuit current and power output varied distinctly that agrees with Takyi *et al.* (2021) where the results showed a linear increase in the short circuit current (I_{sc}) and maximum power with irradiation on their research on performance evaluation of monocrystalline and polycrystalline silicon solar photovoltaic modules under low and high irradiance conditions in Kumasi, Ghana. It also conformed with the study done by Rosyid (2016) provided similar observation where when solar irradiance increases, other variables increase which leads to an increase in power output in tropical climate of Indonesia.

Set3 (FebMarch2021)

Temp = 25 degrees; Polycrystalline.

Irradiance = [1023 848.5 701]

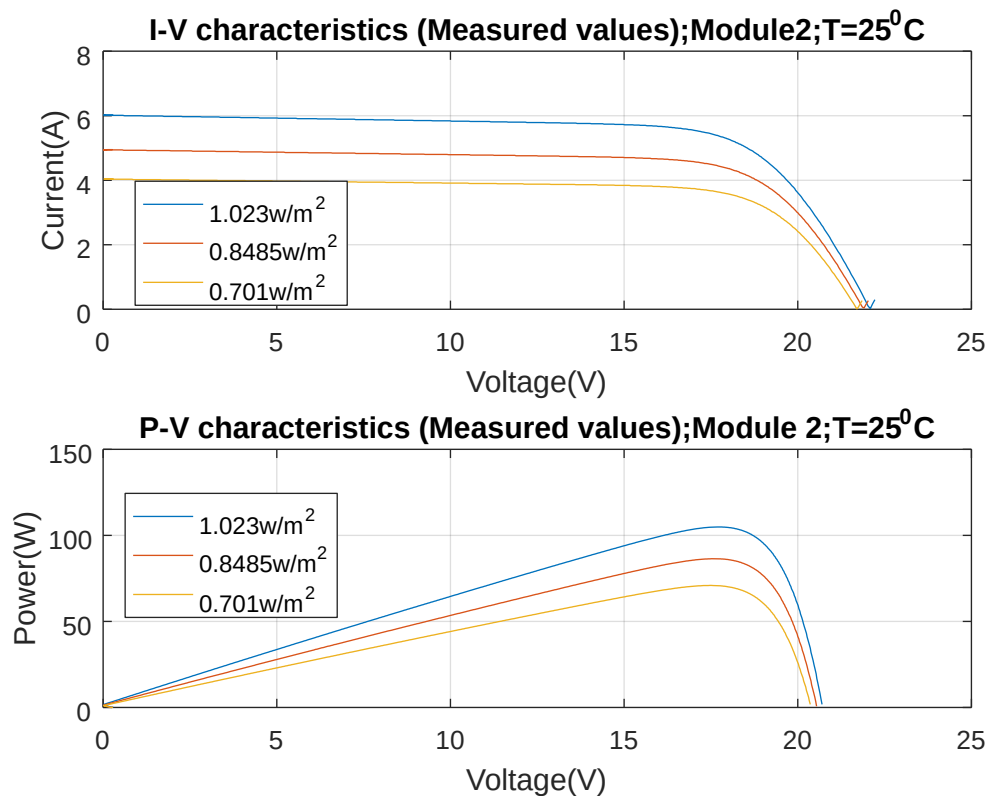


Figure 4.22: I-V and P-V characteristics Polycrystalline module Temperature =25°C

As seen in the fig above, at constant temperature of 25⁰C the polycrystalline module gave an output short circuit current of 6.0 A, 5.0 A, 4.0A at irradiance level of 1023W/m², 848.5W/m², 701W/m² respectively, the maximum power at this irradiance levels were 101W, 79W, 67W respectively, Open circuit voltage of this module was still least affected with irradiance level variation the finding agrees with earlier result by Mandadapu *et al.* (2017) when the irradiance drops, from a high value of 1,000 W/m² to 200 W/m² and below, the PV modules operate around 9% to 10% of their capacities. At this, irradiance levels the open circuit voltage ranged closely between 21V to 22V. Similar results were concluded by Musanga *et al.* (2018) I_{sc} of the module increased significantly with increasing irradiance whilst the V_{oc} was least affected by increasing or decreasing irradiance in their investigation on effect of irradiance and temperature on the performance of monocrystalline silicon solar module under outdoor conditions in Kakamega, Kenya.

4.2.4 Testing parameters for Module 1&2 for the Period of 17th Feb – 31st March 2021

A. Temperature readings

The minimum, average, and maximum temperatures are:

Temperature range: [13.0, 29.0, 45.0]°C

B. Irradiance readings

The minimum, average and maximum irradiance are:

Irradiance Range: [702.0, 862.5, 1023.0] W/m²

4.2.5 The I-V and P-V curves for module 1 under the meteorological conditions

Parameters for plotting I-V and P-V curves from the data collection for the given period

The data of voltage was collected for 58days in 17th Feb – 31st March 2021for 12hours a day and every after 5minutes

At constant irradiance:

Mono-Voltage (V) [10.09 0.02 21.6] at 42 °C

Mono-Voltage (V) [10.87 0.01 20.39] at 28 °C

Mono-Voltage (V) [11.71 0.01 21.60] at 14°C

The Mono_Current: Average, Minimum and Maximum

Mono_Current (A) [54.42 0.01 6.22] at 420 C

Mono_Curren (A) [5.40 0.02 6.12] at 28 °C

Mono_Curren (A) [5.35 0.01 6.02] at 14°C

At constant Temperature

Mono_Voltage (V) [11.01 0.01 20.62] at 1023W/m²

Mono_Voltage (V) [10.90 0.01 20.44] at 848.5W/m²

Mono_Voltage (V) [10.86 0.01 20.38] at 702W/m²

The Mono_Current: Average, Minimum and Maximum

Mono_Current (A) [5.42 0.03 6.15] at 1023W/m²

Mono_Curren (A) [4.51 0.05 5.12] at 848.5 W/m²

Mono_Curren (A) [3.69 0.03 4.19] at 702 W/m²

Table 4.11: Measured parameters for module 1

Parameters for Monocrystalline solar PV	Parameters	Units
A_V	10.91	V
V_{min}	0.02	V
V_{max}	20.84	V
I_{min}	0.00	A
I_{sc}	6.40	A
I_{mp}	5.92	A
V_{oc}	21.8	V
V_{mp}	20.16	V

Irradiance=1000W/m²; Monocrystalline

Temp=[42 29 13]

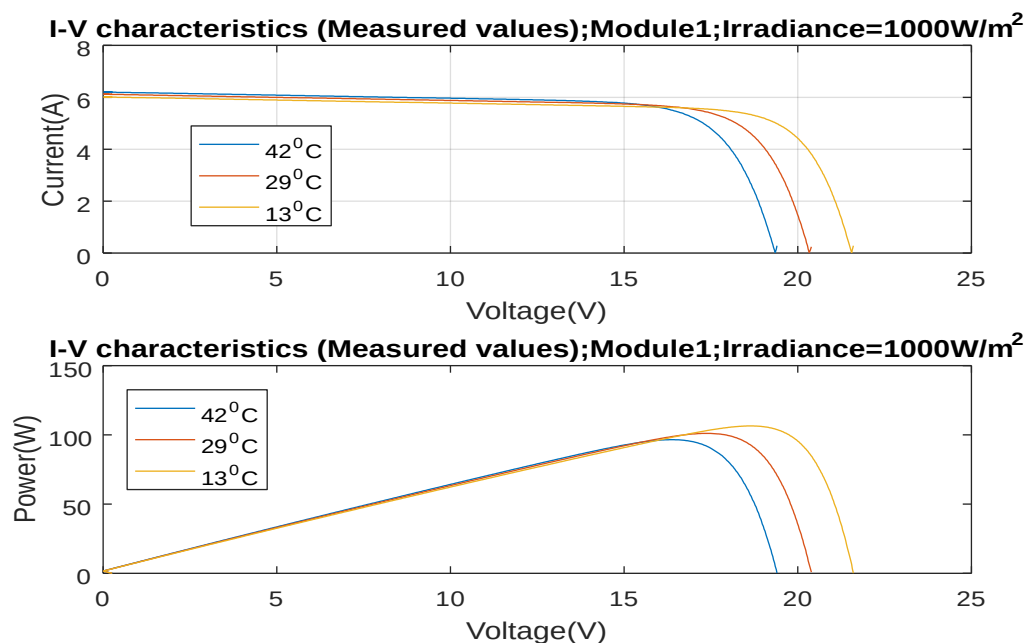


Figure 4.23: I-V and P-V characteristics of monocrystalline Module Irradiance =1000W/m²

At constant irradiance of 1000W/m², variation in temperature on monocrystalline module gave distinct different values of open circuit voltage 19V, 20.5V and 21.8V at 42°C, 29°C, and 13°C respectively; there was still power output variation in this temperatures, 90W, 98W and 108W respectively. At higher temperature there was a slight increase in short circuit current at 42°C it was 6.2A as compared to 6.0 A at 13°C. These findings agreed with Zaini *et al.* (2015) study where they found out that

when temperature rises, the maximum output power and open circuit voltage decreases while the short circuit current increases.

Set3 (FebMarch2021)

4.3 The I-V and P-V curves for module 2 (Polycrystalline)

Parameters for plotting I-V and P-V curves from the data collection for the given period.

The Poly voltage: Average, Minimum and Maximum

Poly_Voltage (V) [10.02 0.01 20.68] at 42°C

Poly Voltage (V) [10.93 0.01 21.82] at 28°C

Poly Voltage (V) [11.72 0.00 22.96] at 14°C

The Ploy Current: Average, Minimum and Maximum

Poly Current (A) [5.18 0.05 5.89] at 42°C

Poly Current (A) [5.12 0.06 5.80] at 28 °C

Poly Current (A) [5.09 0.05 5.71] at 14°C

At constant Temperature

Poly_Voltage (V) [11.11 0.02 22.12] at 1023W/m²

Poly Voltage (V) [10.89 0.02 20.44] at 848.5W/m²

Poly Voltage (V) [10.88 0.01 21.30] at 702W/m²

The poly_Current: Average, Minimum and Maximum

Poly Current (A) [5.24 0.01 5.46] at 1023W/m²

Poly Curren (A) [5.18 0.05 5.3] at 848.5 W/m²

Poly Curren (A) [3.54 0.42 3.94] at 702W/m²

Table 4.12: Measured parameters for Polycrystalline solar PV

Parameters for Polycrystalline solar PV	Values	Units
A_V	12.33	V
V_{\min}	0.00	V
V_{\max}	22.00	V
I_{\min}	0.00	A
I_{sc}	5.8	A
I_{mp}	5.18	A
V_{oc}	22.00	V
V_{mp}	18.48	V

Irradiance=1000W/m²; Polycrystalline.

Temp= [42 28 14]

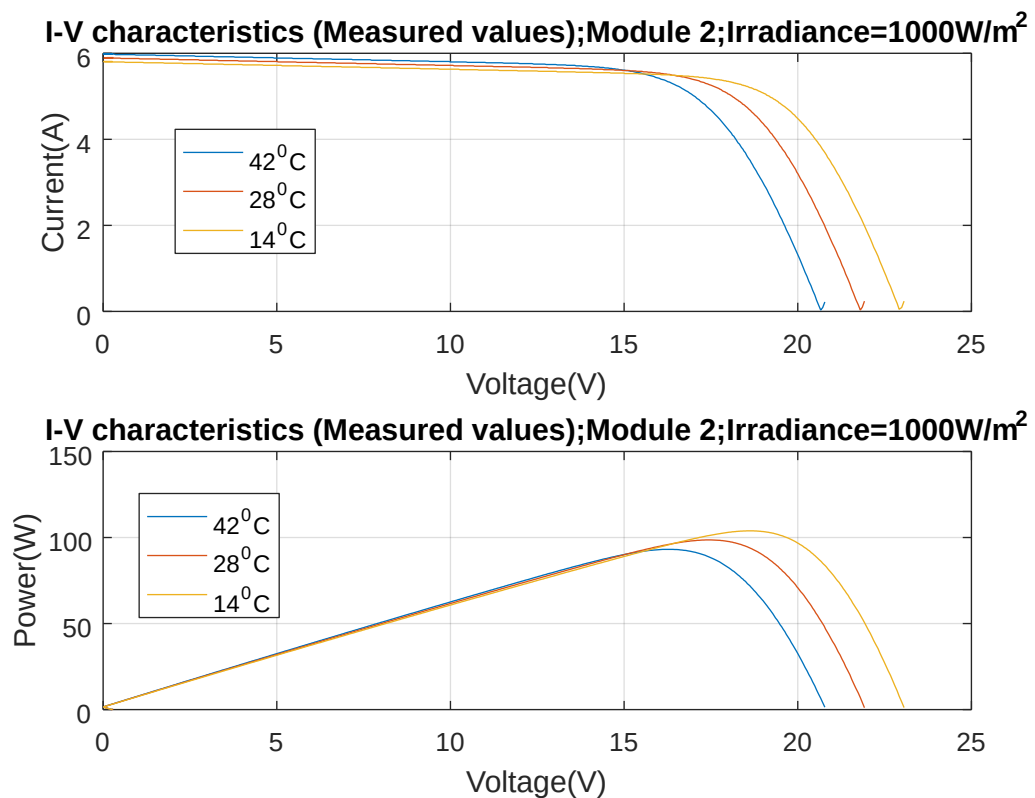


Figure 4.24: I-V and P-V characteristics of polycrystalline Module Irradiance =1000W/m²

At constant irradiance of 1000W/m², polycrystalline module's open circuit voltage and maximum power output varied at different temperature levels of 42°C, 28°C, and 14°C this were 20.8V, 22V, 23V and 90W, 98W, and 102W respectively; from this observation it agrees with study carried out by Malik *et al.* (2017) which showed that

when the temperature rises, the band gap of the semiconductor shrinks, resulting in a decrease in open circuit voltage and, as a result, output power. Unlike voltage the short circuit current for the three temperatures didn't show great variation from each other at 42⁰C it gave 6.0A while at 14⁰C it gave 5.8A which indicates that current is less affected by temperature variation. This observation agreed with those of Chedid *et al.* (2014) which stated that as temperature increases, the voltage decreases substantially while the current undergoes insignificant increase. As a result, the power decreases with increasing temperature.

4.4 SIMULATED GRAPHS

4.4.1 The I-V and P-V curves for monocrystalline (November 2020)

The curves were done using MATLAB-Simulink

Simulink setup

Constant temperature=25 degrees; Irradiances= [1023 848.5 675 W/m²]

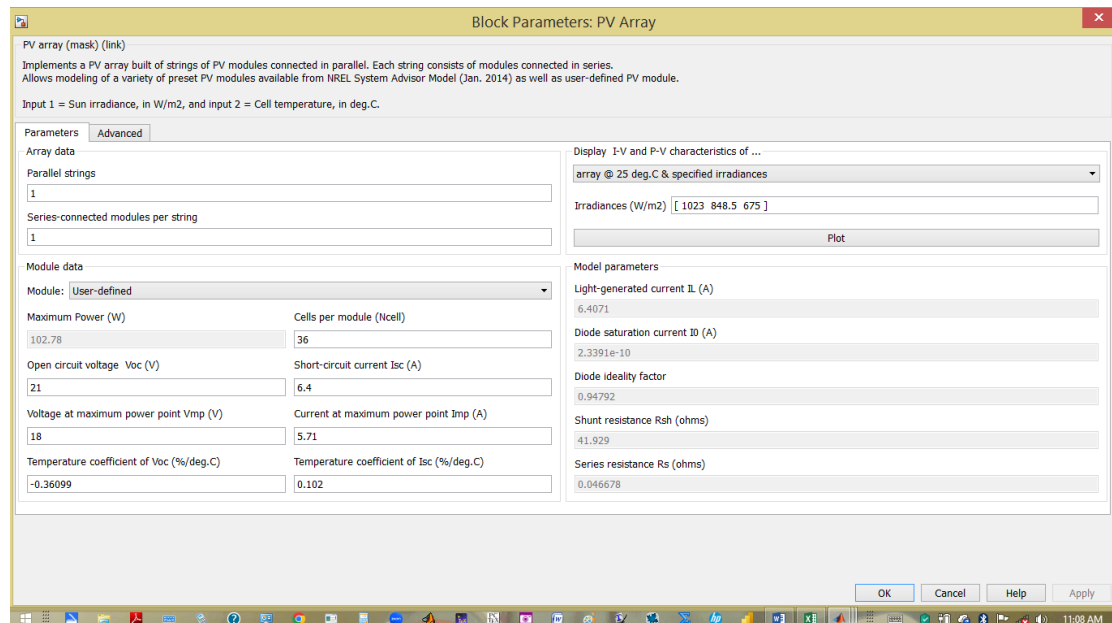


Figure 4.25: Simulink setup for mono-crystalline at constant Temperature

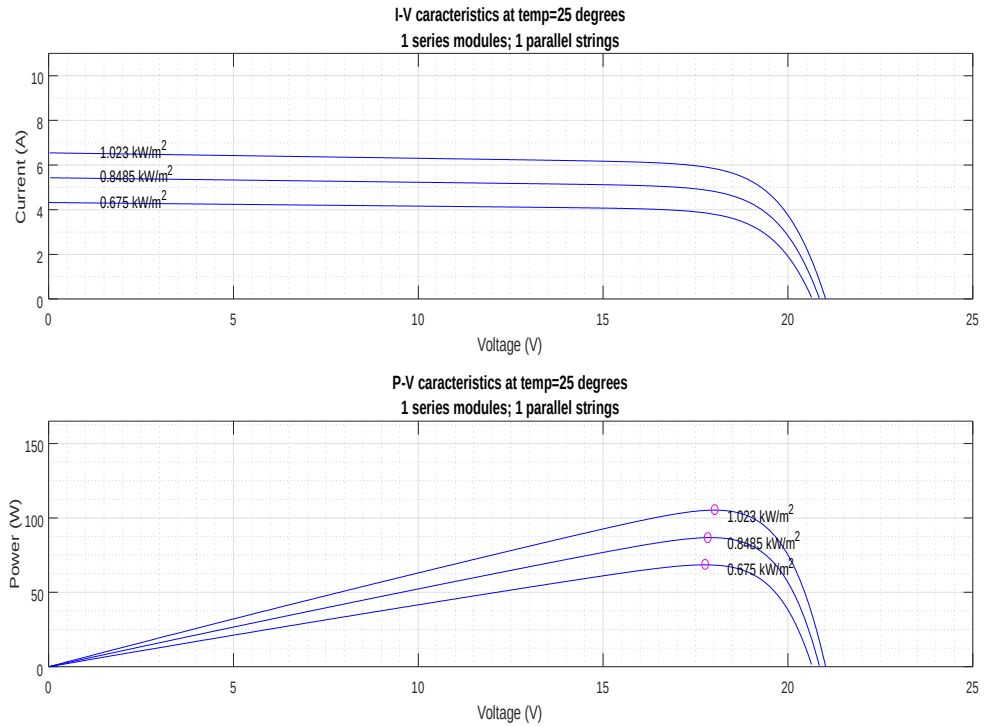


Figure 4.26: I-V and P-V characteristics of monocrystalline Module Temperature =25°C

From the Simulated graph of November period at constant temperature of 25⁰ C monocrystalline module gave a short circuit current of 6.6A, 5.6A, 4.2A at 1023W/m², 848.5 W/m² and 675W/m² respectively. While at the same period and same irradiance levels power output were 102.78W, 87.5W and 68.75W respectively.

I-V and P-V curves at constant irradiance but varying temperature

Constant Irradiance=1000W/m²; Temperature = [44, 28.5, 14°C]

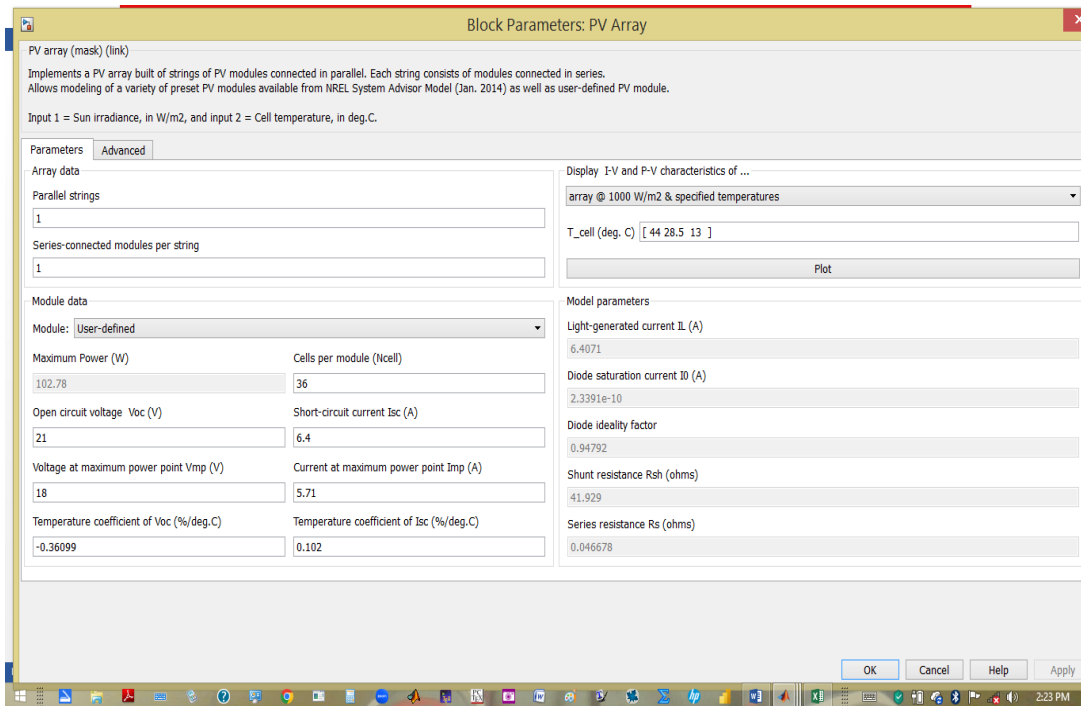


Figure 4.27: Simulink setup for mono-crystalline at constant irradiance

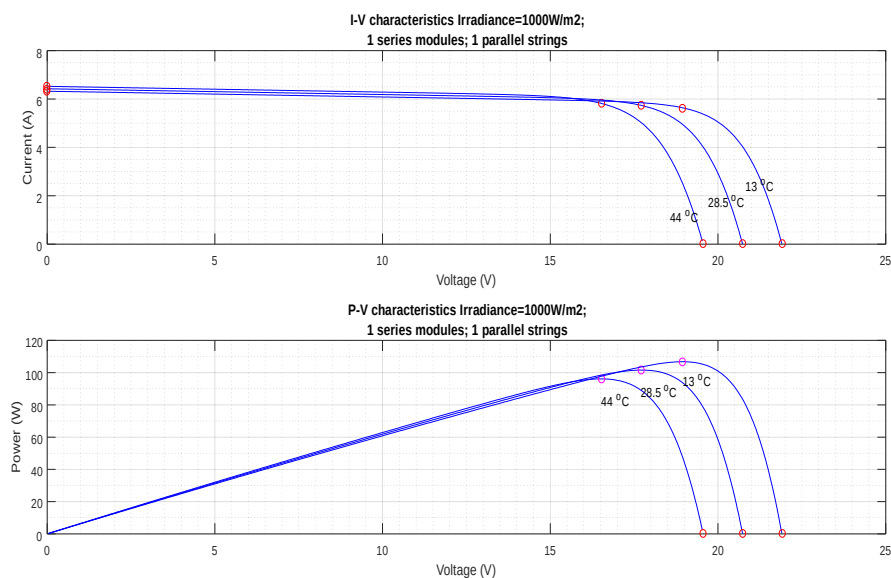


Figure 4.28: I-V and P-V Curves at constant irradiance 1000W/m² (mono-crystalline)

From the Simulated graph of November period at constant irradiance of 1000W/m^2 monocrystalline module gave a short circuit current of 6.5A, 6.3A, 6.2A at 44°C , 28.5°C and 13°C respectively. While at the same period and same temperature levels power output were 96W, 101.2W and 108W respectively.

4.4.2 The I-V and P-V curves for module 2 (polycrystalline)

I-V and P-V curves for module 2 at constant temperature but varying irradiance

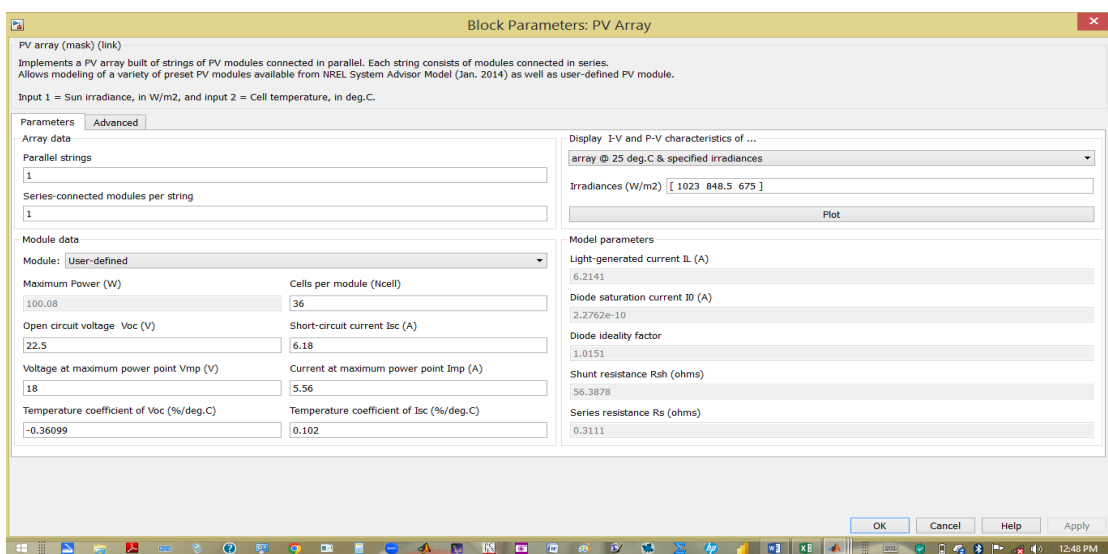


Figure 4.29: Simulink set-up for poly-crystalline

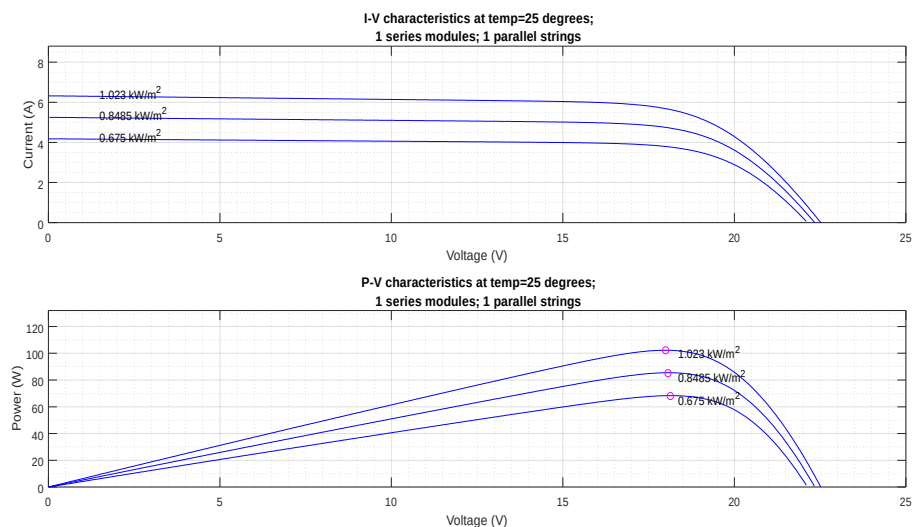


Figure 4.30: I-V and P-V Curves at constant temperature at 25°C (Poly-crystalline)

From the Simulated graph of November period at constant temperature of 25⁰ C polycrystalline module gave a short circuit current of 6.3A, 5.25A, 4.2A at 1023W/m², 848.5 W/m² and 675W/m² respectively. While at the same period and same irradiance levels power output were 102W, 85W and 70W respectively

MODULE 2 (NOV2020 data set)

Constant Irradiance=1000W/m²; Temperature= [44 28.5 14°c]

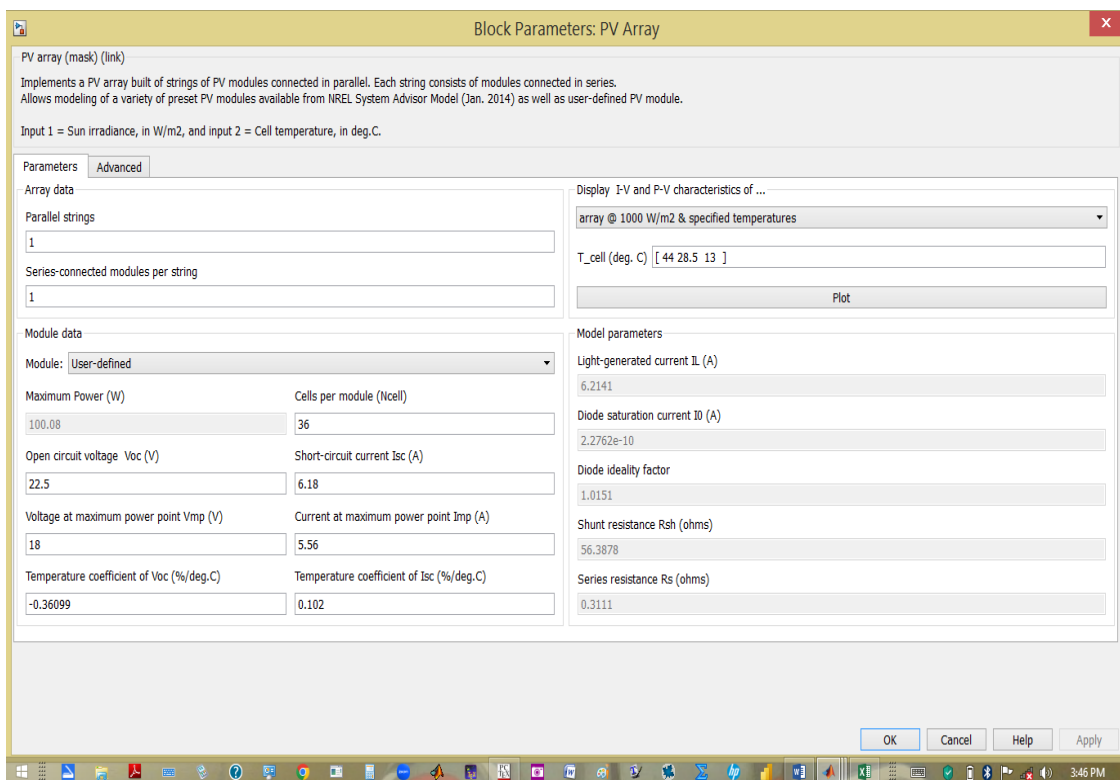


Figure 4.31: Simulink set-up for poly-crystalline at constant irradiance

From the Simulated graph of November period at constant irradiance of 1000W polycrystalline module gave a short circuit current of 6.3A, 6.2A, and 6.1A at 44⁰C, 28.5⁰C and 13⁰C respectively. While at the same period same temperature levels power output were 92W, 98W and 104W respectively

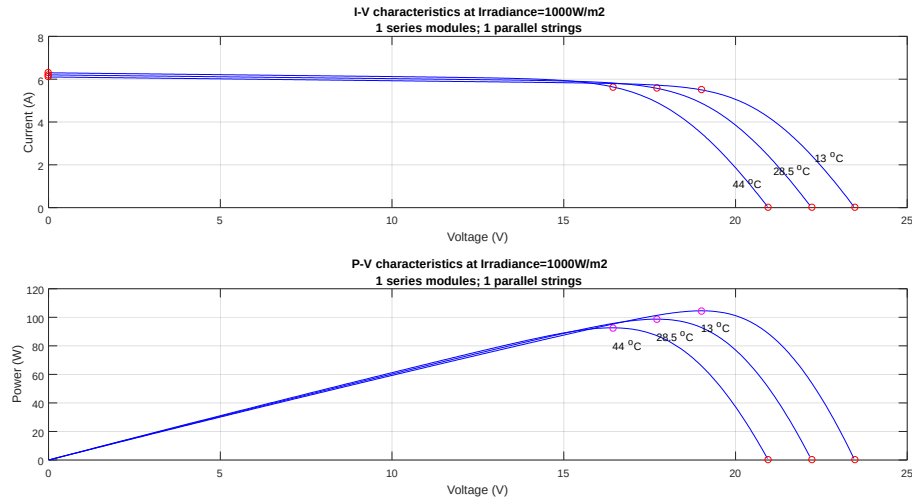


Figure 4.32: I-V and P-V Curves at constant irradiance 1000 W/m^2 (Poly-crystalline)

4.4.3 I-V and P-V curves at constant temperature but varying irradiance

Simulink setup

Constant temperature=25 degrees; Irradiances=[1023 848.5 701 W/m^2]

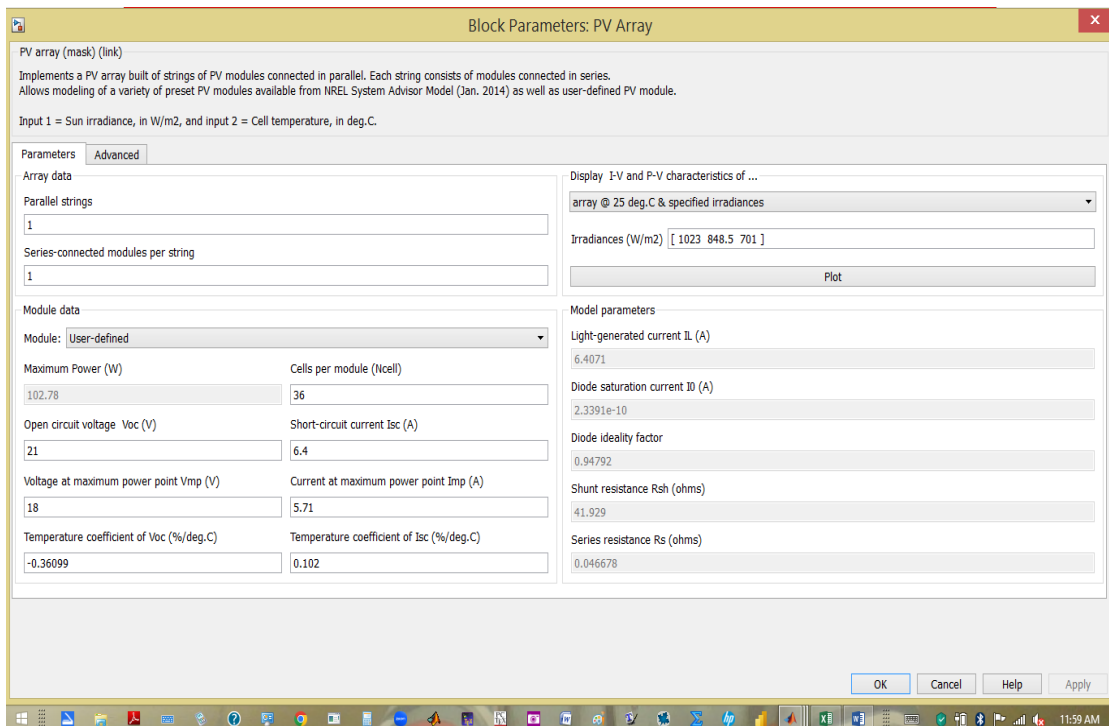


Figure 4.33: Simulink set-up for mono-crystalline for constant temperature

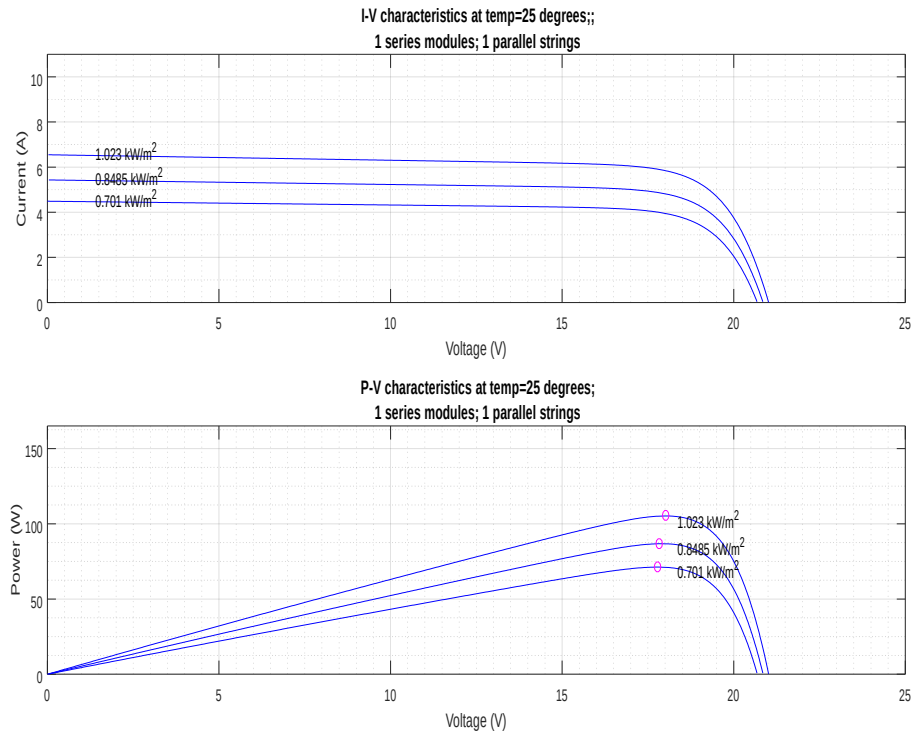


Figure 4.34: I-V and P-V Curves at constant temperature (mono-crystalline)

From the Simulated graph of January/February period at constant temperature of 25°C monocrystalline module gave a short circuit current of 6.5A, 5.5A, 4.5A at 1023W/m^2 , 848.5 W/m^2 and 701W/m^2 respectively. While at the same period and same irradiance levels power output were 105W, 87.5W and 72.5W respectively.

I-V and P-V curves at constant irradiance but varying temperature

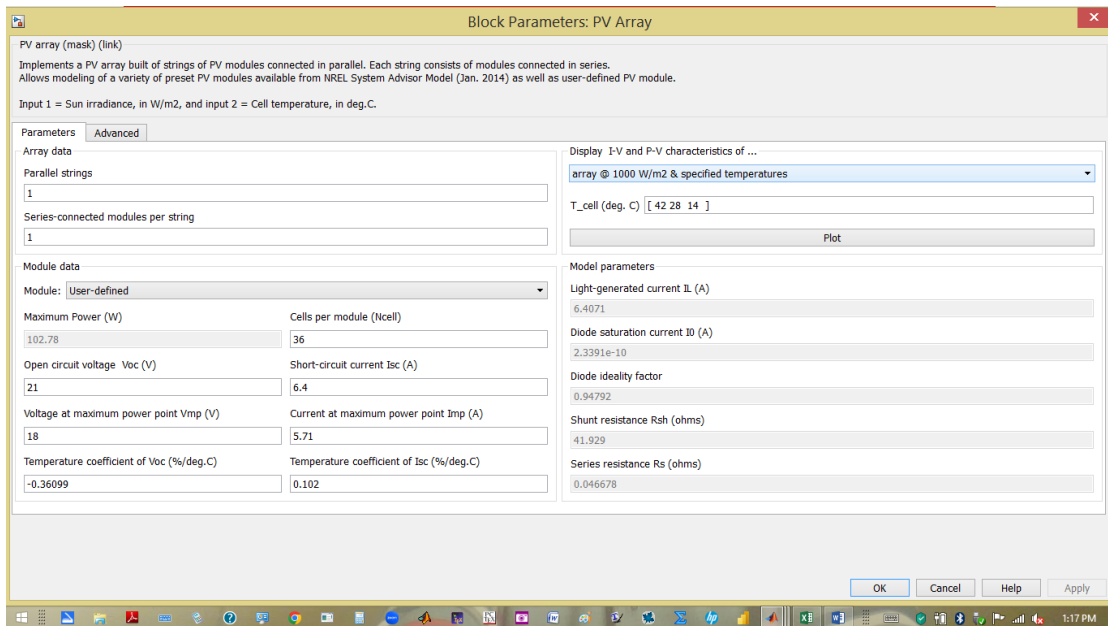


Figure 4.35: Simulink set-up for mono-crystalline at constant irradiance

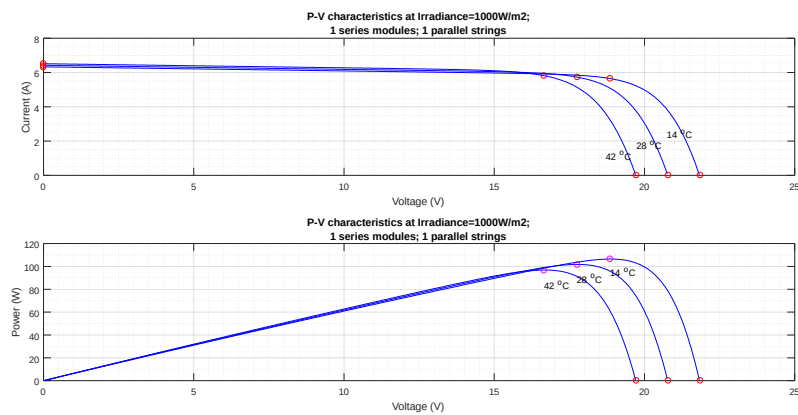


Figure 4.36: I-V and P-V Curves at constant irradiance (mono-crystalline)

From the Simulated graph of January/February period at constant irradiance of 1000W/m^2 monocrystalline module gave a short circuit current of 6.4A, 6.3A, 6.2A at 42°C , 28°C and 14°C respectively. While at the same period and same temperature levels power output were 96W, 100W and 108W respectively.

4.4.4 I-V and P-V curves at constant temperature but varying irradiance

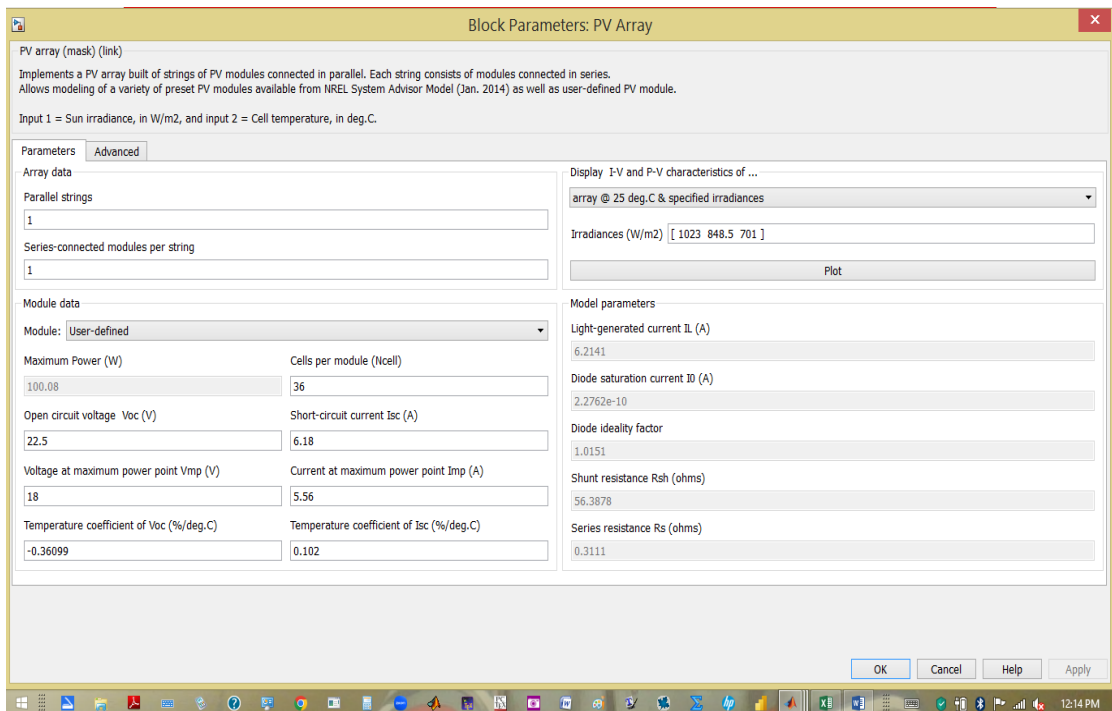


Figure 4.37: Simulink set-up for poly-crystalline at constant temperature

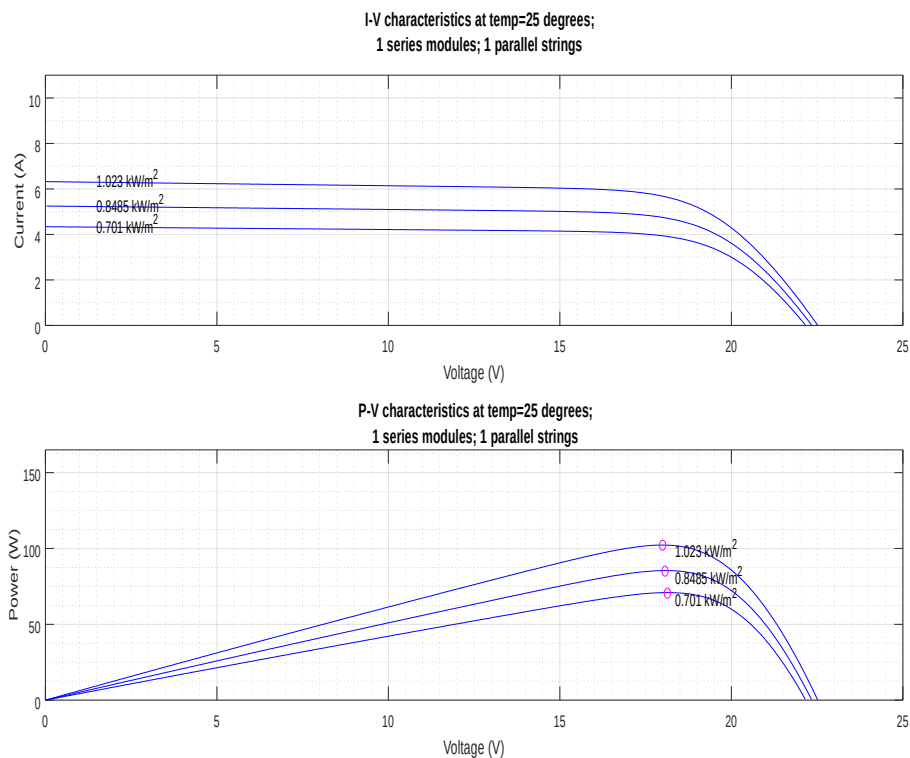


Figure 4.38: I-V and P-V Curves at constant temperature (poly-crystalline)

From the Simulated graph of January/February period at constant temperature of 25⁰ C polycrystalline module gave a short circuit current of 6.2A, 5.2A, 4.2A at 1023W/m², 848.5 W/m² and 701W/m² respectively. While at the same period and same irradiance levels power output were 102W, 86W and 73W respectively

I-V and P-V curves at constant irradiance but varying temperature

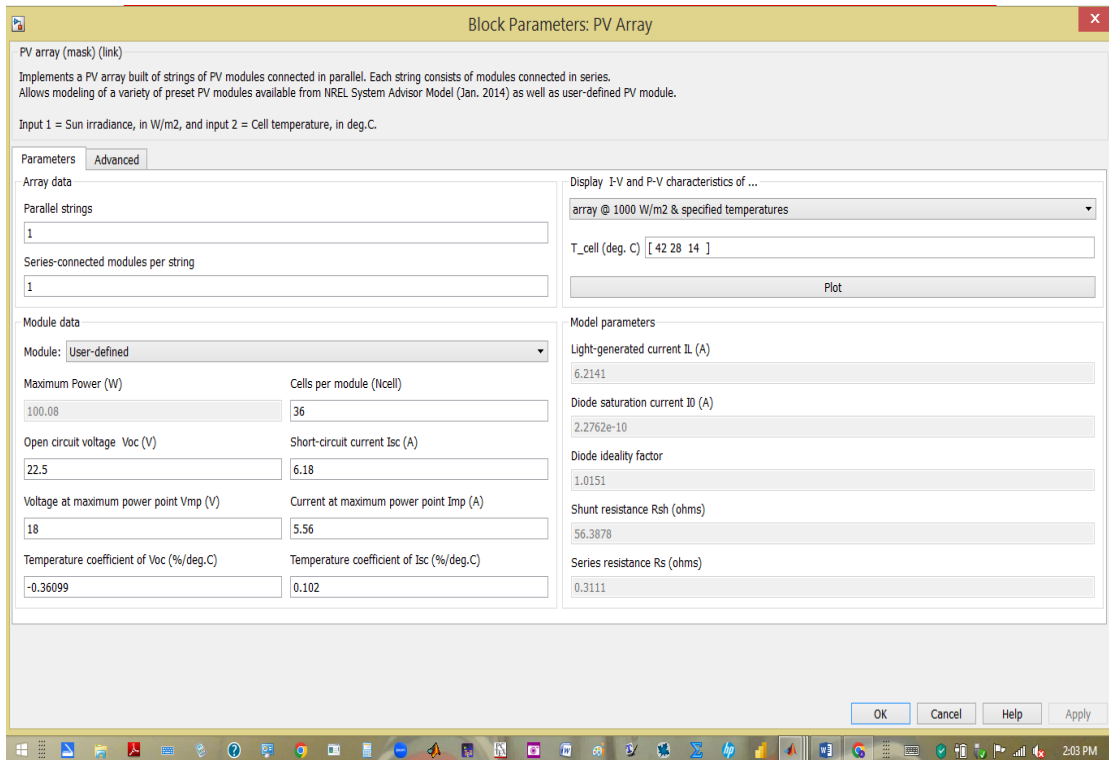


Figure 4.39: Simulink set-up for poly-crystalline at constant irradiance

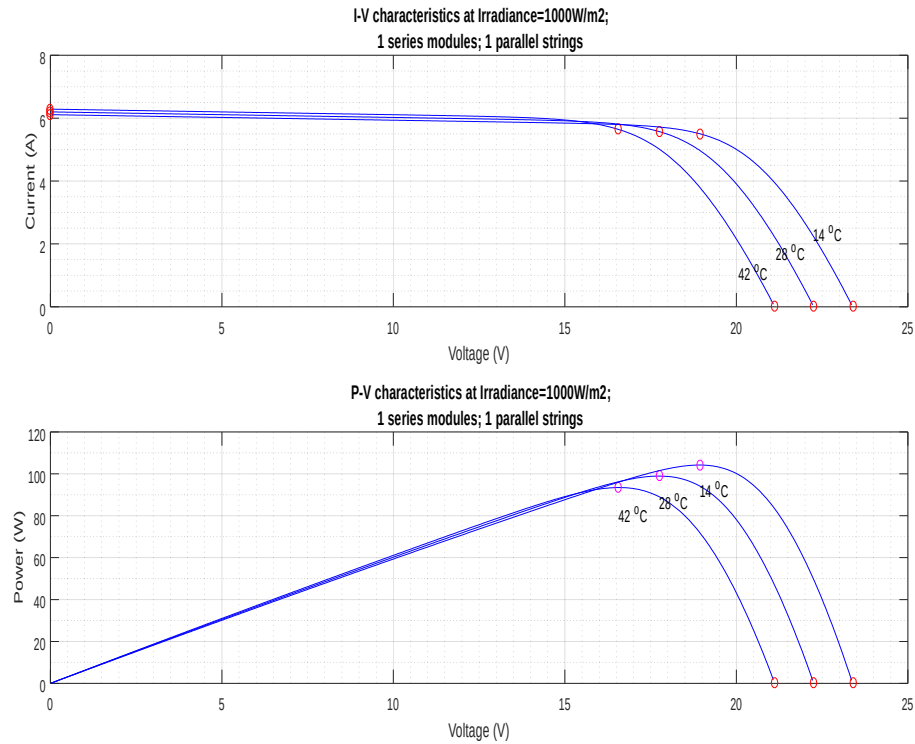


Figure 4.40: I-V and P-V Curves at constant irradiance (poly-crystalline)

From the Simulated graph of January/February period at constant irradiance of 1000W polycrystalline module gave a short circuit current of 6.2A, 6.1A, and 6.0A at 42°C, 28°C and 14°C respectively. While at the same period same temperature levels power output were 93W, 98W and 105W respectively

4.4.5 I-V and P-V curves at constant temperature but varying irradiance

Simulink setup

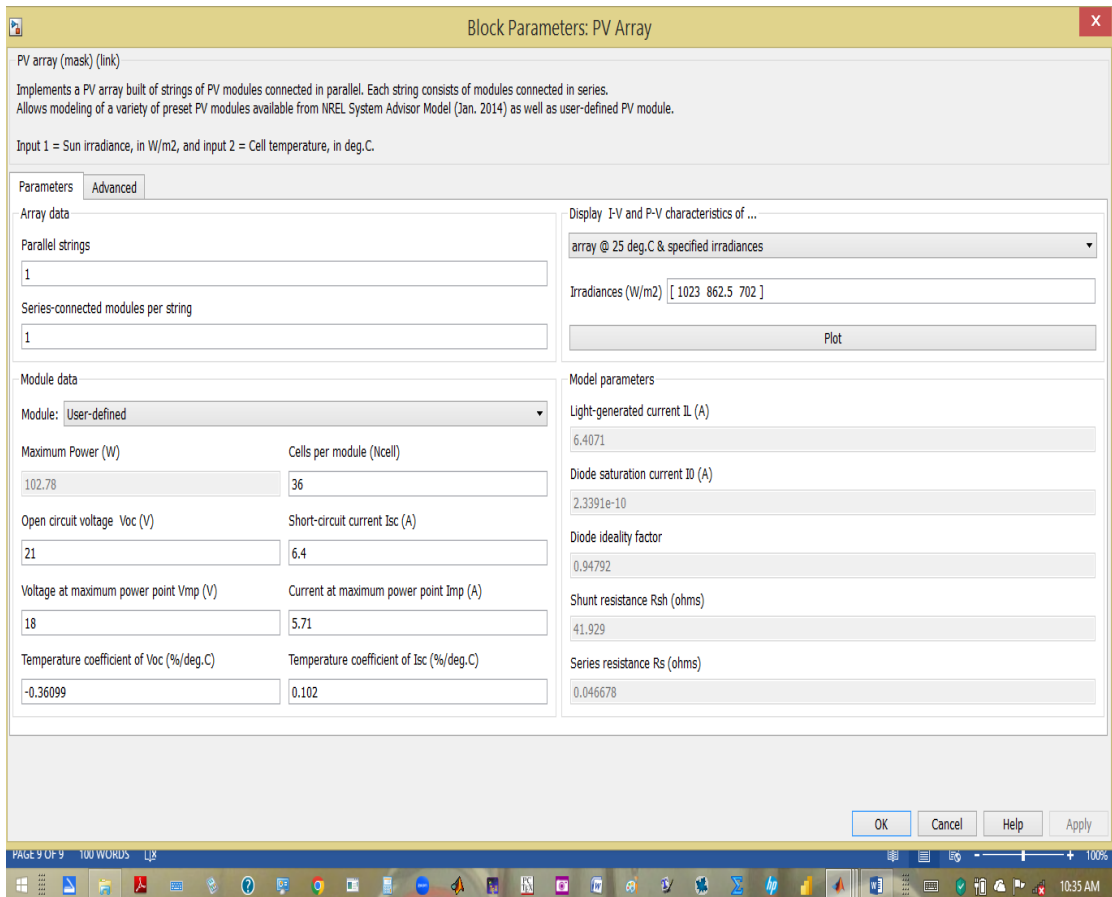


Figure 4.41: Simulink set-up for mono-crystalline at constant temperature

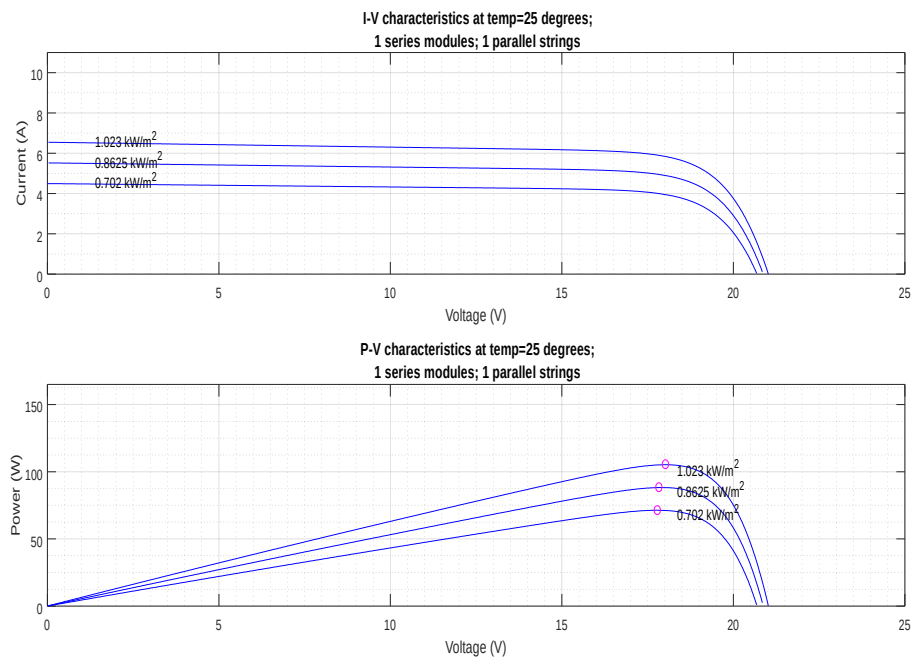


Figure 4.42: I-V and P-V Curves at constant temperature (mono-crystalline)

From the Simulated graph of March period at constant temperature of 25°C monocrystalline module gave a short circuit current of 6.6A, 5.6A, 4.2A at $1023\text{W}/\text{m}^2$, $862.5\text{ W}/\text{m}^2$ and $702\text{W}/\text{m}^2$ respectively. While at the same period and same irradiance levels power output were 106.3W, 87.5W and 68.8W respectively.

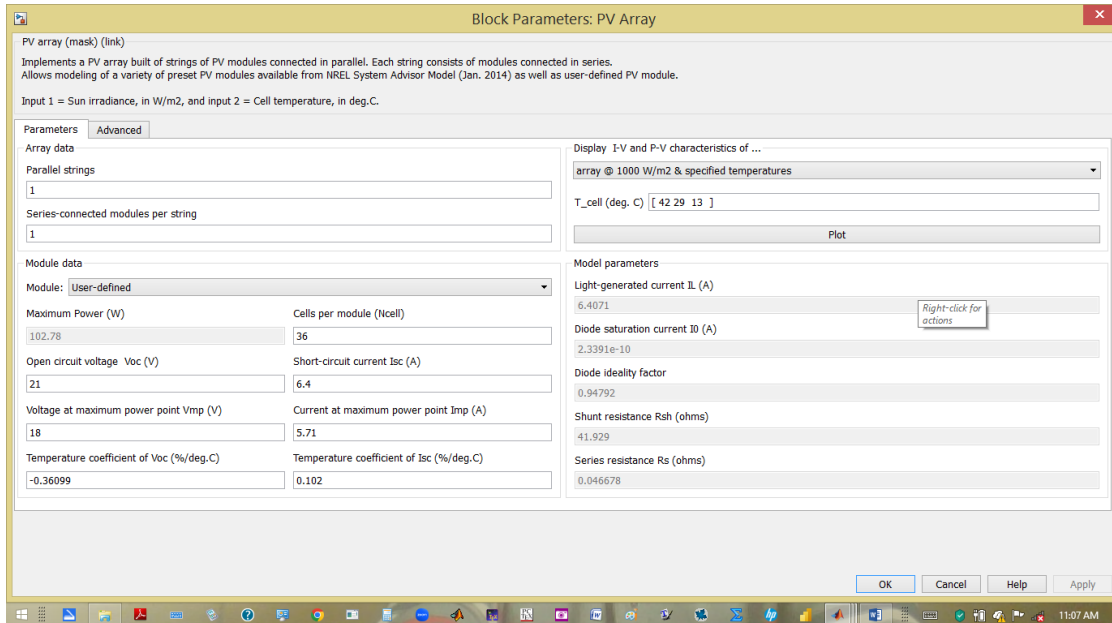


Figure 4.43: Simulink set-up for mono-crystalline at constant irradiance

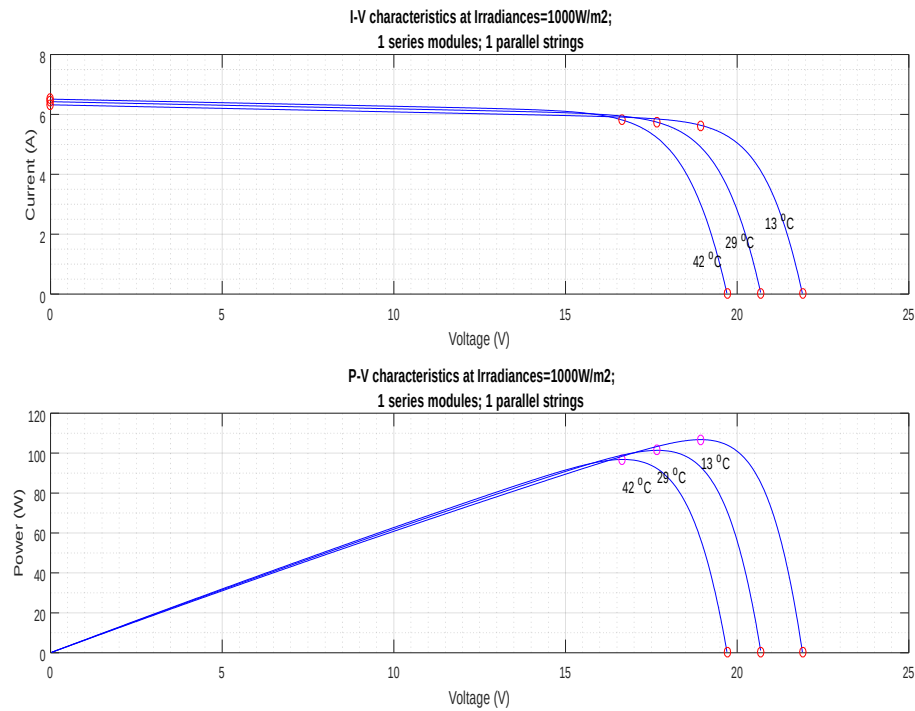


Figure 4.44: I-V and P-V Curves at constant irradiance (mono-crystalline)

From the Simulated graph of March period at constant irradiance of 1000W/m^2 monocrystalline module gave a short circuit current of 6.5A, 6.3A, 6.2A at 42°C , 29°C and 13°C respectively. While at the same period and same irradiance levels power output were 98W, 100W and 108W respectively.

4.3.6 I-V and P-V curves at constant temperature but varying irradiance (Feb-March 2021)

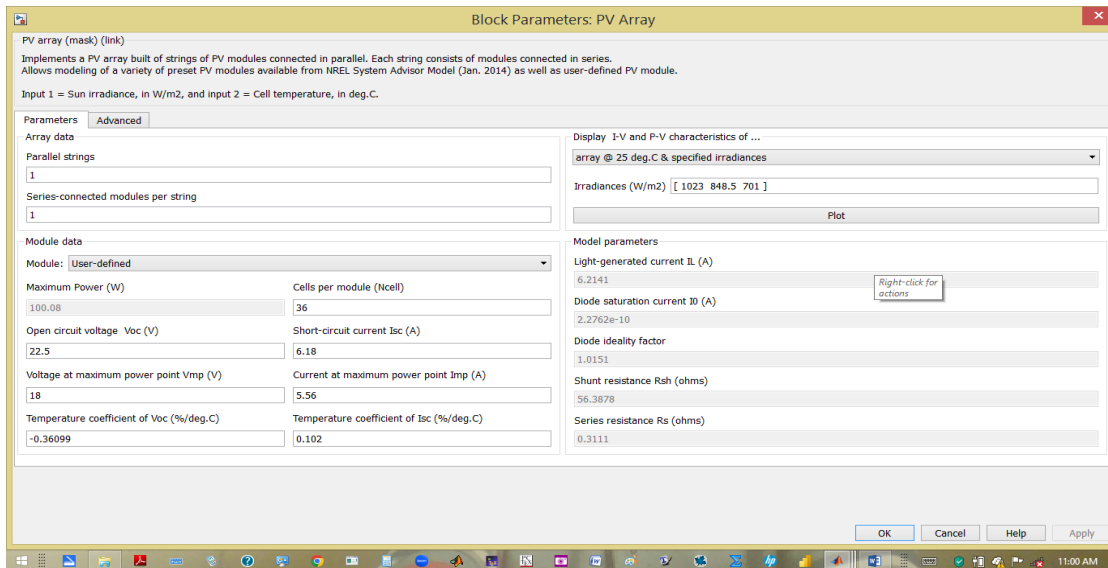


Figure 4.45: Third Simulink set-up for poly-crystalline

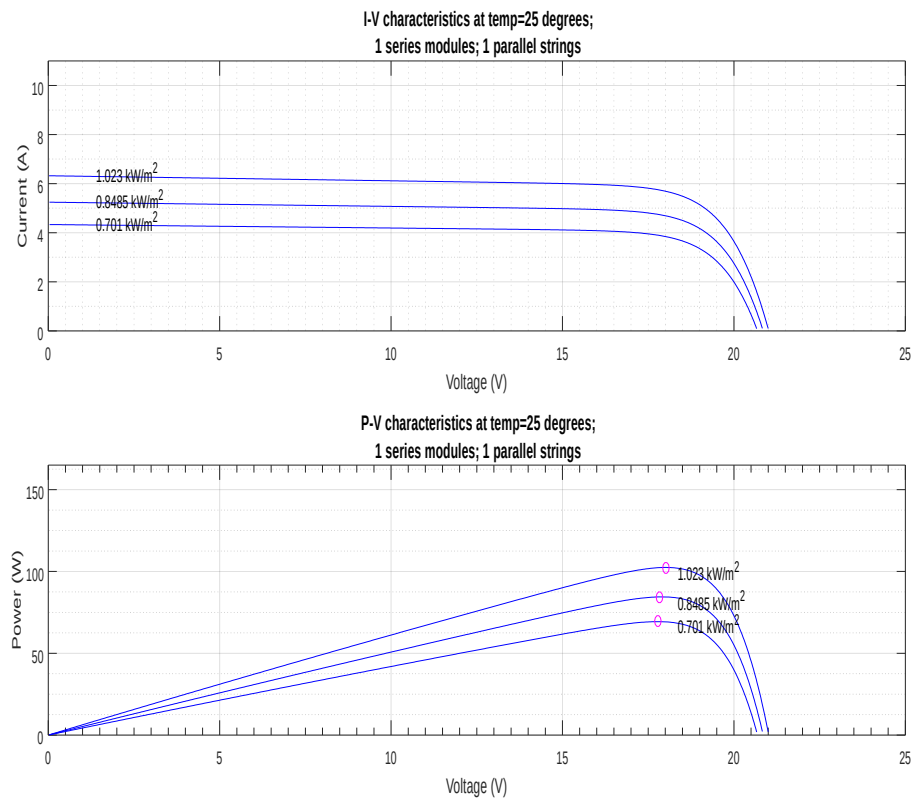


Figure 4.46: I-V and P-V Curves at constant temperature (poly-crystalline)

From the Simulated graph of March period at constant temperature of 25°C polycrystalline module gave a short circuit current of 6.2A, 5.1A, and 4.2A at 1023W, 848.5W and 701W respectively. While at the same period and same irradiance levels power output were 103W, 85W and 68W respectively.

I-V and P-V curves at constant irradiance but the varying temperature

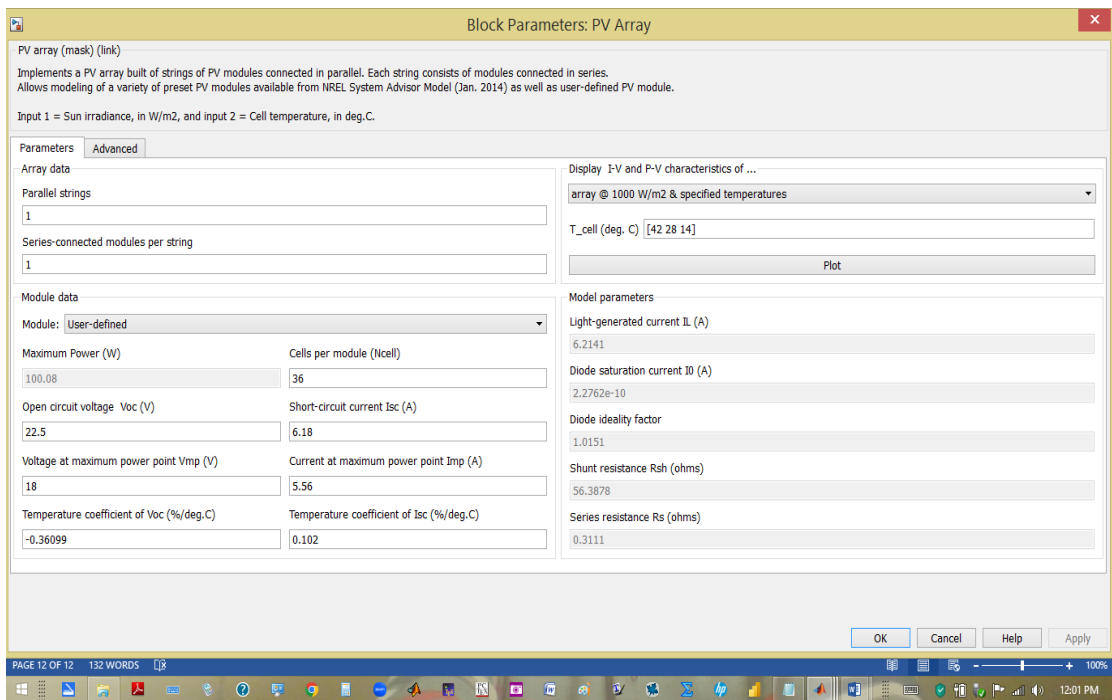


Figure 4.47: Third Simulink set-up for poly-crystalline

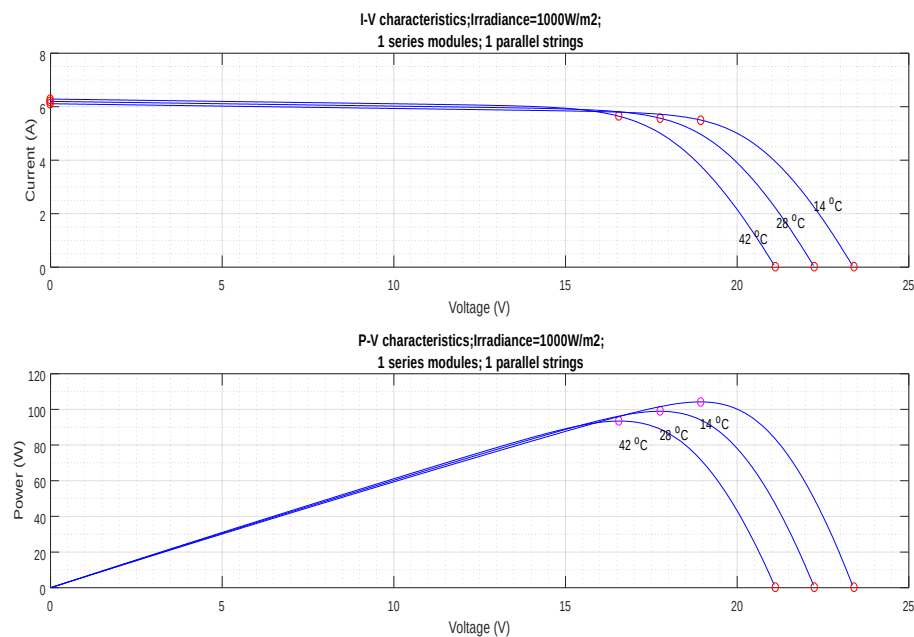


Figure 4.48: I-V and P-V Curves at constant irradiance (poly-crystalline)

From the Simulated graph of March period at constant temperature of 1000 Wm^2 polycrystalline module gave a short circuit current of 6.2A, 6.1A, and 6.0A at 42°C ,

28°C and 14°C respectively. While at the same period and same irradiance levels power output were 94W, 98W and 10W respectively.

4.5 SIMULATED AND MEASURED VALUES COMPARED

Monocrystalline

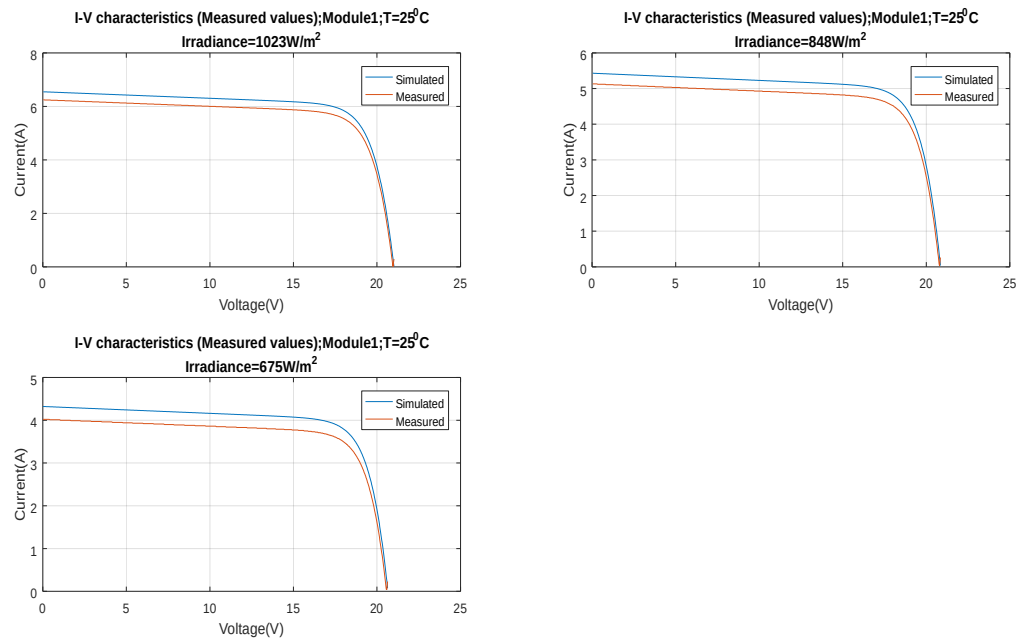


Figure 4.49: I-V characteristics for simulated and measured values for monocrystalline

For monocrystalline simulated gave a higher short circuit current as compared to the measured as shown where simulated at 1023W/m² gave 6.4A while measured gave 6.1A. At 848W/m² simulated had 5.4A and measured 5.05A. Lastly, at 675W/m² simulated gave 4.4A while measured had 4.0A. It indicated that there is slight difference in manufacturers' module specification and the modules performed optimally as specified by the manufacturer.

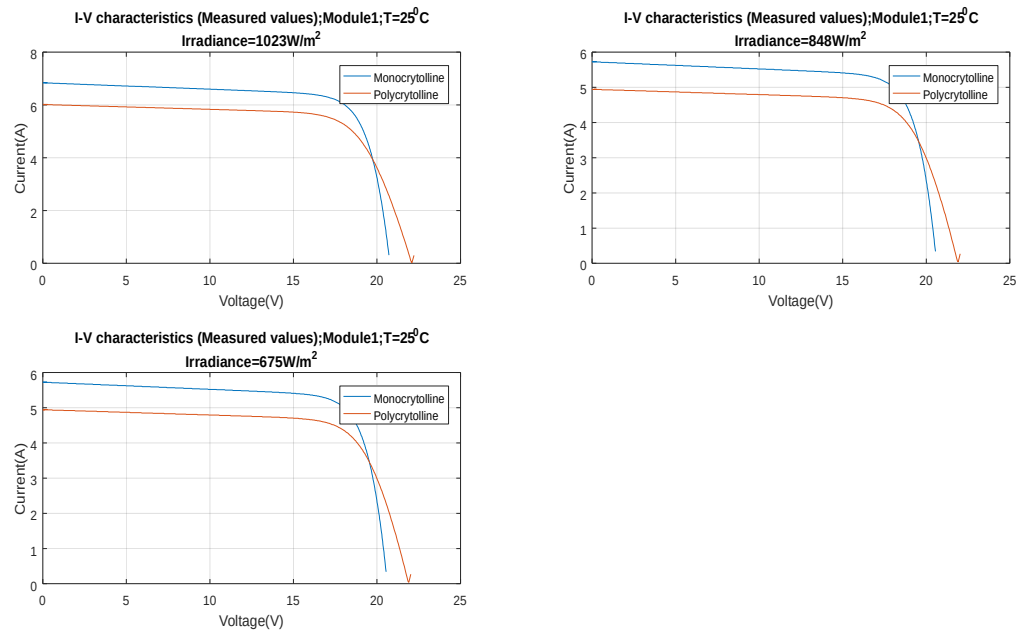


Figure 4.50: I-V characteristics for monocrystalline and polycrystalline measured values at varied irradiance

Performance of monocrystalline and polycrystalline when compared, at 1023W/m² Mono gave 6.8A while poly gave 6.0A. At the same irradiance open circuit voltage of poly was 22V while mono was 20.5V. At, 848W/m² and 675W/m² provided 5.8A and poly 5.0A with their voltage maintained at 20.5V and 22V respectively.

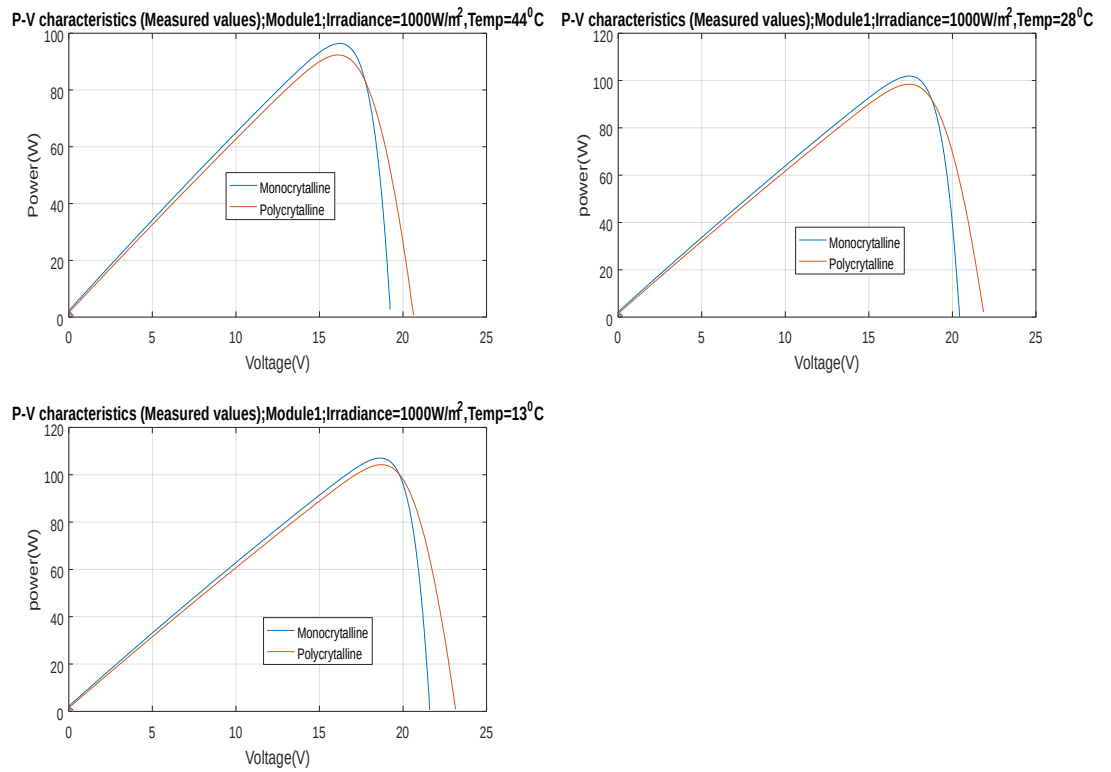


Figure 4.51: P-V characteristics for monocrystalline and polycrystalline at varied temperatures

Power out comparison of Mono and Poly at constant irradiance but varying temperatures, at 44°C mono produced 96W while poly 93W, at 28°C mono gave 102W while poly 98W and finally mono provided 106W and Poly gave 104W. This is a clear indication there is no so much difference in performance for both modules though mono still performed better.

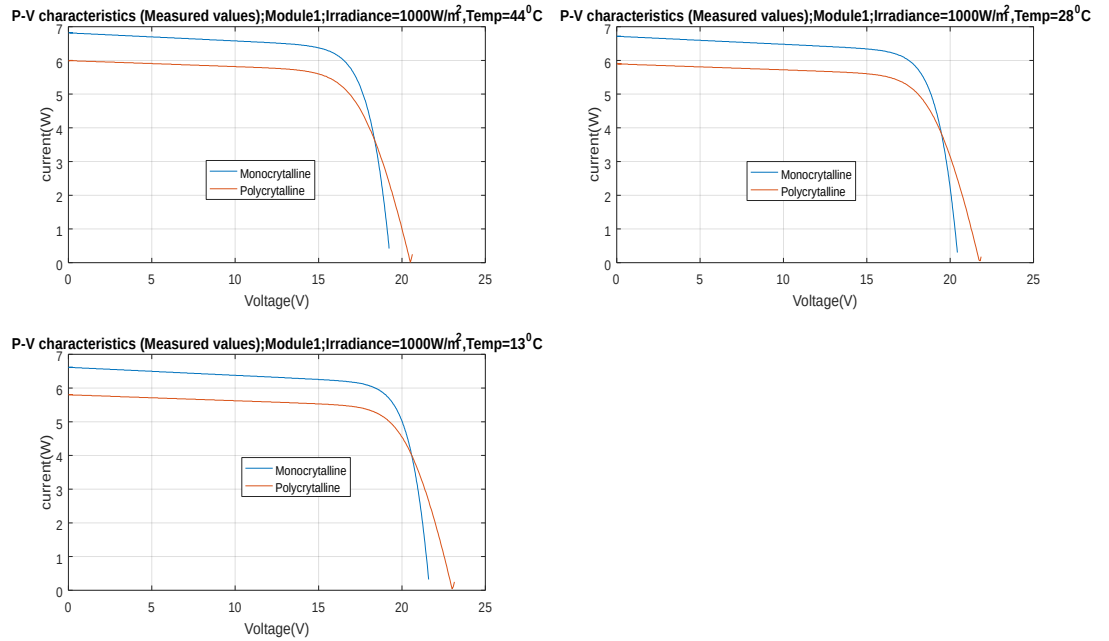


Figure 4.52: I-V characteristics comparison between Mono and Poly at different temperature level but constant irradiance

At 44°C monocrystalline short circuit current was 6.9A, while that of Polycrystalline was 5.0A, at 28°C mono gave 6.8A, poly, gave 5.9A and at 13°C monocrystalline produced 6.6A while poly 5.8A. this shows that monocrystalline module still gave better short circuit current at higher temperatures, though both modules shorts circuit current is temperature depended, where lower temperatures produces slightly lower short circuit current.

4.6 Schematic Simulink setup

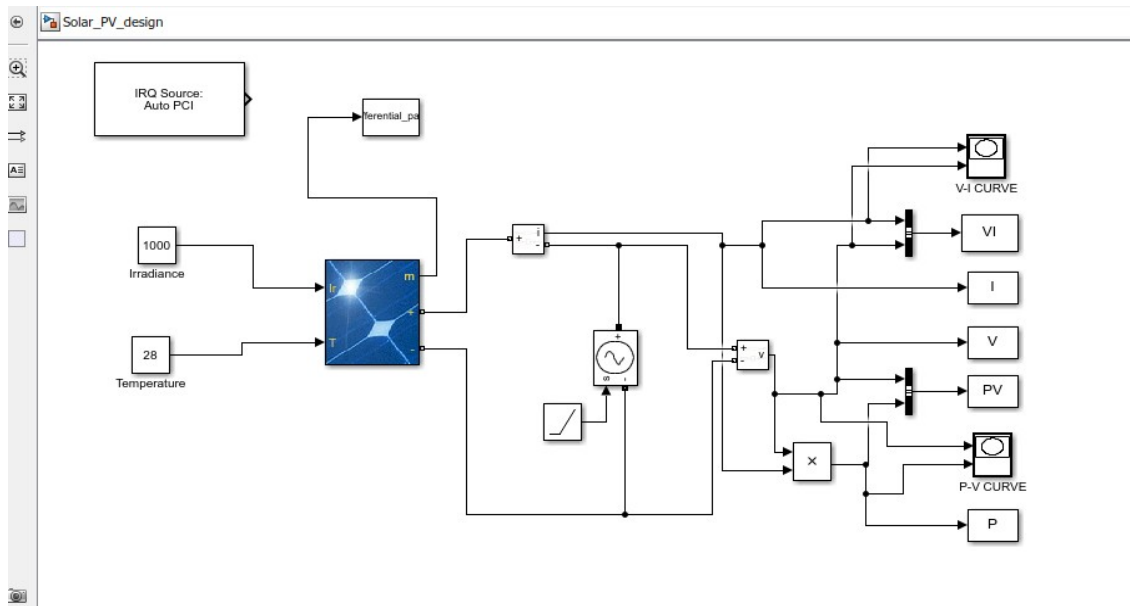


Figure 4.53: Simulink Setup for the simulation

CHAPTER FIVE: CONCLUSIONS AND RECOMMENDATIONS

6.1 Conclusions

The purpose of this study was to evaluate and simulate the performance of two 100W monocrystalline and polycrystalline modules in tropical weather. The conclusion suggests that both the type of solar cells utilized and the environment have an impact on how well photovoltaic panels operate. Monocrystalline module was able to attain a maximum power of 110W while polycrystalline 101W. This surpassed the one indicated by the manufacture, which is 100W. This is a clear indication that modules can even perform better when subjected certain environmental conditions.

Experimentally monocrystalline module performed better, producing a current of 6.4A than poly-crystalline, which produced 6.0A. At higher irradiance both modules produced more current and power while voltage was least affected. At high temperatures power and open circuit voltage decreased for both modules while short circuit current increased slightly. It was noticed that at each instant (irradiance and temperature) polycrystalline produced more voltage, less current and less power while monocrystalline there was more current, more power and less voltage.

In general, the simulation outcomes are a little bit better than the experimental outcomes. It is evident from the simulation results that the output is influenced by the solar irradiation striking the PV modules as well as its surface temperature. The maximum power and open circuit voltage fall as the temperature rises, while the short circuit current rises slightly. When the sun irradiation is high, a lot of power is produced for both modules. Though, monocrystalline has better performance than polycrystalline at tropical savannah climatic condition of Uasin Gishu.

The weather in Uasin Gishu varied slightly in terms of temperature and irradiance, with maximum solar irradiance of 1.023KW/m^2 minimum of 0.675KW/m^2 and a maximum module temperature of 44 degrees, with a minimum of 13°C within the study period.

6.2 Recommendations

Residents are advised to adapt solar PV modules of monocrystalline technology because of its performance against polycrystalline.

It was noticed that at each instant (irradiance and temperature) polycrystalline produced more voltage, less current and less power while monocrystalline there was more current, more power and less voltage. The researcher was not able to ascertain the cause of such variation thus proposes for further probe.

More research must be done in order to determine which specific conditions caused each kind of module to perform better.

REFERENCES

- Abdelkader, M. R., Al-Salaymeh, A., Al-Hamamre, Z., & Sharaf, F. (2010). A comparative Analysis of the Performance of Monocrystalline and Multicrystalline PV Cells in Semi Arid Climate Conditions: the Case of Jordan. *Jordan Journal of Mechanical & Industrial Engineering*, 4(5).
- Abdullahi, N., Saha, C., & Jinks, R. (2017). Modelling and performance analysis of a silicon PV module. *Journal of Renewable and Sustainable Energy*, 9(3), 033501. Accessed on 5th May, 2019 from; <https://pureportal.coventry.ac.uk/en/publications/modelling-and-performance-analysis-of-a-silicon-pv-module>
- African Development Bank (ADP) (2018). Why Africa is the next renewables powerhouse. It is increasingly clear that Africa has the potential to lead the world in scaling-up and generating renewable energy. Retrieved on 12th June, 2019 from: <https://www.afdb.org/en/news-and-events/why-africa-is-the-next-renewables-powerhouse-18822/>
- Agroui, K., Hadj, A., Pellegrino, M., Giovanni, F. & Mahammad, I. (2011). Indoor and Outdoor Photovoltaic Modules Performances Based on Thin Films Solar Cells. *Research and Applications. Renewable Energy*, 14: 469-480.
- Akorede, M. F. (2022). Design and performance analysis of off-grid hybrid renewable energy systems. In *Hybrid Technologies for Power Generation* (pp. 35-68). Academic Press.
- Amankwah-Amoah, J. (2015). Solar energy in sub-Saharan Africa: The challenges and opportunities of technological leapfrogging. *Thunderbird International Business Review*, 57(1), 15-31.
- Arjyadhara P, M AS, Chitrlekha J. (2013). Analysis of solar PV cell performance with changing irradiance and temperature. *International Journal of Engineering And Computer Science*. 2:214-20
- Awad Atia, G. A., Osman, M. M. M., Abdelrahim, M. E. K. A., & Mohammed, W. A. A. (2015). *Design of Digital Temperature Sensor* (Doctoral dissertation, Sudan University of Sciences and Technology).
- Azhar, G & Abdul, M. (2012). The performance of Three Different Solar Panels for Solar Electricity Applying Solar Tracking Device Under The Malaysian Climate Condition. *Energy and Environment Research*, 2: 235-243.
- Barman, J. (2011). Design and feasibility study of PV systems in Kenya.
- Bimenyimana, S., Asemota, G.N.O., Kemunto, M.C & Li, L. (2017). Shading effects in Photovoltaic Modules: Simulation and experimental Results. *Conference Proceedings*. 2nd International Conference on Power and Renewable Energy
- Bioudun, A. D., & Adeleke D. K. O. T. A. (2017). Experimental Evaluation of the Effect of Temperature on Polycrystalline and Monocrystalline Photovoltaic Modules. *IOSR Journal of Applied Physics*, 9(2), 5-10.
- Bisquert, J. (2020). *The Physics of Solar Energy Conversion*. CRC Press.

- Biwott, P. K. (2018). *Assessing The Solar Energy Resource Potential In Trans-Nzoia County For Decentralized Domestic Power Generation* (Doctoral dissertation, University of Nairobi).
- Buni, M. J., Al-Walie, A. A., & Al-Asadi, K. A. (2018). Effect of solar radiation on photovoltaic cell. *International Research Journal of Advanced Engineering and Science*, 3(3), 47-51.
- Carr A. (2005). A Detailed Performance Comparison of PV Modules of Different Technologies and the Implications for the PV System design Methods. *Phd Thesis*; Murdoch University. Western Australia.
- Charfi, W., Chaabane, M., Mhiri, H., & Bournot, P. (2018). Performance evaluation of a solar photovoltaic system. *Energy Reports*, 4, 400-406.
- Chedid, R., Tajeddine, R., Chaaban, F., & Ghajar, R. (2014, April). Modeling and simulation of PV arrays under varying conditions. In *MELECON 2014-2014 17th IEEE Mediterranean Electrotechnical Conference* (pp. 536-542). IEEE.
- Chenni, R., Makhlouf, M., Kerbache, T., & Bouzid, A. (2007). A detailed modeling method for photovoltaic cells. *Energy*, 32(9), 1724-1730.
- Cheruiyot, W. K., Tonui, J. K., & Limo, S. C. Performance Evaluation of 780 Wp Rooftop Solar PV Power Backup System in Western Kenya
- Chikate, B. V., & Sadawarte, Y. (2015). The factors affecting the performance of solar cell. *International journal of computer applications*, 1(1), 0975-8887.
- Choge, D. K. (2015). Analysis of wind and solar energy potential in Eldoret, Kenya. *Journal of Energy Technologies and Policy*, 5(2), 7-13.
- Cornaro, C. & Musella, D. (2010). Performance Analysis of PV Modules of Various Technologies after More than One Year of Outdoor Exposure in Rome, Italy.
- Cui, Y., Wang, Y., Bergqvist, J., Yao, H., Xu, Y., Gao, B., ... & Hou, J. (2019). Wide-gap non-fullerene acceptor enabling high-performance organic photovoltaic cells for indoor applications. *Nature Energy*, 4(9), 768-775.
- Daily Nation (2018). Kenya ranked high for renewable energy. Retrieved from: <https://www.nation.co.ke/news/Kenya-ranked-high-for-renewable-energy/1056-4597554-30vswa/index.html>
- Dash, P. K., & Gupta, N. C. (2015). Effect of temperature on power output from different commercially available photovoltaic modules. *International Journal of Engineering Research and Applications*, 5(1), 148-151.
- David, K., & Berndt, H. (2018). 6G vision and requirements: Is there any need for beyond 5G?. *IEEE vehicular technology magazine*, 13(3), 72-80.
- Dubey, S., Sarvaiya, J. N., & Seshadri, B. (2013). Temperature dependent photovoltaic (PV) efficiency and its effect on PV production in the world—a review. *Energy Procedia*, 33, 311-321.

- Duke, R. D., Jacobson, A., & Kammen, D. M. (2002). Photovoltaic module quality in the Kenyan solar home systems market. *Energy Policy*, 30(6), 477-499.
- Ekpenyong, E. E., & Anyasi, F. (2013). Effect of shading on photovoltaic cell. *IEEE*, 01-06.
- El Amin, A. A., & Al-Maghrabi, M. A. (2018). The Analysis of Temperature Effect for mc-Si Photovoltaic Cells Performance. *Silicon*, 10(4), 1551-1555.
- Ennison, I., & Dzobo, M. (2018). Nuclear Power and Ghana's Future Electricity Generation. IAEA Publication, IAEA-CN-164-1P01.
- Ethan, W. & Hsinjin, E. (2012). Failure Modes Evaluation of PV Materials Degradation Approach. *PV Asia Pacific Conference. Energy Procedia*, 33: 256-264.
- Fares, M. A., Atik, L., Bachir, G., & Aillerie, M. (2017). Photovoltaic panels characterization and experimental testing. *Energy Procedia*, 119, 945-952.
- Fouad, M. M., Shihata, L. A., & Morgan, E. I. (2017). An integrated review of factors influencing the performance of photovoltaic panels. *Renewable and Sustainable Energy Reviews*, 80, 1499-1511.
- Gatakaa, N. E. (2010). Performance Evaluation of Silicon-Based Photovoltaic Modules Found in The Kenyan Market.
- Ghoneim, A. A., Kandil, K. M., Al-Hasan, A. Y., Altouq, M. S., Al-Asaad, A. M., Alshamari, L. M., & Shamsaldeen, A. A. (2011). Analysis of performance parameters of amorphous photovoltaic modules under different environmental conditions. *Energy Science and Technology*, 1(1), 43-50.
- Gorjian, S., & Ghobadian, B. (2015). Solar desalination: A sustainable solution to water crisis in Iran. *Renewable and Sustainable Energy Reviews*, 48, 571-584.
- Grace, J., José, J. S., Meir, P., Miranda, H. S., & Montes, R. A. (2006). Productivity and carbon fluxes of tropical savannas. *Journal of Biogeography*, 33(3), 387-400.
- Gupta, N., Garg, R., & Kumar, P. (2017). Sensitivity and reliability models of a PV system connected to grid. *Renewable and Sustainable Energy Reviews*, 69, 188-196.
- Hamdi, R. T., Hafad, S. A., Kazem, H. A., & Chaichan, M. T. (2018). Humidity impact on photovoltaic cells performance: A review. *International Journal of Recent Engineering Research and Development (IJRERD)*, 3(11), 27-37.
- Hamrouni, N., Jraid, M., & Cherif, A. (2008). New control strategy for 2-stage grid-connected photovoltaic power system. *Renewable Energy*, 33(10), 2212-2221.
- Hansen, F. H. (2018). *A case study: off-grid solar PV in rural Kenya-Analyzing technology diffusion with inspiration from Appropriate Technology* (Master's thesis).
- Hashim, I. D., Ismail, A. A., & Azizi, M. A. (2020). Solar Tracker. *International Journal of Recent Technology and Applied Science*, 2(1), 59-65.

- IEA (International Energy Agency), 2013. World Energy Outlook. Retrieved from: <http://www.worldenergy-outlook.org/publications/weo-2013/>
- International Renewable Energy Agency (IRENA) (2018). Renewable capacity highlights. Accessed on 12th June, 2019 from: https://www.irena.org/-/media/Files/IRENA/Agency/Publication/2018/Mar/RE_capacity_highlights_2018.pdf?la=en&hash=21795787DA9BB41A32D2FF3A9C0702C43857B39C
- Jain, M., Rawat, P. S., & Morbale, J. (2017). Automatic floor cleaner. *International Research Journal of Engineering and Technology (IRJET)*, 4(4), 2395-0056.
- Kabir, E., Kumar, P., Kumar, S., Adelodun, A. A., & Kim, K. H. (2018). Solar energy: Potential and future prospects. *Renewable and Sustainable Energy Reviews*, 82, 894-900.
- Kambli, M. N. A. (2017). *Automatic power factor detector and corrector using arduino uno* (Doctoral dissertation, University of Mumbai).
- Karki, I. B. (2015). Effect of temperature on the IV characteristics of a polycrystalline solar cell. *Journal of Nepal Physical Society*, 3(1), 35-40.
- Khodzhaev, Z. (2016). Monitoring different sensors with ATmega328 microprocessor. *Istanbul Technical University, Faculty of Science and Letters, Advanced Physics Project Report*.
- Korir, D. K. (2020). *Factors Affecting Consumer Adoption of Solar Energy Technology in Uasin Gishu County in Kenya* (Doctoral dissertation, United States International University-Africa).
- Kricher, J. C. (2011). *Tropical ecology*. Princeton University Press.
- Kumar, N. M., Gupta, R. P., Mathew, M., Jayakumar, A., & Singh, N. K. (2019). Performance, energy loss, and degradation prediction of roof-integrated crystalline solar PV system installed in Northern India. *Case Studies in Thermal Engineering*, 13, 100409.
- Kuria, K. P., Robinson, O. O., & Gabriel, M. M. (2020). Monitoring temperature and humidity using arduino nano and module-DHT11 sensor with real time DS3231 data logger and LCD display. *Health Hyg*, 6(7), 8
- Laakso, L., Laakso, H., Aalto, P. P., Keronen, P., Petäjä, T., Nieminen, T., ... & Kerminen, V. M. (2008). Basic characteristics of atmospheric particles, trace gases and meteorology in a relatively clean Southern African Savannah environment. *Atmospheric Chemistry and Physics*, 8(16), 4823-4839.
- Letcher, T. M. (2018). Why Solar Energy?. In *A Comprehensive Guide to Solar Energy Systems* (pp. 3-16). Academic Press.
- Louwen, A., de Waal, A. C., Schropp, R. E., Faaij, A. P., & van Sark, W. G. (2017). Comprehensive characterisation and analysis of PV module performance under real operating conditions. *Progress in Photovoltaics: Research and Applications*, 25(3), 218-232.

- Malik, A., Ming, L., Sheng, T. & Blundell, M. (2010). Influence of Temperature on the Performance of Photovoltaic Poly crystalline Silicon Module in the Bruneian Climate. *A SEANJournal for Science and Technology Development*, **26**: 61-72.
- Manuel, V. & Ignacio, R. (2008). Photovoltaic Module Reliability Model Based on Field Degradation Studies. *Progress Report on Photovoltaics: Research and Applications*, **10**: 825-1002.
- Ministry of Energy (2015). Kenya Sustainable Energy for All Action Agenda. Kenya
- Monk, S. (2016). *Programming Arduino: getting started with sketches*. McGraw-Hill Education.
- Moodbidri, A., & Shahnasser, H. (2017). Child safety wearable device. In *2017 International Conference on Information Networking (ICOIN)* (pp. 438-444). IEEE.
- Muchiri, K., Kamau, J. N., & Wekesa, D. W. (2021). Solar pv potential and energy demand assessment in machakos county.
- Muok, B., Makokha, W., & Palit, D. (2015). Solar PV for Enhancing Electricity Access in Kenya: What Policies are Required?.
- Murgor, D. K. (2015). *Farmers Access to Climate and Weather Information and its Impact on Maize and Wheat Production in Uasin Gishu County, Kenya* (Doctoral dissertation, University of Eldoret).
- Musanga, L. M., Barasa, W. H., & Maxwell, M. (2018). The effect of irradiance and temperature on the performance of monocrystalline silicon solar module in Kakamega. *Physical Science International Journal*, 1-9.
- Mustafa, R. J., Gomaa, M. R., Al-Dhaifallah, M., & Rezk, H. (2020). Environmental impacts on the performance of solar photovoltaic systems. *Sustainability*, *12*(2), 608.
- Muzathik, A. M. (2014). Photovoltaic modules operating temperature estimation using a simple correlation. *International Journal of Energy Engineering*, *4*(4), 151.
- Mwende, R. (2021). *Photovoltaic (Pv) System Performance Forecasting and Modelling Using Real-time Observation and Weather Data* (Doctoral dissertation, University of Nairobi).
- Nagarjun, K. (2019). Autonomous vehicle navigation and mapping system
- Ngeno, G., Otieno, N., Troncoso, K., & Edwards, R. (2018). Opportunities for transition to clean household energy in Kenya: application of the household energy assessment rapid tool (HEART).
- Njoku, H. O., Ifediora, K. M., Ozor, P. A., & Dzah, J. M. (2020). Typical performance Reductions in PV modules subject to soiling in a tropical climate. *Nigerian journal of technology*, *39*(4), 1158-1168.
- Novelan, M. S., & Amin, M. (2020). Monitoring System for Temperature and Humidity Measurements with DHT11 Sensor Using NodeMCU. *International Journal of Innovative Science and Research Technology*, *5*(10), 123-128.

- Ojha, M., Mohite, S., Kathole, S., & Tarware, D. (2016). Microcontroller based automatic plant watering system. *International Journal of Computer Science and Engineering*, 5(3), 25-36.
- Oloo, F. O., Olang, L., & Strobl, J. (2015). Spatial modelling of solar energy potential in Kenya. *International Journal of sustainable energy planning and management*, 6, 17-30.
- Opiyo, N. (2015). Modelling PV-based communal grids potential for rural western Kenya. *Sustainable Energy, Grids and Networks*, 4, 54-61.
- Osma-Pinto, G., & Ordóñez-Plata, G. (2019). Measuring factors influencing performance of rooftop PV panels in warm tropical climates. *Solar Energy*, 185, 112-123.
- Otakwa, R. V. M. (2012). *Performance characterization of a dye-sensitized photovoltaic module under tropical weather conditions: the case of Nairobi, Kenya* (Doctoral dissertation, University of Nairobi, Kenya).
- Pan, T., & Zhu, Y. (2018). Getting started with Arduino. In *Designing embedded systems with arduino* (pp. 3-16). Springer, Singapore.
- Pang, W., Cui, Y., Zhang, Q., Yu, H., Zhang, X., Zhang, Y., & Yan, H. (2019). Comparative investigation of performances for HIT-PV and PVT systems. *Solar Energy*, 179, 37-47.
- Passago, S., Yodying, C., Monatrakul, W., & Santiboon, T. T. (2020). Research and development of renewable energy: Prototype of LED street lighting from solar energy. *Systematic Reviews in Pharmacy*, 11(2), 765-776.
- Performance study of Monocrystalline and Polycrystalline solar PV modules in tropical environments. In *International Conference on Advanced Engineering Theory and Applications* (pp. 193-203). Springer, Cham.
- Phalan, B., Bertzky, M., Butchart, S. H., Donald, P. F., Scharlemann, J. P., Stattersfield, A. J., & Balmford, A. (2013). Crop expansion and conservation priorities in tropical countries. *PloS one*, 8(1), e51759.
- Preece, N. (2002). Aboriginal fires in monsoonal Australia from historical accounts. *Journal of Biogeography*, 29(3), 321-336.
- Puccinelli, R. R., Cabrera, J. P., Huynh, E., Lebel, P. M., & Gómez-Sjöberg, R. (2021). Portable low-cost optical density meter. *bioRxiv*.
- Qian, Z. (2015). Getting started—Programming Arduino Yún Microcontroller. *Application Note, ECE*, 480.
- Quansah, D. A., Adaramola, M. S., Takyi, G., & Edwin, I. A. (2017). Reliability and degradation of solar PV modules—Case study of 19-year-old polycrystalline modules in Ghana. *Technologies*, 5(2), 22.
- Quaschnig, V. V. (2019). *Renewable energy and climate change*. Wiley.
- Rani, P. S., Giridhar, M. S., & Prasad, M. R. S. Effect of Temperature and Irradiance on Solar Module Performance.

- Reese, M. O., Glynn, S., Kempe, M. D., McGott, D. L., Dabney, M. S., Barnes, T. M., ...&Haegel, N. M. (2018). Increasing markets and decreasing package weight for high-specific-power photovoltaics. *Nature Energy*, 3(11), 1002.
- René J. (2005). *Introduction to polymer solar cells*. Eindhoven University of Technology, Netherlands. 3Y280.
- Ribeyron, P. J. (2017). Crystalline silicon solar cells: Better than ever. *Nature Energy*, 2(5), 17067.
- Rob, R., Tirian, G. O., & Panoiu, C. (2017). Temperature controlling system using embedded equipment. In *IOP Conference Series: Materials Science and Engineering* (Vol. 163, No. 1, p. 012046). IOP Publishing.
- Rong P., Joseph K., Govindasamy T. (2011). Degradation analysis of Solar Photovoltaic Modules: Influence of Environment Factor. In *the proceedings of Reliability and Maintainability Symposium*, 15: 24-27.
- Roy, A., Kedare, S. B., & Bandyopadhyay, S. (2010). Optimum sizing of wind-battery systems incorporating resource uncertainty. *Applied Energy*, 87(8), 2712-2727.
- Salman, A., Qamran, T., & Abu Dayya, S. (2020). Design and Implementation of a monitoring and control system for power conversion networks.
- Santos, J. A. F. D. A., Cunha, F. B. F., Costa, C. A. D., & Torres, E. A. T (2021). Exploratory study about wind-solar hybrid power plants in Brazil. In *16th SDEWES-Conference on sustainable development of energy, water and environment systems*. Outra instituição.
- Sarker, P. C., Islam, M. R., Paul, A. K., & Ghosh, S. K. (2018). Solar Photovoltaic Power Plants: Necessity and Techno-Economical Development. In *Renewable Energy and the Environment* (pp. 41-69). Springer, Singapore.
- Sathyanarayana, P., Ballal, R., Sagar, P. L., & Kumar, G. (2015). Effect of shading on the performance of solar PV panel. *Energy and Power*, 5(1A), 1-4.
- Sawin, J. L., Martinot, E., Sonntag-O'Brien, V., McCrone, A., Roussell, J., Barnes, D., ...&Ellenbeck, S. (2010). Renewables 2010-Global status report.
- Siddiqui R., Kumar R., Jha G. and Bajpai U. (2014). Performance Analysis of Polycrystalline Silicon PV Modules on the Basis of Indoor and Outdoor Conditions. *International Journal of Current Engineering and Technology*, 14: 35-47.
- Takase, M., Kipkoech, R., & Essandoh, P. K. (2021). A comprehensive review of energy scenario and sustainable energy in Kenya. *Fuel Communications*, 7, 100015.
- Taşcıoğlu, A., Taşkın, O., & Vardar, A. (2016). A power case study for monocrystalline and polycrystalline solar panels in Bursa City, Turkey. *International Journal of Photoenergy*, 2016.

- Tobnaghi DM, Naderi D. (2015) The effect of solar radiation and temperature on solar cells performance. *Extensive Journal of Applied Sciences*. 3:39-43.
- Tyagi, V. V., Kaushik, S. C., & Tyagi, S. K. (2012). Advancement in solar photovoltaic/thermal (PV/T) hybrid collector technology. *Renewable and Sustainable Energy Reviews*, 16(3), 1383-1398.
- Ulrich, B. (2019). Open-source wideband (DC to MHz range) isolated current sensor. *HardwareX*, 5, e00057.
- Vera, Y. E. G., Castillo, O. D. D., Pardo, L. Á. C., & Pérez, L. F. S. (2019, November).
- Wen, C., Fu, C., Tang, J., Liu, D., Hu, S., & Xing, Z. (2012). The influence of environment temperatures on single crystalline and polycrystalline silicon solar cell performance. *Science China Physics, Mechanics and Astronomy*, 55(2), 235-241.
- Yang, G. (2007). *Life cycle reliability engineering* (Vol. 10, p. 9780470117880). New Jersey: Wiley.
- Yang, H., He, W., Wang, H., Huang, J., & Zhang, J. (2018). Assessing power degradation and reliability of crystalline silicon solar modules with snail trails. *Solar Energy Materials and Solar Cells*, 187, 61-68.

APPENDICES

8.1 Appendix A: Installation on the roof



8.2 Appendix B: More measured results

